Bursts Identification in Water Distribution Systems

Irina Borovik

PhD

August 2008

Bursts Identification in Water Distribution Systems

Irina Borovik

Submitted in partial fulfilment of the requirements for the degree of Doctor of Philosophy

awarded by

De Montfort University

August 2008

Abstract

The presented thesis investigates the identification of burst locations in water distribution systems (WDS) by analysis of field and simulation experimental data. This required the development of a new hybrid method of burst detection and sizing, and also a burst location identification algorithm. Generally, existing practice relies on a combination of some simple procedure and experience of the involved staff and cannot be easily automated. The practical methods are based on direct manifestation of burst on the surface or on systematically surveying suspected areas e.g. by using listening sticks, such methods are very time consuming. The proposed burst location algorithm is based on comparing data by means of statistical analysis of field data with results of water network simulation. An extended network hydraulic simulator is used to model pressure dependent leakage terms. The presence of a burst changes the flow pattern and also pressure at network nodes which may be used to estimate the burst size and its location. The influence of such random factors as demand flows and background leakage on the process of burst detection is also considered. The field data is from a generalised fixed area and variable area (FAVOR) test where inlet pressure is being stepped up and down and the following variables are measured: inlet flow, inlet pressure (head) and pressure at a number of selected sensitive nodes. The method has three stages and uses two different models, one is inlet flow model (IFM) to represent the total inlet flow and another is the extended hydraulic model to simulate different burst locations. Initially the presence of a potential burst is investigated. If this is confirmed precise values of the demand, background leakage flow and burst flow in IFM are subsequently estimated. They are used to identify the burst site at the third stage of the method. The method can be easily adapted for practical use. It requires data from experiments carried out at night between 1am and 5am and involves placing typically about 20 temporary loggers to collect the measurements during this period. It also requires the availability of a hydraulic model which normally is in the possession of a water company. The program has been implemented in the Matlab package and is easy to use. The current methodology is tuned to identify a single burst but can be generalised to identify locations of multiple bursts.

Acknowledgement

The author would like to thank Prof. Bogumil Ulanicki for his guidance and members of the De Montfort University Water Software Systems research group for their help in preparation of the present research.

The author would like also to thank John May and South Staffordshire Water company for providing experimental data and for taking part in informative discussions.

Contents

Lists of tables

Lists of figures

1 Introduction

1.1 Aims and objectives of the research

Water is the most widespread substance in nature (hydrosphere occupies 71% of the Earth surface). It plays the most important role in the geological history of our planet and the existence of humanity without water would be impossible (about 65% of the human body consists of water). Water is an essential component of practically all technological processes. For this reason high emphasis is given to the matter of water supply without which further development of civilized society and modern production becomes impossible.

The current state and fast growth of urban water supply systems, expansion in a number of simultaneously used sources of water supply, in pump plants and in storage capacities are calling for improvement in analysis and control methods for water distribution systems (WDS). WDS are rather complicated entities of special constructions, interconnected by their parameters and operational condition. They provide, with sufficient reliability, water extraction from water sources, water treatment, accumulation and storage, water supply to the point of consumption, as well as distribution of the water among consumers. The systems are constructed in different environments using standard projects and serially manufactured for this purpose consisting of equipment, pipes and building constructions. Usually a WDS serves a rather wide circle of water consumers, who are dispersed over a wide area. In such complex conditions to take rational decisions about separate matters of water supply is difficult and requires the use of computer technology. One of the most important tasks is rational management of water resources. The UK water industry is addressing the major challenge of leakage management for WDS, driven by a mixture of economic, political and social factors (WRc 1994a, and b) and (Lambert et al. 1998). The water companies are making major investments to reduce leakage through traditional solutions and the evaluation and application of new technology. The savings arising from reduced leakage must be balanced against the cost of implementation of leakage detection schemes and the notion of an economic or optimum level of leakage at the distribution network scale is widely accepted throughout the industry.

The leakage reduction problem as a whole is complex and requires co-ordinated actions in different areas of water network management, such as:

- Direct detection and repair of existing bursts
- General pipe rehabilitation programmes
- Operational pressure control

Water companies undertake a mixture of these complementary actions. General pipe rehabilitation is the most costly and long term action, but is undertaken to improve a number of different factors including leakage and water quality. Operational pressure control is a cost-effective action for reducing leakage over whole sub-networks, and for reducing the risk of further leaks by smoothing pressure variations and is the subject of ongoing research (Vairavamoorthy and Lumbers 1998), (Ulanicki et al. 1999), (Ulanicki and Prescott 2000). Detection and repair actions are targeted at sub-networks where bursts are present. Benefits of quick burst repair include reduced water losses, reduced disruption to traffic, reduced consequential losses (e.g. from flooding), and also reduced disruption to customers' supplies, which is an important water industry performance measure.

There are a number of procedures for detecting bursts. Water from some bursts appears on the surface but the water does not necessarily emerge at the point of the burst. Many bursts remain invisible with the water draining away and never reaching the surface. Undetected bursts cause significant damage to the network and urban infrastructure. Listening sticks and leak noise correlation methods are frequently used by water companies (Cascetta and Vigo 1992). This involves systematically surveying areas suspected of having bursts. These areas are identified from the night flow or from historical records of bursts and pipe condition. Leak noise correlation involves teams in the field surveying mains in sections, it is time consuming and costly. Some companies are now considering permanently installed leak noise monitors. Generally, burst detection requires a combination of activities depending upon the burst itself and the experience of the staff performing the tasks.

Recently UK water companies have heavily invested into restructuring water networks into smaller sub-networks known as Demand Management Areas (DMAs). A DMA is a sub-network where the boundary flow is monitored in order to assess leakage. Its boundary is closed except for inputs and outputs with flow and pressure metres. This facilitates leakage management in terms of pressure control and bursts detection.

The first internationally applicable concept is the bursts and background estimates (BABE) which was developed by Allan Lambert for the UK National Leakage Control Initiative. The findings of this Initiative have been published in 'Managing Leakage' Reports (WRc- UK Water Industry, 1994). In BABE analysis, components of Real Losses are considered to consist of background leakage, reported and unreported leaks and bursts. Pressure in a water distribution system varies with demands during 24 hours a day (through the 24-hour day). For systems served by gravity from reservoirs, pressure is normally the highest at night, between 02.00 hrs and 04.00 hrs, when consumption is at its lowest. The minimum flow, measured during the night when the flow is at its lowest, is generally used in the BABE analysis as the initial basis for calculating losses from the system. When a new burst occurs it causes a noticeable increase in night boundary flow - such bursts should be located and repaired as quickly as possible. This approach is effective only for detecting new bursts and not for their localisation. DMAs which are supplied by a small number of mains can be investigated by successively closing valves across the DMA and observing the corresponding changes in flow. This allows the operator to narrow the search to a small area where leak noise correlation methods can be applied. This common sense procedure can be developed further into formal estimation techniques for burst detection (Pudar and Liggett 1992) but so far, there is no firm practical evidence that this approach is fully effective. This can be attributed to the fact that the method is based on passive identification and inaccurate models, which do not reflect the true nature of leakage. Attempts were made to use the transient response of a network to detect bursts (Covas and Ramos 1999), although the model is complicated and the effectiveness of the approach is questionable especially for looped networks.

The hypothesis behind this research is that a truly effective method for burst detection can be formulated by exploiting different behaviour of background leakage and bursts under varying pressure (May 1994). The first step of the method is to perform an active identification experiment which involves changing inlet pressure and observing corresponding changes in the inlet flow and in pressure at a number of internal nodes.

1.2 Summary of personal achievements

The following are personal contributions that represent significant and original advances over existing work:

- Development and validation of the concept that the different behaviour of background leakage and bursts under varying pressure can be used for burst detection.
- Verification that it is possible to precisely define the level of background leakage and presence of bursts in a network.
- Verification that it is possible to estimate the total water demand from night flow as well as demand distribution.
- Creating a hybrid method for burst size determination.
- The investigation of the effects of burst presence on pressure changes in the network and validation of the hypothesis that this can be used for the burst location identification.
- Creating a burst location identification algorithm together with the criterion to evaluate its accuracy.
- Investigation of the sensitivity of the burst location identification algorithm to different logger placement strategies.
- Validation of the developed methodology on two practical case studies
- Participation in Moscow University conference "Information and Control Systems in XXI century" (Borovik & Pavlov 2000) and publication of reports (Borovik & Pavlov 2007, Borovik & Yanov 2007).

1.3 Organization of thesis

The thesis comprises six chapters representing the development of the research. The content of individual chapters is as follows:

- Chapter 2 contains a review of the literature in the leakage management area.
- Chapter 3 contains general equations of main physical laws and phenomena governing water distribution systems.

- Chapter 3 consists of two sections, Chapter 3.1 is dedicated to the description of a network mathematical model and Chapter 3.2 to the physics of leaks.
- Chapter 4 is dedicated to verification of the hypothesis that the different behaviour of background leakage and bursts under varying pressure can be used to develop a method for burst detection. It consists of three parts: validation of the FAVOR test, high precision leakage modelling studies, and the formulation of a burst presence identification algorithm.
- Chapter 5 is dedicated to the task of finding burst location and is divided into three main parts: development of the hybrid method to quantify the leakage flows (Chapter 5.1), investigation of sensitive indicators of burst presence (Chapter 5.2) and finally the development of the burst location identification algorithm in Chapter 5.3. The approach is based on calculating parameter estimates using the least squares method followed by statistical analysis based on the chi-square criterion. Chapter 5.1.1 describes an algorithm for selecting sensitive nodes where pressure loggers are to be placed, while the effects of different placing strategies are investigated in Chapter 5.3.2. Special emphasis is placed on the definition of a criterion which is able to assess the reliability of the obtained results.
- Chapter 6 describes three practical case studies in order to validate the proposed approach.
- Conclusions and an outline for future research are outlined in Chapter 7.

1.4 Leakage characteristics

There are numerous types of leaks, each one with different typical flow ranges. The AWWA manual, Water Audits and Leak Detection, describes six such categories (Manual of Water Supply Practices AWWA M36 1990). Hirner also uses six categories for causes of leaks identified in a German city network (Hirner 1997):

- Bad and defective materials, whether of the pipes and joints or in the bedding and surroundings, due to insufficient planning.
- Pipe breaks resulting from poor workmanship in their laying – bridging pipes, stones in contact with pipes, non-adherence to required joint gaps, damage arising from heavy traffic, excessive joint deflection within sockets.

- Operational errors – excess pressure, filling pipelines too rapidly, closing valves too rapidly, water hammer.
- Corrosion – internal due to aggressive water, external due to insufficient corrosion protection of metallic materials from aggressive soil and groundwater.
- Leaking fittings (valves, air valves, saddles, hydrants), leaking stuffing boxes, leaking gate seating with stones in the seating, encrustation, old valves with inadequate construction, broken spindles caused by excessive force during operation, badly located saddle clamps.
- Accidental or deliberate damage to hydrants and taps removed from standpipes.

Examples of leaks from a joint between two pipes and from a connection are shown in Fig.1.1 and Fig.1.2 respectively.

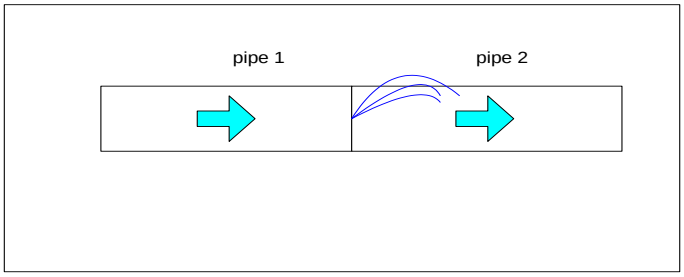

Fig. 1.1 Leak at a pipe joint

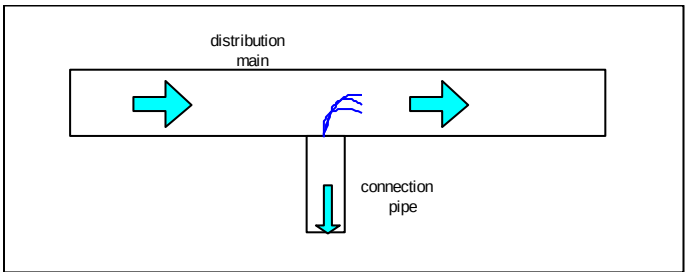

Fig. 1.2 Leak at a connection

The flow rates of individual leaks depend on the size of the hole, split or crack, and network pressure. They cover a wide range from a few litres/hour to many thousands of litres/hour. In Hirner (1997) categorization of the causes of leaks, all the items under the heading of operational faults such as excess pressure, filling pipelines too rapidly, closing valves too rapidly, water hammer – are associated with operating pressures, either directly or indirectly.

For the purposes of practical calculations and modelling it is appropriate to aggregate the numerous categories of leaks into a smaller number of broader groupings. The choice of groupings needs to reflect the fact that the total annual volume of losses from leakage depends not only on frequencies, flow rates and average duration of different types of leak but also on the practicalities of becoming aware of, and locating, the leaks. The following groupings are now widely used in the UK, with some variation in terminology (Lambert et al. 1998).

- Reported leaks generally have such high flow rates that they cause visible flows at the ground surface, loss of supply or low pressure for consumers. They are therefore normally reported to the water company by third parties soon after they occur.

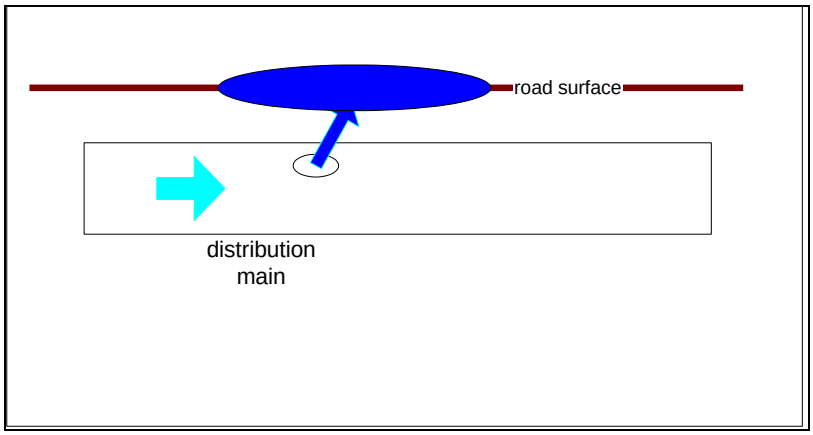

Fig. 1.3 Reported leaks

Reported leaks tend to have quite high individual flow rates, typically between 500 and 50,000 litres/hr, but average duration of only a few hours or days if repairs are carried out promptly.

- Unreported leaks have flow rates, which are generally less than those for reported leaks, but because they are only found through special investigations, they can run for months or even a year, and cause larger losses of water than reported leaks.

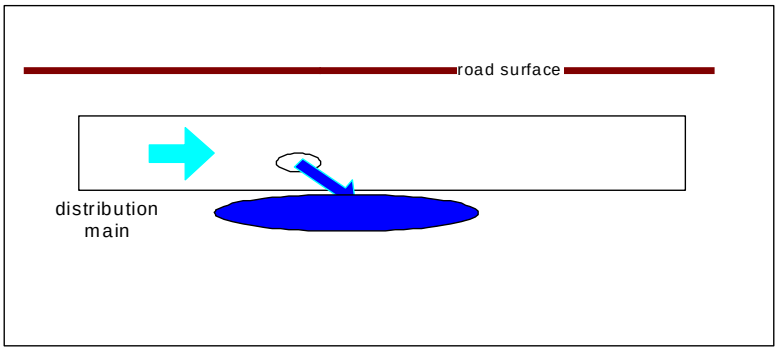

Fig. 1.4 Unreported leaks

However, some leaks are so small, so deep below ground, or come from pipes or fittings constructed of materials with poor sound conductivity (e.g. plastic pipes) that they cannot be detected at all. These relatively small undetectable leaks give rise to a third category of leakage.

- Background leakage for which individual flow rates are quite low – from less than 10 litres/hour to several hundred litres/hour – but they can account for a considerable proportion of the annual volume of losses, because they run continuously. They occur mainly at joints and fittings, and in the initial stages of development of small corrosion holes.

The unreported and reported leaks are combined into one group called bursts (or fixed area leakage) and the following categorization is proposed:

- flow of an individual burst is from 0.1 litres/second to 10 litres/second
- flow of an individual background leak is from 0.005 litres/second to 0.05 litres/second

for the purpose of numerical and practical experiments.

The main task of the research is to detect the location of a possible burst in water distribution systems.

2 Literature review

At the present time the water loss due to leaks in water distribution systems is a major problem for water companies. The economic cost related to water pipe bursts depends on frequency of pipe breaks which decreases overall hydraulic performance of WDS. For example, current water losses in WDS in Serbia and Montenegro are 40% or more of delivered water (Babich, Prodanovich and Ivetich 2005). In Italy real losses represent 27% of the entire supplied volume, but in many cases they reach and exceed 50% and similar conditions are common in many other countries (Magini, Pallavicini & Verde 2007). Leakage makes up a large part, sometimes more than 70% of the total water losses (WHO 2001). As a consequence of these economic and water-quality related issues, the interest of the scientific community in leak detection methodologies increased, with many papers on this topic published in recent years.

In general, two approaches of solving the problem of water loss due to leaks are available. The first one is prevention of leak occurrences. Usually a combination of factors and conditions influences the probability of leak occurrences (Ragani and Tesfamariam 2005), both static (e.g., pipe material, size, age, soil type) (Economou et al 2007) and dynamic (e.g., climate, cathodic protection, pressure zone changes) (Kleiner & Rajani 2007). Skipworth (2001) and Unwin (2003) showed an increase in the burst rate with pipe age, where the relationship depends on material types. Various modelling approaches are used for prediction of the failures, depending upon the failure type, the nature and complexity of the network and the availability, scope and reliability of relevant data (Kleiner & Rajani 2001; Giustolisi & Berardi 2007; Berardi L., Giustolisi O., Primativo F. 2007; Boxall at al 2005). Predictions create a possibility of preventing burst occurrences by carrying out jobs on reconstruction and renewal of pipes (Hetenyi, Tolnai and Zimmer 2007). An economic analysis of this problem was performed in pioneering works on the subject (Shamir & Howard 1979, Walski & Pellicia 1982). Renewal works are needed which ensure the continuity of the service access, but where the strategy of renovation needs to take into account economic, technical and social criteria (Nafi & Werey 2007). During development of a multi-objective strategy different algorithms are used for solving the task of planning optimisation and

renovation: a genetic algorithm (Giustolisi, Laucelli and Savic 2005, Dandy and Engelhardt 2001), a fuzzy rule based, non-homogeneous Markov process (Kleinner et al 2004, 2005), the method of Cullinane (Trifunovich, Umar 2003), statistical methods (Mays, 2000), a nonsorting genetic algorithm (Devi & Nam-Sik 2004), a Strength Pareto Evolutionary Algorithm (SPEA) (Cheung et al. 2003), a Non-Sorting Genetic Algorithm II (Deb et al 2000). At present the pipe rehabilitation practice and theory is being actively developed, new materials for pipes are investigated and new factors influencing the probability of burst occurrences are investigated, but it needs sufficient time, efforts and resources to be fully realized, that is why the problem of water losses will remain important in the near future.

In this context the detection of leaks is of high importance and both methodologies of the prediction of pipe failures and the detection of leaks are based on analysis of statistical data of already detected leaks (Berardi, Savic & Giustolisi 2005).

The detection of a burst and identification of its size and location is not possible without system monitoring providing information about flow changes (Burnell 2003) and pressure changes (Stephens et al. 2005). The quality of collected information from monitors depends on the placement of pressure loggers in a water distribution system. To solve the problem of optimal placement of pressure loggers various methods based on Genetic Algorithms (Xi, Bin, Jie & Fang 2007), cluster analysis (Huang & Cong 2001, Zhou & Hu 2005) and regression analysis (Guo, Liu & Chen 2004) are suggested, but the essence of all these methods is in discovering sensitive nodes in the network, which represent behaviour of all other nodes. The matter of selection of sensitive nodes is examined in detail in Chapter 5.1.1.

There were different leak detection methods proposed in 1990s which are reviewed in (Simpson and Vitkovsky 1997, Vitkovsky and Simpson 1997), for example, a leak detection method by means of solving the inverse steady-state problem was introduced by Pudar and Liggett (Pudar & Liggett 1992). More recently, several techniques for leaks detection based on transient models have been investigated. For instance, (Brunone & Ferrante 2001, Covas at al. 2003, Covas et al. 2004, Al-Khomairi 2005) have developed methods based on time analysis of a travelling wave. (Zecchin et al. 2005), (Mpesha et al. 2000, Stoianov et al. 2002, Ferrante & Brunone 2003, Wang et al. 2002) have investigated similar ideas in the frequency domain. Inverse transient analyses have been proposed by (Soares, Covas & Reis 2007, Liggett & Chen 1994,

Nash & Karney 1999, Vitkovsky et al. 2000, Kapelan et al. 2003). The basic idea is to deliberately generate transient waves or impulses and to measure the responses with highly sensitive pressure transducers. Optimisation (search) methods such as genetic algorithms are used for the burst location (Wu & Sage 2007). The burst is placed at different nodes of the WDS model to minimize the difference between the simulated and measured transient pressure (Vitkovsky et al. 1999). The overwhelming majority of research papers concerned with this methodology have been applied for the single pipeline cases and not to real distribution systems. The main shortcoming of the approach is that the transient wave is heavily damped throughout a WDS due to storage tanks, junctions, network cross connections and various demands. It is unlikely that it will be possible to measure transient pressure accurately enough to be used for inverse analysis. In general such methods are not suitable for leak detection in DMAs.

Currently, other methods for burst detection are appearing. This is linked to the increase in computer power and consequently with the possibility of fast information processing in large databases and with the availability of new numerical methods for WDS analysis (Tabesh & Delavar 2003, Giustolisi & Laucelli 2007) e.g. modeling pressure dependent leakage.

The burst finding pilot study using the Calibration Module of SynerGEE® Water (Deagle etal. 2007) has been successful and it has proven that network models can be employed to identify system anomalies and areas of interest within the distribution network. However, according to the authors of the paper the required period of observation over the real network is very long: "A plot of a DMA inflows over a number of months prior to study and for the 24 hour period during the study and pressure data for a full 24-hour period for all pressure logger points are required".

There are other methods, which require continuous monitoring of the concerned area. For instance, (Garcia, Cabrera, Cabrera 2006) have developed a method based on the observation of the minimum night flow (MNF), (Mounce, Boxall & Machell 2007) used the Artificial Neural Networks/Fuzzy Logic approach to analyze a DMA inflow including MNF, (Buchberger & Nadimpalli 2004) have developed the leak screening method based on repeatedly computing the mean and standard deviation of the measured inlet night flows. An annual balance method has been proposed by (Tabesh et al. 2005). (Araujo, Coelho & Ramos 2003) have developed a method for estimating distributed pressure-dependent leakage and consumer demands. Typical limitations of

the above methods are that they identify only new burst events whilst the existing leaks may go undetected and they estimate the total water losses rather than precise location of a burst.

Puust (Puust et al. 2006) proposed a methodology which is based on the Shuffled Complex Evolution Metropolis (SCEM-UA) algorithm and is capable of estimating the posterior probability density functions for unknown leak areas and their respective locations in an artificial network case-study. It seems that this approach is similar to the hybrid method presented in this report, but it has not been developed completely and unfortunately comparative analysis of these methods cannot be carried out.

3 General concepts

In the epoch of computer technology the solution to many engineering tasks is accomplished by computer algorithms which use mathematical models of physical phenomena occurring in the examined system. In this chapter the equations governing WDS are given, which underlie the method developed by the author.

3.1 Network model without leaks.

At the present time there are a number of packages for computer simulation of WDS, such as: GINAS (Coulbeck 1989), EPANET (Rossman 2000), FINESSE (WSS 1999) and InfoWorks WS (Wallingford Software 2008).

All of them are based on the hydraulic laws (in Greek language *hydro* means water, *aulos* – pipe, chute) – the science, that began to develop in the ancient period (250 years B.C.). A conceptual model of a WDS can be presented as an input-output system illustrated in Figure 3.1.

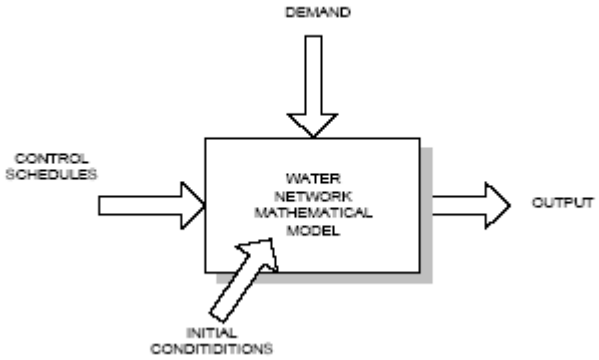

Fig. 3.1 Input-output models (conceptual model) of a water network

The following terms are associated with the model:

Control Schedules are pump, valve and source schedules.

Demands are node outflows representing water consumption.

Initial Conditions are the initial reservoir levels.

Output comprises heads at nodes, flows in elements, and operating costs.

Water Network Mathematical Model is the set of mathematical equations simulating behaviour of the physical system.

Topology describes connections between components.

A computer model of a water distribution system is a collection of links connected to nodes. The links represent pipes, pumps and control valves. Nodes are points in the network where links join together and where water enters or leaves the network. It is useful to distinguish between the basic two terminal components with regular characteristics and the complex components with local control loops that potentially have irregular (non-monotonic, non-smooth) characteristics.

The two terminal components are described by an equation relating component flow q and the head loss Δh: e.g. $\Delta h - r(q)q = 0$ where *r(q)* is flow dependent resistance.

For complex components the origin and destination heads may appear explicitly as separate variables, e.g. $f(q, h_{origin}, h_{destination}) = 0$.

The basic components are reservoirs, pipes, simple valves, pumps, and demands. The components with local control loops are control elements such as pressure reducing valves (PRVs), pressure sustaining valves (PSVs), pressure control pumps (PCPs), etc.

In a computer implementation, a water network model is represented by a set of network data (network topology, water demands and components data) and a set of equations (that define physical operation of the model).

The fundamental model is formulated using laws of physics. Three physical laws are employed for water network models: conservation of mass – flow continuity (Kirchhoff's I law), conservation of energy - head-loss continuity (Kirchhoff's II law), and component equations (head/flow law).

The hydraulic head loss caused by water flowing in a pipe due to friction can be computed using one of two different formulas:

- Hazen-Williams formula

  The Hazen-Williams equation is an empirical formula which relates the flow of water in a pipe with the physical properties of the pipe and the pressure drop caused by friction.

- Darcy-Weisbach formula

  The Darcy–Weisbach equation is an important and widely used phenomenological equation in hydraulics. It relates the head loss or pressure loss due to friction along a given length of pipe to the average velocity of the fluid flow.

Each formula uses the following equation to compute head-loss between the origin and destination node of the pipe:

$\Delta h = Rq^B$

where Δh is head-loss (Length), q – flow rate (Volume/Time), R – resistance coefficient, and B – flow exponent. The table 3.1 lists expressions for the resistance coefficient for each of the formulas (Streeter & Wylie 1998).

Table 3.1 The resistance coefficients

Formula	Resistance Coefficient (R)
Hazen-Williams	$10.075 \times C^{-1.852} (d[m])^{-4.87} L[m]$
Darcy-Weisbach (Colebrook –White)	$f \times 0.082627 \times (d[m])^{-5} \times L[m]$

where

C - Hazen-Williams roughness coefficient

d – pipe diameter [m],

L – pipe length [m]

f – friction factor is a combination of geometric factors such as the Reynolds number and (outside the laminar regime) the relative roughness of the pipe (the ratio of the roughness height to the hydraulic diameter) and is obtained by solving the Colebrook equation $\frac{1}{f^{0.5}} = -2.0 \log\left(\frac{e/d}{3.7} + \frac{2.51}{\mathrm{Re} \times f^{0.5}}\right)$, where

e - Darcy-Weisbach roughness coefficient [m]

d – pipe diameter [m],

q – flow rate [m^3/s]

Re - the Reynolds Number of the flow (Reynolds numbers are used to characterize different flow regimes, such as laminar or turbulent flow: laminar flow occurs at low Reynolds numbers, where viscous forces are dominant, and is characterized by smooth, constant fluid motion, while turbulent flow occurs at high Reynolds numbers and is dominated by inertial forces, which tend to produce random eddies, vortices and other flow fluctuations.)

.

The pipe headloss formulas for full flow:

- Hazen-Williams formula

$$\Delta h[m] = Rq^{1.852} = 10.075 \times C^{-1.852}(d[m])^{-4.87} L[m](q[l/s])^{1.852}$$

- Darcy-Weisbach (Colebrook –White) formula

$$\Delta h[m] = Rq^2 = f \times 0.082627 \times (d[m])^{-5} \times L[m] \times (q[l/s])^2$$

The Darcy–Weisbach equation are considered to be the most accurate model for estimating frictional head loss in steady pipe flow, but it is difficult to use. That is why an alternative empirical head loss calculation like the Hazen-Williams equation may be preferred. The Hazen-Williams equation can be expressed in slightly different units commonly used by hydraulic engineers:

$$\Delta h[m] = 1.21216 \times 10^{10} C^{-1.852}(d[mm])^{-4.87} L[m](q[l/s])^{1.852}$$

For convenience of calculations in this thesis the above network equation can be expressed using a vector-matrix notation, as given below:

$$\frac{dh_f}{dt} = -S^{-1} q_f(t) \qquad \text{reservoir dynamics} \qquad (3.1)$$

$$R(q)q = \Lambda^T h \qquad \text{component equations} \qquad (3.2)$$

$$\Lambda_c q = -d \qquad \text{mass balance at connection nodes} \qquad (3.3)$$

$$\Lambda_f q = q_f + q_s \qquad \text{mass balance at the reservoir nodes} \qquad (3.4)$$

where

S is a diagonal matrix of the reservoir cross-sectional areas

$h = \begin{bmatrix} h_f \\ h_c \end{bmatrix}$ is the vector of node heads, h_f is the vector of heads at reservoir nodes (fixed grade nodes) and h_c is the vector of heads at the connection nodes.

q is the vector of branch flows.

q_f and q_s are nodal flows, the vector of reservoir flows and the vector of source flows respectively.

d is the vector of nodal demands.

Λ_c, Λ_f are the node branch incidence matrices for connection nodes and reservoir nodes respectively.

$R(q)$ is the component resistance matrix:

$$R(q)=\begin{bmatrix} r_1(q_1) & 0\ldots & 0 \\ 0 & r_2(q_2) & 0\ldots \\ 0 & 0\ldots & r_b(q_b) \end{bmatrix}$$

$r_i(q_i)$ is a resistance for q_i flow from component headloss function $\Delta h_i = R_i \mid q_i \mid^{0.852} q_i = r_i(q_i) q_i$

b is a number of branches.

The system of equations (3.1) to (3.4) can be classified as a system of differential algebraic equations (DAEs) where equation 3.1 represents the differential part and equations (3.2) to (3.4) the algebraic part. Variables h_c, q, h_f , q_f are internal variables of the model, vector h_f is called a differential variable and h_c , q, q_f are called algebraic variables.

3.2 Physics of leaks

Initially, a model must be obtained which includes standard hydraulic data and additionally leakage information. It is standard industrial practice that the leakage flow is aggregated together with demands. Germanopoulos (1985), using results of field experiments, proposed a non-linear formula relating leakage flow to pressure. May (1994) suggested an approach to leakage representation, which has a direct physical interpretation and can be incorporated into a simulation algorithm comparatively easily. Consider a vessel containing fluid with an opening in its wall depicted in Fig. 3.2.

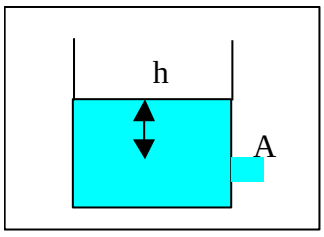

Fig. 3.2 A vessel containing fluid

Speed of the water through the opening is $v=\sqrt{2gh}$ and the flow $q=c_d A\sqrt{2gh}=c_d A(2gh)^{0.5}$, where c_d is the discharge coefficient, A is the orifice area, g is the acceleration due to gravity and h is the pressure head.

A slightly more general form of this power law will be applied to express the leak flow in pipes:

$$q = cp^{\alpha},$$

where c is the leak coefficient (equivalent area of the leak), α is the leak exponent and p is the pressure which is the difference between the head and the node elevation.

May's theory demonstrated that the cross-sectional area of certain types of leakage paths - holes, tears or breaks in pipes, joints and fittings - vary with pressure, while the velocity of flow continued to vary in proportion to the square root of pressure. This would give rise to different types of leakage paths in which the flow rates vary with pressure as follows:

- fixed areas (in case of a burst) to the power 0.5

  The burst flow is calculated as $q = c_1 p^{0.5}$, where c_1 is the burst coefficient.

- areas which vary along a single axis (in the case of the background leakage) to the power 1.5

  The background leakage's flow is calculated as $q = c_2 p^{1.5}$, where c_2 is the background leakage coefficient.

In the UK large scale water distribution systems are decomposed into zones and the zones are decomposed into district metering areas (DMA). The concept of DMA management was first introduced to the UK water industry in the early 1980s (WAA 1980) where a district is an area of a distribution system which is specifically defined, e.g. by the closure of valves, and in which the quantities of water incoming and going out of the district are metered (Morrison 2004). Assessments of the aggregate water losses for the whole WDS are derived indirectly from water balance calculations, as the difference between a measured volume of input and aggregate, and measured or estimated volume of output over the same period of time. It is possible to write an equation for the balance of water in a DMA as follows:

$$Flow_{inlet} = Demand + Leakage$$

The corresponding equation for the estimation of the inlet flow can be written as follows:

$$q = Demand + Leakage = d + c_1 p_1^{0.5} + c_2 p_2^{1.5}$$

where p_1 and p_2 are appropriate pressures which will be discussed in detail later.

A simulation model including hydraulic equations and pressure dependent leakage has been created and implemented in the advanced modelling environment GAMS (Brooke, Kendrick, & Meeraus 1992). Such a model provides freedom to model different scenarios, for example simulating just background leakage, which cannot be tested in a physical network. The effects of bursts on flows and heads throughout the system can be observed and sensitive indicators of the presence of bursts can be derived. Because precision is of paramount importance, the Darcy-Weisbach (Colebrook –White) formula has been used rather than the Hazen-Williams model (Streeter and Wylie 1998). The standard hydraulic equations (3.1)-(3.4) have been complemented with additional terms representing pressure dependent leakage $q = c\, p^{\alpha}$, where the leakage exponent α is equal to 0.5 for a burst and 1.5 for the background leakage. The value of *c* for each node is estimated by distributing the total background leakage flow between nodes. This equation constitutes the basis for further investigation.

4 Detection of a burst presence

The aim of this part of the research is to formulate and verify a method for identification of the burst presence using the fixed and variable orifice area (FAVOR) test proposed by May (1994) as a starting point. The investigation will progress in three stages: validation of the FAVOR test, high precision leakage simulating studies and formulation of a burst presence identification algorithm. Leakage has two components - the burst leakage through larger holes and the background leakage predominantly through pipe connections and joints. These two terms respond differently to varying pressure. A power law with exponent 0.5 governs flow through fixed areas (bursts). Flows through small holes and pipe-joints are governed by a power law with exponent 1.5. There are two possible explanations for this: the elasticity of pipes and/or inherent properties of fluid flowing through very small orifices.

The hypothesis is that applying step pressure changes to a DMA input and monitoring boundary flows can be used to separate the two terms of leakage in a DMA. This active identification experiment provides measurements from which equivalent constant and varying areas of the bursts and background leakage respectively can be evaluated. Hydraulic simulations are an important part of the method.

4.1 Validation of the proposed experimental method

The fixed and variable orifice area (FAVOR) test is based on Fixed and Variable Area Discharge (FAVAD) concept (May 1994), which describes the leakage and pressure relationship considering bursts as a fixed area discharge whereas background loss is considered as a variable area discharge. This concept is integrated with BABE methodology (Breaks and Background Estimates (BABE) 2008). In this concept, certain relationship between pressure and leakage exist depending on the leakage paths. Losses from fixed area leakage paths vary according to the square root of the system pressure, whilst discharges from variable area paths vary according to pressure to the power of 1.5. As there will be a mixture of fixed and variable area leaks in any distribution system, loss rates vary with pressure to a power that normally lies between the limits of 0.5 and 1.5. The simplest versions of the FAVAD concept, suitable for most practical

predictions, are Leakage flow Q (l/s) which varies with Pressure according to an exponent $N1(P^{N1})$ or

$$\frac{Q_1}{Q_0} = \left(\frac{P_1}{P_0}\right)^{N1}$$

So, if pressure is reduced from P_0 to P_1, flow rates through existing leaks change from Q_0 to Q_1, and the extent of the change depends on the exponent $N1$. The higher the $N1$ value, the more sensitive existing leakage flow rates will be to changes in pressures. The FAVAD concepts have for the first time allowed accurate forecasting of the increase or decrease of Real Losses due to a change in pressure. The $N1$ values might be in the order of 0.5 to 1.5, depending upon the type(s) of leak present (Thornton, Lambert 2005).

With the help of collaborating water companies seven single-input Demand Management Areas (DMAs) were selected by Water Software System research group (DMU). Multiple-input areas were tested as well. A typical FAVOR test was carried out by DMU during the night between 1 a.m. and 5 a.m. During the period of recordings, the inlet pressure was changed stepwise over a typical range of values at 20-minute or 30-minute intervals. The recorded variables with 10-seconds or 20-seconds intervals were the inlet pressure and flow (Fig.4.1 for Down Ampney and Appendix A for other six DMA).

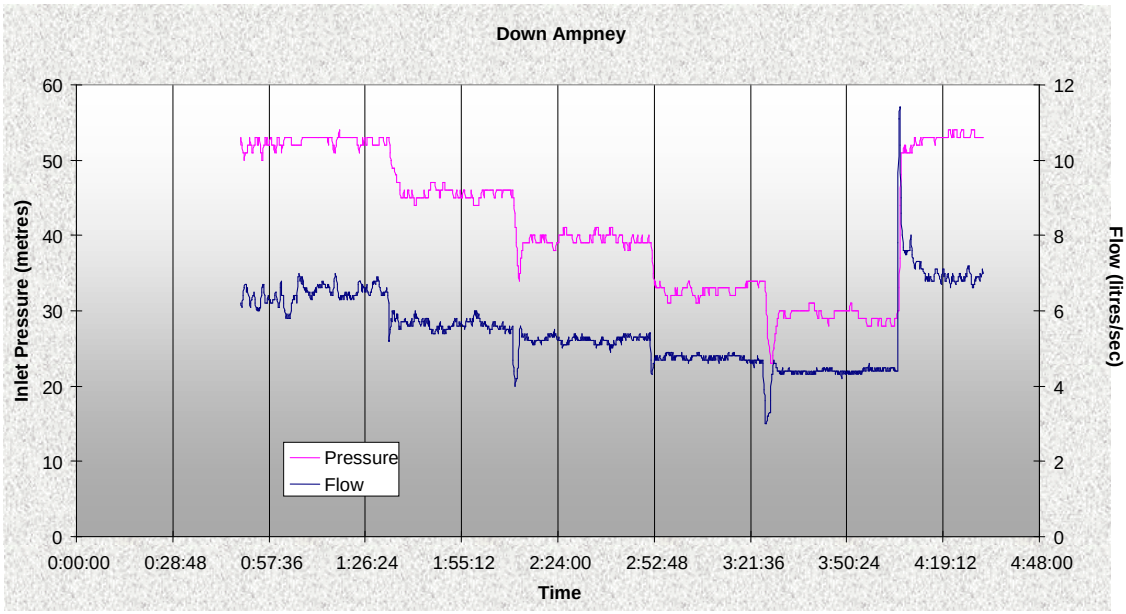

Fig. 4.1 FAVOR Test Data of Down Ampney

It can be observed from the data (Fig.4.1) that when the inlet pressure is changed stepwise, the flow changes in a similar manner. The data from the transient phase between steady states should be neglected to decrease errors.

A three term inlet flow model (IFM) is fitted to this data.

$$q = d + c_1 p_1^{0.5} + c_2 p_2^{1.5} \tag{4.1}$$

It is assumed that the demand variation within half an hour is insignificant. *d* is the average total demand that can be assumed to be irrespective of pressure. The total demand at night consists of the sum of small customers demands. Some customers demands (such as washing hands, cleaning plates and dishes and so on) are independent of pressure, as they have (controllers of water rates) possibility to control water head, while the other customers demands of automated devices (such as washing mechines, toilet cisterns, etc.) depend on pressure, because the time period of direct water demand depends on water head and on tank volume. But the ratio of time period of direct water demand by separate devices to the whole period of observation (about 4 hours) is insignificant. Variation of a specific demand, resulting from a pressure change at the given point of time can be considered only as a deviation from average demand at the same point of time. The average total demand is the sum of consumers demands at each specific point of time averaged for the whole night period of observation and can be assumed to be independent of pressure.

From a data set it is possible to find the coefficients *d*, c_1 and c_2. For the purpose of this investigation pressures p_1 and p_2 were assumed to be related to the average zonal night pressure (AZNP) (Maksimovic et al 2003). The average zonal night pressure taking account of the zonal demand distribution, p_{AZNP}, as herein defined as

$$p_{AZNP} = \frac{\sum_{i \in Nodes} p_i \cdot Demand\_Allocation\_Factor_i}{\sum_{i \in Nodes} Demand\_Allocation\_Factor_i}$$

where p_i is pressure at each node of network with demand and $Demand\_Allocation\_Factor_i$ is proportion of total demand *d* applied to node *i*.

Coefficients have been determined by a least squares method. The method of least squares is often applied in statistical contexts. Least squares can be interpreted as a method of fitting data. The best fit in the least-squares sense is that instance of the

model for which the sum of squared residuals has its least value, a residual being the difference between an observed value and the value given by the model.

$$\sum_{1}^{n}\left[q-\left(d+c_1 p^{0.5}+c_2 p^{1.5}\right)\right]^2 \rightarrow \min \qquad (4.2)$$

where q - measured inlet flow

p - measured inlet pressure including AZNP correction

n - the number of measurements

and coefficients $d \geq 0$, $c_1 \geq 0$, $c_2 \geq 0$, because the water cannot enter a network through leakages and cracks.

The suitability of a linear relationship between leakage and pressure has also been investigated. Coefficients and the root-mean square error for seven DMAs for the linear model and the three-term model are shown in Table 4.1 below.

Table 4.1 Coefficients and RMS error for seven DMAs

DMA	Num of measu-rements	Inlet flow linear model $q = d + cp$			Inlet flow three term model $q = d + c_1 p^{0.5} + c_2 p^{1.5}$			
	n	d	c	The root-mean square error	c_2	c_1	d	The root-mean square error
Ashbury	1255	3.517943	0.081812	1.374553	0.0053	0	5.8816	1.034893
Buscot	1288	0.80247	0.003861	3.042027	0.0058	0	0.2311	1.66811
Down Ampney	1332	6.106428	0.32282	1.506813	0.0348	0	10.3239	1.171579
Cirencester	1613	5.942036	0.397712	5.331473	0.0387	0	11.8231	2.777965
Farringdon	1593	1.594479	0.3	9.292015	0.0519	0	0	2.667019
Priorsfield	1536	6.934208	0.305279	5.854758	0.0244	0.9412	6.8909	2.174472
Shellingford	1458	4.747	0.229928	2.641694	0.0119	1.6835	0	1.777046

The root-mean square error in the three-term model, observed in the table, is smaller than the error from the linear model, therefore the three-term model can be used in the subsequent considerations. For the time being it is impossible to comment on the values of the coefficients in the table without further research.

4.2 Simulating leakage including background leakage and bursts

The general purpose environment GAMS (Brooke, Kendrick, & Meeraus 1992) was used for simulating leakages for this stage of the research. The water network model simulation program realized in GAMS was provided by Water Software System research group (DMU). A GAMS simulation model provides freedom to model different scenarios that cannot be tested in a physical network. The effects of bursts on flows and heads throughout the system can be observed and sensitive indicators of the presence of bursts can be derived by using the GAMS simulation model. The pipe equation is represented by the Darcy-Weisbach (Colebrook –White) pipe formula (Streeter and Wylie 1998).

The Frizinghall network shown Fig. 4.2 is used for the experiments. In this network there is one inlet node (node 5), by which water enters the network, and some demands at nodes 20, 30, 40, 50, 65, 75, 80, 95, 105, 110, 115, 120, 125, 140, 145, 165, 175, 180, 195, 225, 226, 230, 241, 250, 255, 265, 305, 310, 320, 335, 345, 350, 360, 365, 375, 380, 385 (Appendix B).

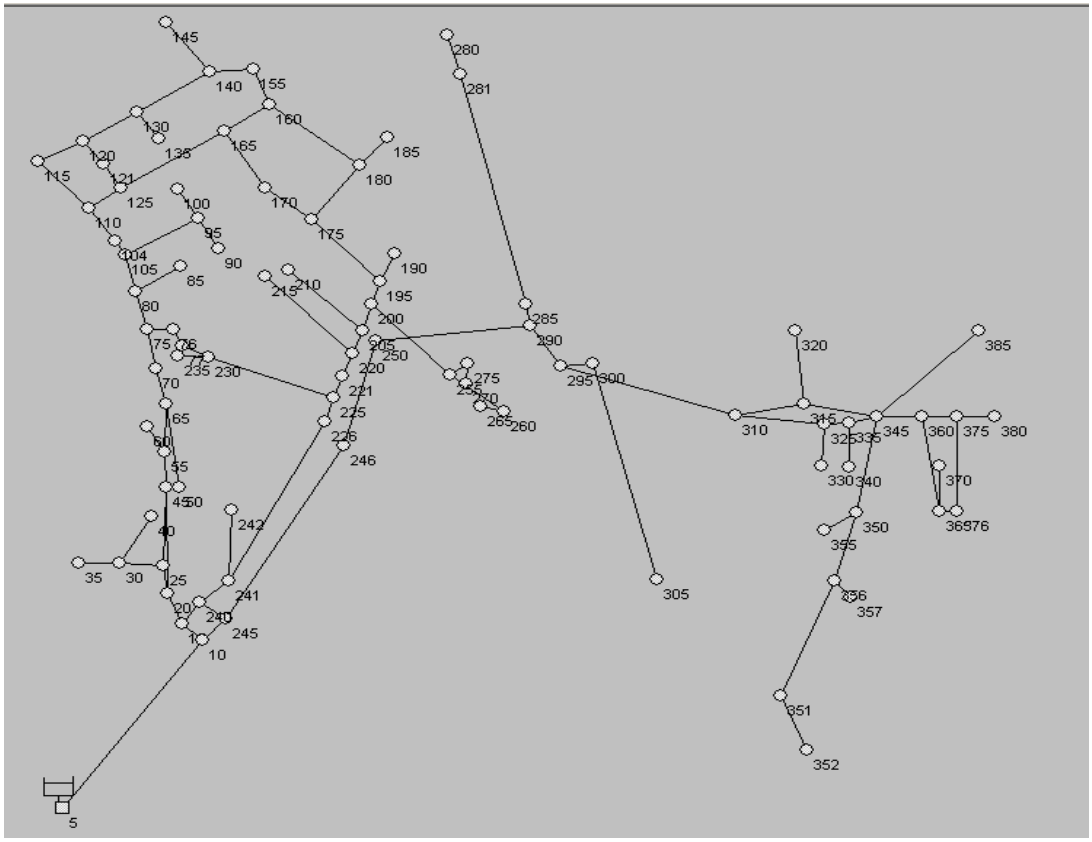

Fig. 4.2 Frizinghall network

The input parameters of the simulation program were: inlet pressure, value of total demand (in l/s), value of background leakage coefficient, and location of background leakages, and value of burst coefficient and location of burst. The values of inlet flow and flow and head at all nodes were output parameters of the simulation program.

4.2.1 Background leakage estimation

Initially, only background leakage was introduced to the model of the network and simulations were carried out for seven different nodal values of total background leakage coefficient to generate the 'experimental' data. In each experiment the inlet pressure was changed stepwise and the inlet flow obtained. The value of total demand was set to 1.798 litres/second. From the generated data the coefficients of the inlet flow model were estimated using a least square method and compared with the set values (input simulation values).

The inlet pressure was changed from 50 to 102 metres in steps of 4 metres. This was repeated for each value of the total background leakage coefficient.

The nodes with background leakage were: 20, 30, 40, 50, 65, 75, 80, 95, 105, 110, 115, 120, 125, 140, 145, 165, 175, 180, 195, 225, 226, 230, 241, 250, 255, 265, 320, 335, 345, 350, 360, 365, 375, 380, 385.

The inlet flow model equation (4.1) was adapted by removing the second term (the burst term) and assuming that pressure p_2 represents the DMA inlet pressure. Comparison of the set and estimated values of the total background leakage coefficients are given in Table 4.2 below.

Table 4.2 Background leakage coefficients (for inlet pressure)

Set value of background leakage coefficient for every node (for seven experiments)						
0.000309	0.00144	0.00288	0.0144	0.0308571	0.0514286	0.085371
Set value of total background leakage coefficient (35 nodes * set value)						
0.0108	0.0504	0.1008	0.504	1.08	1.8	2.988
Estimated value of total background leakage coefficient (for seven experiments)						
0.03502	0.152592	0.287413	0.927504	1.409213	1.808084	2.28326

The values of the inlet flow for each experiment can be found by substituting obtained coefficients into the IFM equation. The total flow is the same for both the set up and the estimated values but demand flow and background leakage flow differ from the estimated ones. Because these differences have the same magnitude the total flow is the same. The coefficients of background leakage are not linearly correlated as illustrated in Fig. 4.3.

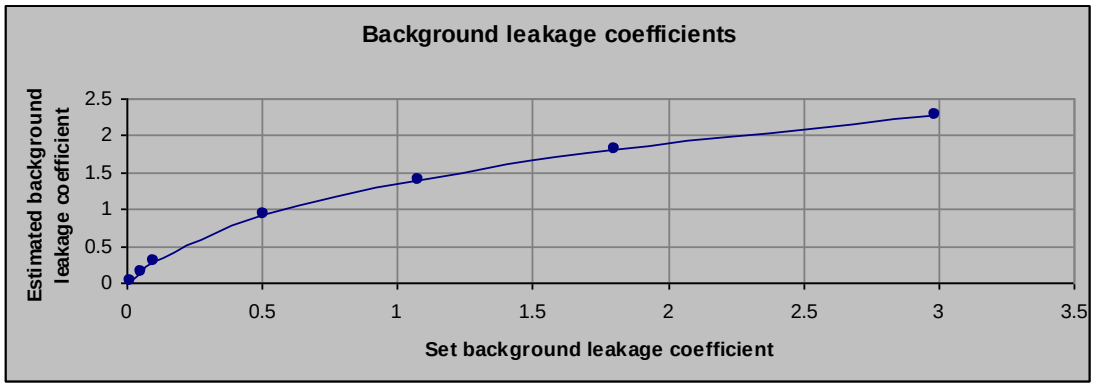

Fig. 4.3 Estimated background leakage coefficients using inlet pressure

This outcome can be explained because of an unsuitable choice of pressure variable for the inlet flow model (IFM). In this model the inlet pressure was used to represent the

pressure at all background leakage nodes, it would be better to use the average zonal night pressure p_{AZNP} defined as

$$p_{AZNP} = \frac{\sum_{i \in Nodes} p_i \cdot Demand\_Allocation\_Factor_i}{\sum_{i \in Nodes} Demand\_Allocation\_Factor_i} \qquad (4.3)$$

where p_i is pressure at each node of network with demand and $Demand\_Allocation\_Factor_i$ is proportion of total demand d applied to node i.

Let's test this hypothesis using the simulation model developed in GAMS; $Demand\_Allocation\_Factors$ and inlet pressure are input data. The inlet pressure was changed from 52 to 96 metres in steps of 4 metres. The pressures p_i are received from the simulation program. The average zonal night pressure is calculated from equation 4.3:

Inlet Pressure (metres)	52	56	60	64	68	72	76	80	84	88	92	96
AZNP (metres)	101.60	105.59	109.58	113.58	117.57	121.56	125.55	129.55	133.54	137.53	141.52	145.52

The results are depicted in Figure 4.4.

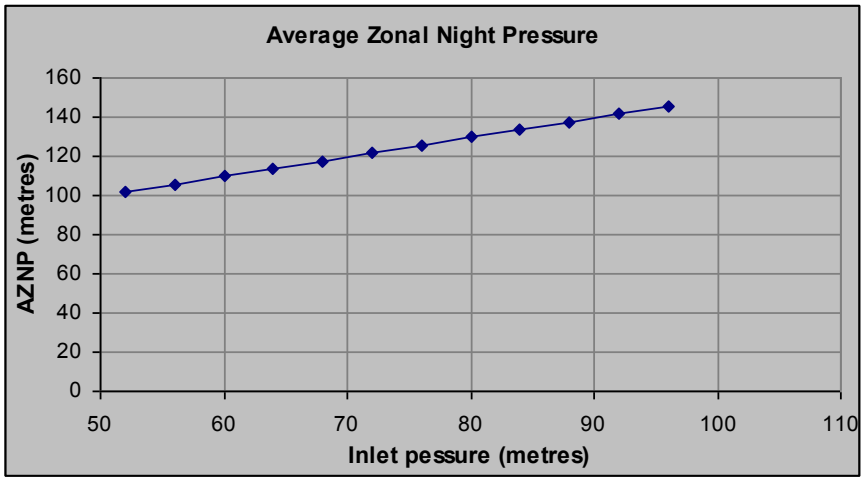

Fig. 4.4 Relationship between AZNP and inlet pressure

It can be observed from the chart that this is an affined relationship and can be described by a straight line equation:

$$p_{AZP} = a + b \cdot p_{input}$$

where *a* and *b* are coefficients, which can be calculated by regression analysis, and for the selected network:

a = 49.7 b= 0.998078 with the RMS error = 0.00000721

The experiment with background leakage only and step changing inlet pressure was repeated again but this time the average zonal night pressure was used in the IFM. The following results shown in Table 4.3 were obtained:

Table 4.3 Background leakage coefficients (for AZNP)

Set value of Background leakage coefficient for every node (for seven experiments)						
0.0003	0.0014	0.0028	0.014	0.03	0.05	0.083
Set value of total background leakage coefficient (35 nodes * set value)						
0.0108	0.0504	0.1008	0.504	1.08	1.8	2.988
Estimated value of total background leakage coefficient (for seven experiments)						
0.01019	0.04724	0.09317	0.42703	0.86817	1.39947	2.26402

Coefficients of the background leakage are linearly correlated (Fig. 4.5)

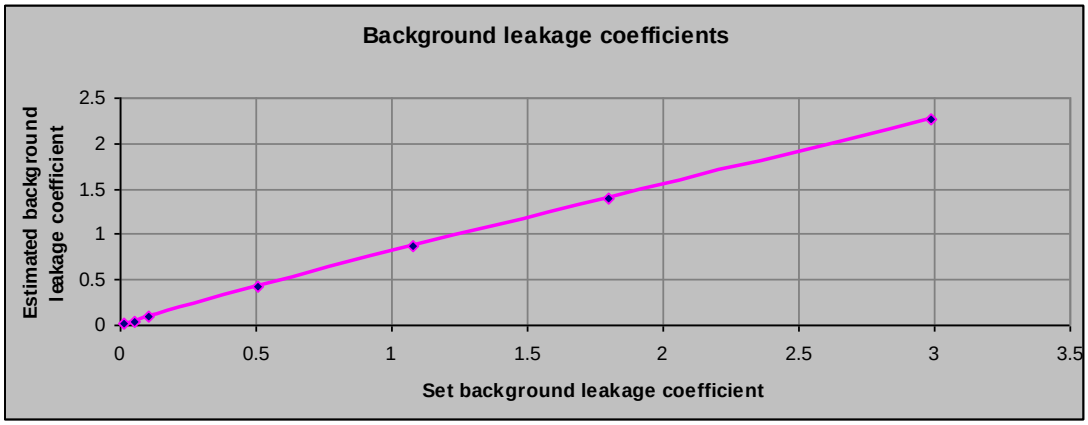

Fig. 4.5 Background leakage coefficient using AZNP.

By substituting the obtained coefficients in the equation of the IFM the flows for each experiment are determined. The total flow, flow of the background leakage and the demand coincides with the given ones (Fig. 4.6).

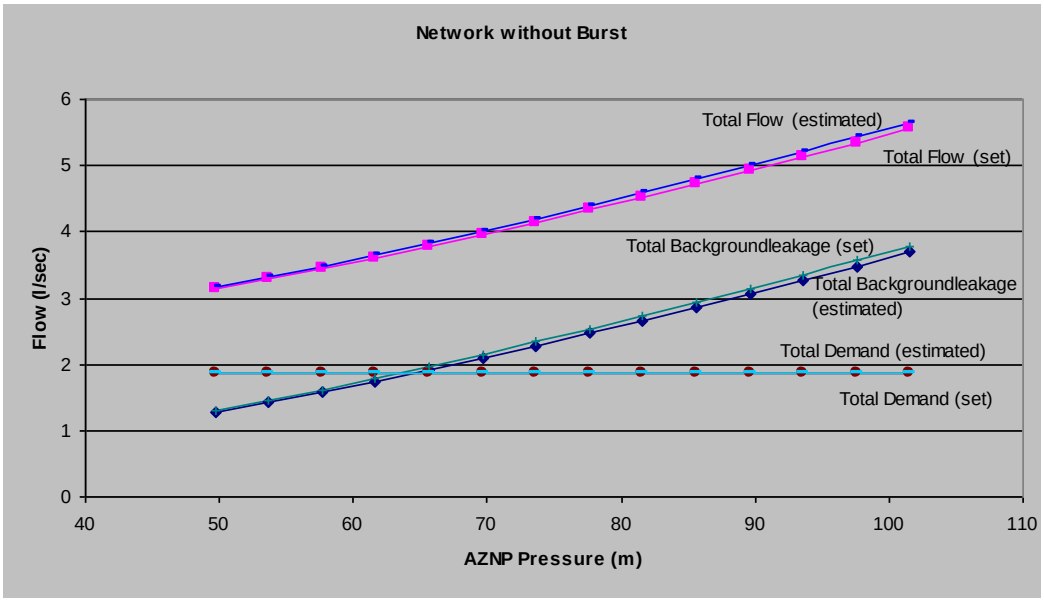

Fig. 4.6 Comparison of estimated and actual (set) flows

The outcome of the experiment proves that it is better to use the Average Zone Night Pressure for p_2 in IFM (equation 4.1) to represent background leakage.

4.2.2 Burst estimation

Now it is time to focus on an investigation of properties of the leakage flow caused by bursts. It is necessary to test the hypothesis that the burst is represented by the power term $c_1 p^{0.5}$, and consider which pressure should be used, inlet pressure, AZNP as in the case of the background leakage or something else. With the help of the GAMS simulation program the network from Fig.4.2, with the known demand *(d=1.736 l/s)* and with a burst at node 246 but without the background leakage, was simulated.

Eight different values of the burst coefficient were selected and, for each value of burst coefficient, the inlet pressure was changed from 50 to 98 metres stepwise and the inlet flow was recorded.

The inlet flow model is reduced to two terms:

$$q = d + c_1 p_1^{0.5}$$

where q is the inlet flow, p_1 is the inlet pressure and d is the demand value.

Comparison of the set and estimated by the method of least square values of the burst coefficients is presented below in Table 4.4 and in Fig.4.7.

Table 4.4 Burst coefficients

Set value of burst coefficient (for eight experiments)							
0	0.02651	0.13245	0.26447	0.39561	0.65438	1.26551	2.28602
Estimated value of burst coefficient using least square analysis of simulated results							
0	0.01	0.05	0.1	0.15	0.25	0.5	1

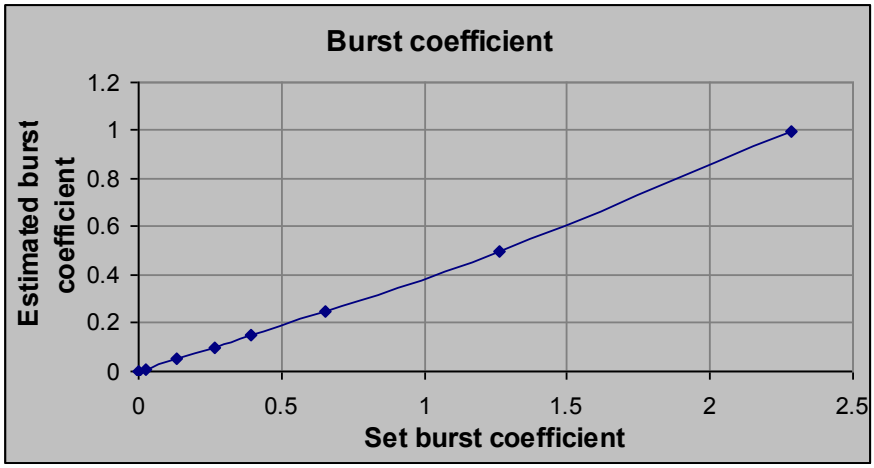

Fig. 4.7 Estimated burst coefficients using inlet pressure

One can note that at small values of the coefficient (that correspond to a burst flow of 2-4 litres/seconds) the relationship is linear but as the burst flow increases the burst flow is underestimated.

The comparison between simulated (set) and estimated flows is presented in Fig.4.8, it is worth noticing that although the estimated burst coefficients are not accurate the corresponding flow components are estimated accurately.

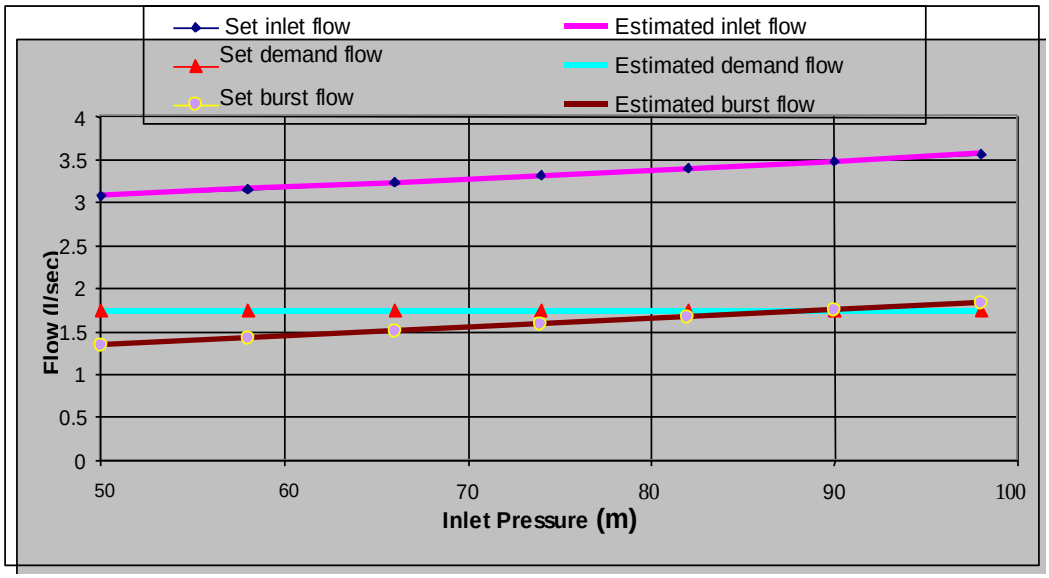

Fig. 4.8 Experiment results

Table 4.5 Simulated (set) and estimated flows

Set inlet flow (l/sec)	3.571	3.486	3.403	3.32	3.24	3.16	3.082
Estimated inlet flow (l/sec)	3.57	3.49	3.40	3.32	3.24	3.16	3.08
Set burst flow (l/sec)	1.836	1.750	1.666	1.584	1.504	1.425	1.346
Estimated burst flow (l/sec)	1.84	1.75	1.67	1.58	1.50	1.42	1.35
Set demand flow (l/sec)	1.736	1.736	1.736	1.736	1.736	1.736	1.736
Estimated demand flow (l/sec)	1.74	1.74	1.74	1.74	1.74	1.74	1.74

The outcomes of the repeated experiment using AZNP for calculations are not very successful either. The set of simulated and estimated coefficients of burst have a nonlinear relationship presented in Fig. 4.9. The demand flow *d* is now bigger than the pre-set demand. This means that the burst has a constant component, which in the estimation model now contributes to the demand.

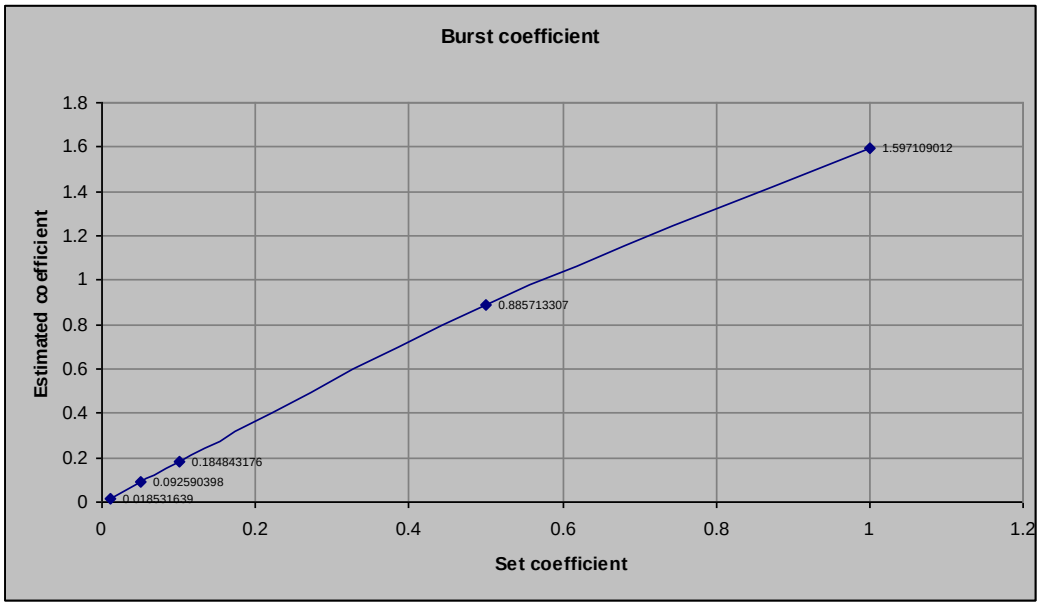

Fig. 4.9 Estimated burst coefficients using AZNP pressure

To check again the use of the inlet pressure in the IFM for the burst term, the previous experiment is repeated with the burst at node 352. The inlet pressures, coefficient of the burst and the demand remain the same. The estimated coefficient differs significantly from the simulation (pre-set) one (Fig.4.10).

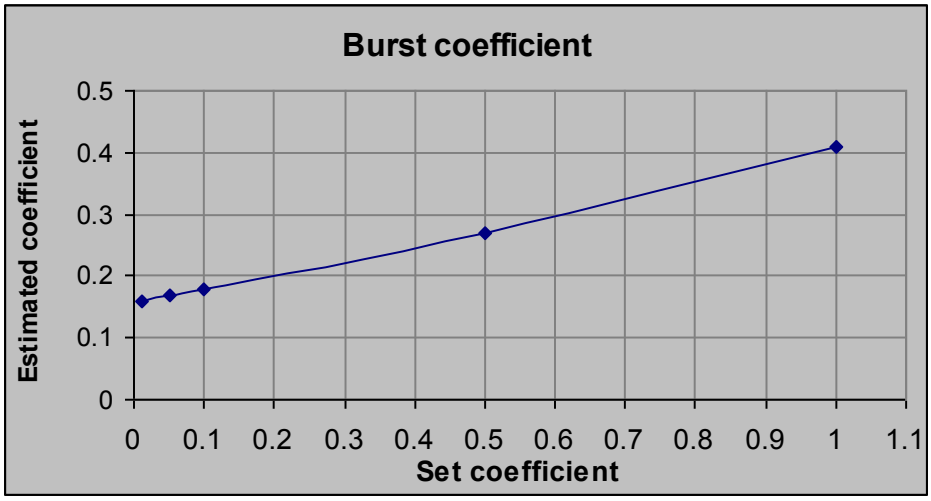

Fig. 4.10 Estimated burst coefficients using inlet pressure (burst at node 352)

Although the estimated total inlet flow is equal to the simulated one, the estimated demand is higher than that specified in the simulation program and consequently the estimated burst leakage flow is smaller than the simulated one. This implies, that the use

of the inlet pressure in the burst term in the IFM does not necessarily lead to an accurate representation of the real burst flow.

In the first experiment the results with the inlet pressure shown in Fig.4.8 are relatively good, because the burst node 246 is very near to the inlet node and has a comparable value to the burst node pressure.

Repeating the experiment with AZNP instead of the inlet pressure gives the similar negative outcome, but with a smaller error.

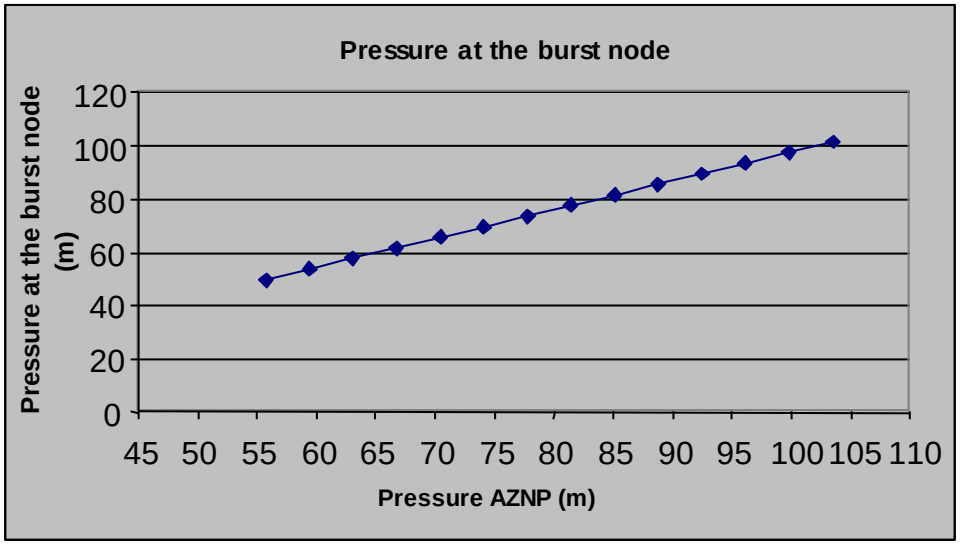

Fig. 4.11 Pressure at the node of the burst

Further investigation of pressures in a network has indicated a linear relationship between pressure at a node and AZNP (Fig. 4.11)

$p_{node} = a + b \cdot p_{AZNP}$ where a and b are the regression coefficients.

In fact, the burst term should be represented by the pressure at the burst as it is indicated in the equation below but unfortunately the burst node and consequently the burst pressure are not known in advance

$$q = d + c_1 p_{burst\_node}^{0.5} = d + c_1 \cdot (a + b \cdot p_{AZNP})^{0.5}$$

where a depends on the elevation of the burst node.

The data described by the model above can be approximated by the different model, which uses AZNP

$$q = \hat{d} + \hat{c}_1 \cdot p_{AZNP}^{0.5}, \qquad (4.4)$$

this results in the overestimation of the demands $\hat{d} \geq d$ due to the contribution of the constant a.

Let's apply the three-term IFM to the network where the background leakage and a burst are present:

$$q = \hat{d} + \hat{c}_1 \cdot p_{AZNP}^{0.5} + c_2 \cdot p_{AZNP}^{1.5} \quad (4.5)$$

The arrangements are: the inlet pressure changes from 50 to 102 metres in steps of 4 metres. There is a burst at node 352. The burst coefficient for the simulation is set to 0.5 corresponding to the burst flow of 3-4*l/sec*. The background leakage is present at the following nodes 20, 30, 40, 50, 65, 75, 80, 95, 105, 110, 115, 120, 125, 140, 145, 165, 175, 180, 195, 225, 226, 230, 241, 250, 255, 265, 320, 335, 345, 350, 360, 365, 375, 380, 385. The aggregate coefficient of the background leakage is set up as 0.0036, corresponding to the background leakage flow of 2-3*l/sec* and finally the demand is equal to 0.852*l/sec.*

The network is simulated using the GAMS program and the inlet flow is recorded for each value of the inlet pressure. The AZNP is calculated for the given inlet pressure data. The coefficients *a* and *b* of the equation $p_{AZNP} = a + b \cdot p_{input}$ were known from the previous simulation experiment in Section 4.2.1.

Coefficients d, c_1, c_2 are calculated by the method of least squares and are collected in Table 4.6.

Table 4.6 Estimated coefficients (for one burst)

Coefficients of model	Set coefficients	Estimated coefficients
d	0.852	1.6896
c_1	0.5	0.4029
c_2	0.0036	0.0038

The calculated coefficients are substituted into the three-term model and flows for each step of the inlet pressure are obtained. The following graphs depicted in Fig. 4.12 are plotted from this experiment.

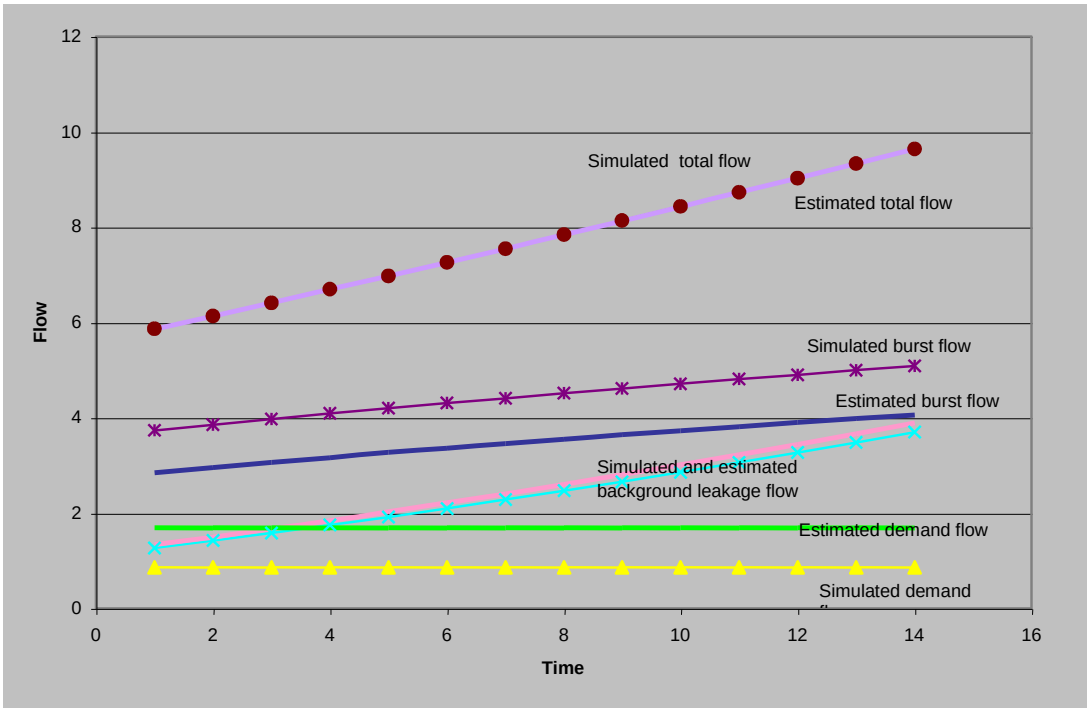

Fig. 4.12 Obtained results

It can be observed from the charts in Fig.4.12 that the extra component of the burst flow is added to the demand flow, but the background leakage flow is determined precisely.

If there is more than one burst in the network the coefficients of bursts are added together.

$$q = d + c_{1,burst\_1} p_{AZNP}^{0.5} + c_{1,burst\_2} p_{AZNP}^{0.5} + c_2 p_{AZNP}^{1.5} = d + c_1 p_{AZNP}^{0.5} + c_2 p_{AZNP}^{1.5}$$

The formula above is applied to a network with two bursts, both with $c_1=0.5$. The experiment is also carried out under the same conditions as the previous experiment with one burst and the corresponding IFM coefficients are obtained using the least-square method:

Table 4.7 Estimated coefficients (for two bursts)

Coefficients of model	Set coefficients	For two bursts	For one burst
d	0.852	2.535	1.6896
c_1	two bursts both with 0.5	0.8246	0.4029
c_2	0.0036	0.0039	0.0038

It follows from the Table 4.7 that the coefficient of the bursts has increased twice and the coefficient of background leakage has remained the same. The true value of the demand is equal to 0.852 so it can be observed that the constant element from the bursts contributes again to the demand:

- for one burst

$$d = demand + burst\_constant \Rightarrow burst\_constant = d - demand = \\ = 1.6896 - 0.852 = 0.8376$$

- for two equal bursts

$$d = demand + first\_burst\_constant + second\_burst\_constant = \\ = 0.852 + 0.8376 + 0.8376 = 2.53$$

More experiments have been carried out with two bursts and then three bursts and the similar pattern has been confirmed.

4.2.3 Burst leakage presence indication.

The real value of the burst flow is the sum of the 'constant' part of the burst flow (resulting from the difference between the pressure at the burst node and the AZNP) and variable part of the burst flow. This can be interpreted that $\hat{c}_1 > 0$ (equation 4.5) is a good indicator of a burst presence and the reminder of this section is dedicated to investigating this hypothesis. The following multiple squared correlation coefficient R^2 (Borovkov 1976) will be used,

$$R^2 = \frac{\sum_n (Flow\_estimated - Flow\_estimated\_average)^2}{\sum_n (Flow\_data - Flow\_data\_average)^2}$$

where R^2 is a number from 0 to 1, to assess how well the estimated values match the actual data,

n - number of measurements,

$Flow\_estimated\_average = \frac{\sum_n Flow\_estimated}{n}$ - the average value of estimated flow values,

$Flow\_data\_average = \frac{\sum_{n} Flow\_data}{n}$ - the average value of simulated (actual) flow values.

The degree of usefulness of the $\hat{c}_1 \cdot p_{AZNP}^{0.5}$ term in the IFM as an indicator of the burst presence can be assessed with the help of this criterion. The term is more indicative for R^2 being close to 1.

The network without bursts is simulated by applying 14 steps of the inlet pressure and the IFM coefficients are determined by the method of the least squares. The results of simulation are presented in Table 4.8 and the estimated coefficients obtained by the least-square method are in Table 4.9.

Table 4.8 Results of simulation (network without burst)

Total boundary flow l/sec	2.056	2.204	2.358	2.517	2.682	2.852	3.027	3.207	3.392	3.581	3.775	3.974	4.176	4.383
Pressure AZNP	48.89	52.84	56.79	60.74	64.69	68.63	72.58	76.52	80.46	84.41	88.35	92.29	96.23	100.17

Table 4.9 The estimated coefficients (network without burst)

	Estimated coefficients	Simulated (set) coefficients
$\hat{d}$	0.84976314	0.85
$\hat{c}_1$	0	0
c_2	0.00352307	0.0035

Coefficient $\hat{c}_1$ is equal to zero, the total flow is calculated from the IFM as the sum of the demand and the background leakage flow $q = \hat{d} + c_2 p_{AZNP}^{1.5}$ and is displayed in Table 4.10.

Table 4.10 The result of calculation (network without burst)

Pressure AZNP	48.89	52.84	56.79	60.74	64.69	68.63	72.58	76.52	80.46	84.41	88.35	92.29	96.23	100.17
Estimated boundary flow	2.05	2.20	2.36	2.52	2.68	2.85	3.03	3.21	3.39	3.58	3.78	3.97	4.18	4.38

The average value of the simulated flow is $\frac{\sum_{1}^{14} Flow\_data}{14}$ =3.156

and the average value of the estimated flow is $\frac{\sum_{1}^{14} Flow\_estimated}{14}$ =3.1557

The parameter R^2 is determined using the previously defined formula as $R^2 = 0.99$ which is a very high value.

A similar experiment is repeated with presence of a burst. In the first stage the burst term is removed from the IFM $q = \hat{d} + c_2 p_{AZP}^{1.5}$ and the following results are obtained. The flows are presented in Table 4.11 and the IFM coefficients in Table 4.12.

Table 4.11 The obtained results (network with burst)

Pressure AZNP	48.89	52.84	56.79	60.74	64.69	68.63	72.58	76.52	80.46	84.41	88.35	92.29	96.23	100.17
Total boundary flow l/sec	16.25	16.86	17.46	18.05	18.63	19.21	19.79	20.36	20.92	21.49	22.05	22.60	23.16	23.71
Calculated boundary flow l/sec	16.53	17.00	17.50	18.01	18.53	19.07	19.63	20.20	20.79	21.39	22.01	22.64	23.28	23.94

Table 4.12 The estimated coefficients (network with burst)

	Estimated coefficients	Simulated (set) coefficients
$\hat{d}$	12.696134	0.85
$\hat{c}_1$	0	2
c_2	0.011216	0.0035

Furthermore, the parameter R^2 is calculated as $R^2=0.8$ indicating that the accuracy of the flow approximation has significantly decreased. Then, the coefficients of the IMF are recalculated including the burst term.

$q = \hat{d} + \hat{c}_1 \cdot p_{AZP}^{0.5} + c_2 \cdot p_{AZP}^{1.5}$

The IMF coefficients and the corresponding flows are given in Table 4.13 and Table 4.14 respectively.

Table 4.13 IFM coefficients

	Estimated coefficients	Simulated (set) coefficients
$\hat{d}$	3.9142	0.85
$\hat{c}_1$	1.5604	2
c_2	0.0042	0.0035

Table 4.14 The obtained results

Pressure AZNP	48,89	52,84	56,79	60,74	64,69	68,63	72,58	76,52	80,46	84,41	88,35	92,29	96,23	100,17
Simulated total boundary flow l/sec	16,25	16,86	17,46	18,05	18,63	19,21	19,79	20,36	20,92	21,49	22,05	22,60	23,16	23,71
Estimated boundary flow l/sec	16,26	16,87	17,47	18,06	18,65	19,23	19,80	20,38	20,94	21,51	22,07	22,63	23,19	23,74

The parameter R^2 is calculated as $R^2=0.99999$ so the accuracy of approximation is very high. The standard deviation of the estimated flow for both cases (with and without the burst term) is given below:

- a model without the burst term

$$\delta^2 = \frac{\sum_n (Flow\_estimated - Flow\_data)^2}{n} = 0.0196591,\ \delta = \sqrt{\delta^2} = 0.14021.$$

- a model with the burst term

$$\delta^2 = \frac{\sum_n (Flow\_estimated - Flow\_data)^2}{n} = 0.000388205\ ,\ \delta = \sqrt{\delta^2} = 0.019702$$

Similar experiments were performed with a burst of different magnitude and at different locations and the obtained results have been very similar to that presented above. From a practical point of view the hypothesis that the coefficient $\hat{c}_1$ can be used as an indicator of burst presence has been confirmed.

4.2.4 Demand estimation

If the demand is known, then it is possible to evaluate the magnitude of the burst flow from $q_{burst} = \hat{d} - d + \hat{c}_1 \cdot p_{AZNP}^{0.5}$. If a DMA has no bursts and only the background leakage it is possible to evaluate the instantaneous demand flow from the formula $d = q_{in} - q_{background} = q_{in} - c_2 p_{AZNP}^{1.5}$.

The demand can be calculated at different time instances and a deeper statistical analysis of this demand can be carried out.

Each field test has a series of pressure steps thirty minutes apart. During each step a portion of the total flow is the demand, which is pressure independent and is random due to numerous customers in the DMA using random volumes of water at random time intervals (Buchberger and Wu 1995). It is assumed here that the demand has a normal distribution, the assumption often used in existing literature, e.g. by Pallavicini & Magini (2007). The normal distribution law is characterized by the exponential formula:

$f(x) = \frac{1}{\delta\sqrt{2\pi}} \cdot e^{-\frac{(x-m)^2}{2\delta^2}}$ where m= expected value (mean) and δ=standard deviation.

There are data available from a number of FAVOR tests carried out for physical DMAs without bursts. For instance, for the first section of the Cirencester area the obtained frequencies are shown in Table 4.15.

Table 4.15 Frequency of occurrence of the demand

Demand (x_I) [l/s]	6	7	8	9	10	11	12	13	14	15	16	17	18
Frequency of occurrence of the demand (n_I)	0	11	0	0	0	202	0	0	99	86	0	0	12

The experimental probability $p(x_i)$ for each value of the demand is determined from the formula $p(x_i) = \frac{n_i}{\sum_i n_i}$ and recorded in Table 4.16.

Table 4.16 The probability of occurrence of a demand

Demand (x_i) [l/s]	6	7	8	9	10	11	12	13	14	15	16	17	18
Probability $p(x_i)$	0	0.027	0	0	0	0.49	0	0	0.24	0.21	0	0	0.03

The estimates for the mean and the standard deviation are $m = \sum_i x_i \cdot p(x_i) = 12.66$ and $\delta^2 = \sum_i p(x_i) \cdot (x_i - m)^2 = 4.634$, $\delta = \sqrt{\delta^2} = 2.15$ respectively.

The theoretical probability density *f(x)* can now be calculated for each demand level from the estimated model $f(x) = \frac{1}{\delta\sqrt{2\pi}} \cdot e^{-\frac{(x-m)^2}{2\delta^2}}$ as illustrated in Table 4.17.

Table 4.17 The probability density

Demand (x_i) [l/s]	6	7	8	9	10	11	12	13	14	15	16	17	18
Probability density $f(x_i)$	0.002	0.006	0.018	0.044	0.086	0.138	0.177	0.183	0.153	0.103	0.056	0.024	0.009

This estimated distribution for the demands is shown in Fig. 4.13 below and compared with the recorded data.

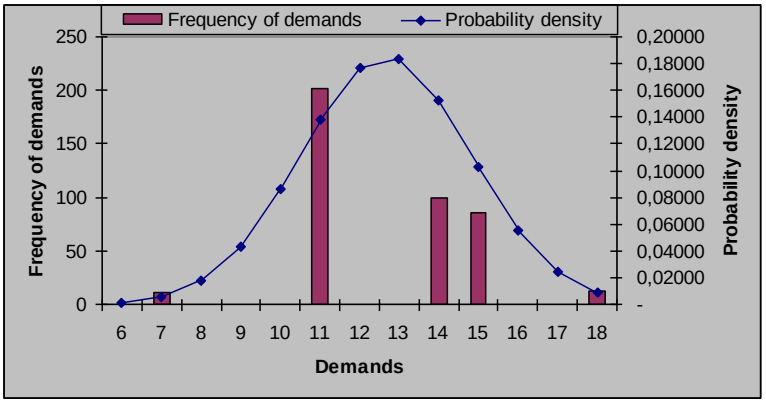

Fig. 4.13 The normal distribution for the demands

From the model distribution, the probability of the demands falling within a particular range can be calculated, examples are given in Table 4.18.

Table 4.18 The demand distribution

Probability (%)	Section of demand value	
99.7%	6.2	19.12
95%	8.3557	16.966
68%	10.5	14.8

Similar calculations have been performed for other water distribution zones. The density distribution for the second section of the Cirencester area is depicted in Fig.4.14.

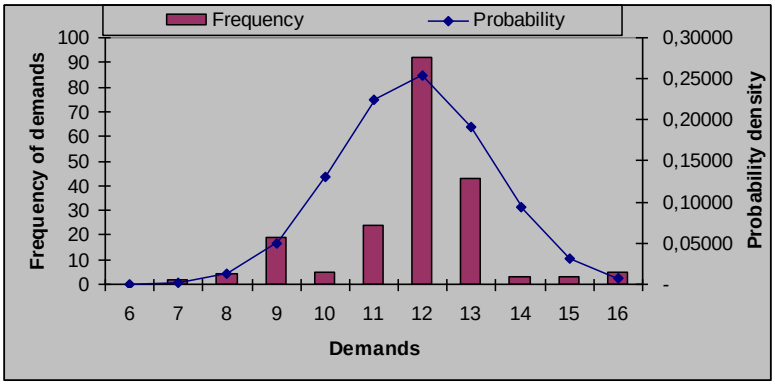

Fig. 4.14 Second section of Cirencester area

The frequency distribution for the Buscot area and the Down Ampney area are presented in Fig.4.15 and Fig.4.16 respectively.

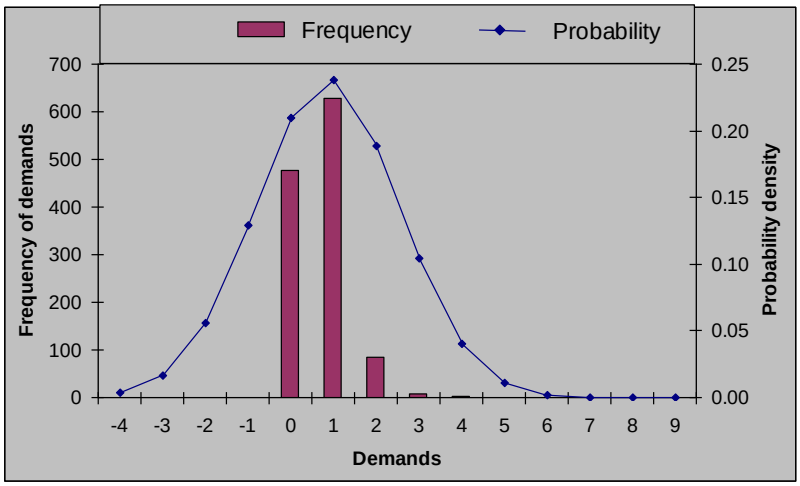

Fig. 4.15 Buscot area

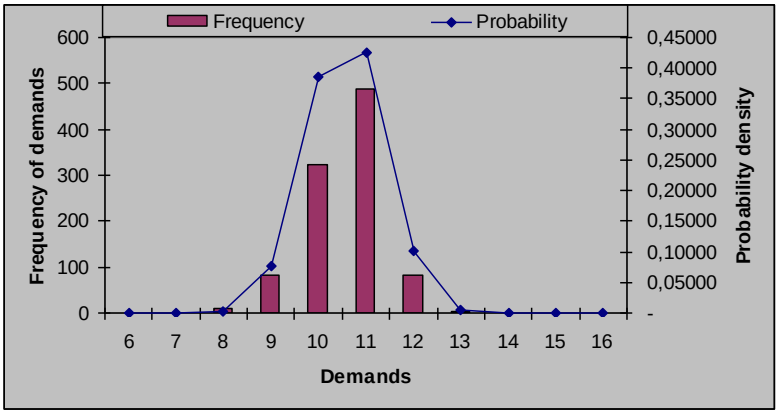

Fig. 4.16 Down Ampney area

The mean value of the demand in each case is equal to the demand value in the IFM.

4.3 Summary

The following conclusions can be made resulting from the carried out research: Applying step pressure changes to a DMA input and monitoring boundary flows can be used to separate the three terms in the inlet flow: demand, the burst flow and the background leakage flow.

- Background leakage in a network can be accurately represented by a pressure dependent term where the Average Zone Night Pressure (AZNP) is raised to the power of 1.5.
- Burst flow is represented by a pressure dependent power term in which it is necessary to use the pressure at the burst node for accurate representation. The use of AZNP in this term creates an additional constant term which incorrectly increases the total demand term. It is impossible on the basis of input data only (inlet flow, inlet pressure and AZNP pressure) to find out precisely the burst size, but it is possible to discover its presence.
- The demand flow has random character with a normal distribution. The probability of a demand falling within a particular range and the demand distribution curves have been estimated from the experimental data. However, for the reasons mentioned in the previous point it is impossible to estimate the demand accurately using only input data (inlet flow and inlet pressure).

But applying step pressure changes to a DMA input and monitoring boundary flows (FAVOR test) only for the detection of the presence of leaks does not make sense. Many Water Companies successfully use the BABE test (WRc- UK Water Industry, 1994) for this purpose. That is why in order to solve the posed problem of identification of a burst size and its location it is necessary to continue the research.

5 Identification of a burst location

The main aim of this chapter is to formulate an identification procedure to estimate the burst coefficient (an equivalent burst area) and the burst location more precisely than is currently possible by other methods. This is a complementary approach to the traditional methods of acoustic monitoring and closing sections of the network and can assist water companies in their leakage management activities.

Two case studies are described in this chapter. The first one is based on numerical experiments where the data are generated from a simulation model of a DMA. This demonstrates the applicability of the method and its susceptibility to noise. In the course of carrying out numerical experiments it has been assumed that the burst exponent was 0.5. A number of field studies have shown that the exponent can be considerably larger than 0.5, and typically varies between 0.5 and 2.5 (Farley & Trow 2003, Van Zyl & Clayton 2005, Ulanicki, Prescott and May 2006). The proposed approach can be adapted to other burst exponent values and this topic is discussed in Chapter 5.4.

The second case study is based on data, obtained by S. Prescott (WSS) out of field experiments performed on a physical DMA.

It is worth recalling that the whole approach is based on an active identification experiment and allows detection of existing bursts, which is a significant advantage compared to other methods.

5.1 Determination of a burst size

The proposed experimental method is based on the FAVOR test, originally developed by May (1994). This involves adjusting the pressure at the inlet to a DMA and monitoring the corresponding changes in inlet flow. The recorded pressure/flow relationship can be used to separate the inlet flow into three components:

- Demand – assumed to be constant over the recording period (between 1am – 5am).
- Fixed area leakage – the leakage flow which is governed by the power law with the exponent of 0.5. This model is applicable for a reasonably large burst.
- Variable area leakage – the leakage flow is governed by the power law with the exponent of 1.5 due to changes in the effective leakage area caused by the

pressure changes. This applies to minor drips, dribbles and seepages through joints and connections often referred to as ‘background leakage’.

$$q = d + q_{burst} + q_{background} = d + c_1 p_i^{0.5} + \sum_j c_{2j} p_j^{1.5} \quad (5.1)$$

where

q	inlet flow
d	demand flow
q_{burst}	burst flow at node i
$q_{background}$	background leakages flow
c_1	the burst coefficient
p_i	pressure at the burst node
c_{2j}	background leakage coefficients
p_j	pressures at background leakages nodes

It is assumed that the demand flow does not depend on pressure variations in a DMA and the average value of demand is constant over the considered period between 1 am – 5 am. The total background leakage flow represents the sum of all separate background leaks in a network and it is possible to use a single (common) coefficient of the background leakage c_2 and the Average Zone Night Pressure p_{AZNP} to evaluate this flow as has been investigated in Chapter 4. However, as is known from Chapter 4 replacement of the pressure at the burst node by the inlet pressure or by the Average Zone Night Pressure leads to an underestimation of the burst size. This is why for accurate burst coefficient (burst flow) identification more measurements are required, for instance, pressure measurements at a number of internal nodes of the DMA. Extended FAVOR (e-FAVOR) test is where additionally pressure (head) at a number of selected internal nodes of a DMA is measured.

5.1.1 Sensitive nodes

It is impossible to monitor all nodes in a DMA due to economic and practical limitations, namely the number of loggers required and the availability of access points (hydrants) for measurements. It is therefore essential to use a comparatively low number

of loggers and place them at representative nodes so called ‘sensitive nodes’ which would allow for identifying the burst flow and the burst location.

The experiment described in Chapter 4.2.2 was revised as follows. The burst was at node 246 and the inlet pressure was used in the IFM to represent this burst with good results but only because the burst node was very close to the inlet.

Looking at the topology of this model, it was easy to observe that a change of pressure at one network node causes similar changes at the neighbourhood nodes. After further investigation of pressure distribution in the network with bursts present, it has been observed that some nodes which are on the path between the source and the burst react more to the bursts than other nodes, and such nodes can be called “sensitive nodes”. In the course of further experiments it has been found that if the pressure of the node, which is near to burst, was used for the calculation of the burst flow, instead of the pressure at the burst node, the error does not exceed 0.5%.

The procedure of finding sensitive nodes has been formalised and is presented below. Once the sensitive nodes have been identified from the model, pressure loggers can be placed at these nodes during the field experiment subject to hydrant availability.

One of the methods of determining sensitive nodes is splitting a network into homogenous areas and choosing a number of nodes inside each area. An area should contain nodes which are strongly hydraulically linked and have a similar reaction to a burst inside the area. The sensitive nodes can be selected by evaluating the root-mean-square deviation of the pressure p_i at each node reaction due to the bursts located at different points of the area, i.e. the most sensitive pressure node is selected for each burst node.

$$\sqrt{\frac{\sum_{1}^{n}\left(p_i - \frac{\sum_{1}^{n} p_i}{n}\right)^2}{(n-1)}} \rightarrow \max \qquad (5.2)$$

where

n number of burst locations

p_i pressure at node i

This method has some shortcomings. The choice of areas directly depends on the topology of a network and for each network the number of areas can be quite different.

The maximum of root-mean-square deviations, as the experiment has shown, are at the extremities of a network, and this may result in a not quite precise identification of bursts, which are in the centre of the network.

The other method of determining sensitive nodes has been developed by Prescott and Ulanicki (2006). They were guided by the idea that the placement of loggers is of paramount importance to ensure that as much information as possible about the network and its operation is collected during data collection. The technique is related to that proposed by Bush and Uber (1998) and uses the sensitivity matrix of the hydraulic model (Jacobian matrix) to determine how the pressure at potential measurement nodes is affected by a burst at any node across the network. This matrix has dimension *m*x*n*, where *m* is the number of potential pressure measurement points and *n* is the number of nodes in the network (possible burst location).

The sensitivity matrix can be calculated directly from the network equations (Chapter 3.1) and it is obtained directly from the simulator.

The algorithm of detection of sensitive nodes works as follows:

1. A network model is simulated and a sensitivity matrix constructed. The matrix has size $m \times n$ where *m* (e.g. 100) is the number of all potential measurement points (location of hydrants) and *n* (e.g. 530) is the number of nodes. The elements of this matrix are derivatives of the measured head at node *m* with respect to the area of a burst at node *n*.

The sensitivity matrix is given by

$$S = \begin{pmatrix} \frac{dh_1}{dc_1} & \frac{dh_2}{dc_1} & \cdots & \frac{dh_m}{dc_1} \\ \frac{dh_1}{dc_2} & \frac{dh_2}{dc_2} & \cdots & \frac{dh_m}{dc_2} \\ \cdots & \cdots & \cdots & \cdots \\ \frac{dh_1}{dc_n} & \frac{dh_2}{dc_n} & \cdots & \frac{dh_m}{dc_n} \end{pmatrix} \tag{5.3}$$

2. The desired number of measurement nodes is selected, which may depend for instance, on the number of available loggers (e.g. 20).
3. The location with the highest total sensitivity over all the network nodes is selected as a measurement point.

4. All nodes that are both within a given proximity, and within a given head difference, of the selected point are eliminated as possible measurement points. These rejected nodes are collated with the chosen measurement point to from a node group.
5. From the remaining available locations, the one with the highest total sensitivity over all the network nodes is selected as the next measurement point.
6. Steps 3, 4 & 5 are repeated until all measurement points are either used or discarded.
7. The network coverage is determined by setting the proximity and head difference limits at step 3. If the number of chosen nodes is different from the desired number, then these limits are adjusted accordingly and the process is repeated from step 2.

This procedure provides a list of measurement points, which ensure that all parts of the network have a measurement nearby. The algorithm has been implemented in MATLAB by Prescott and Ulanicki (2006) and subsequently has been used in the present research.

5.1.2 Determination of the IFM coefficients.

To corroborate the hypothesis, that from the additional measurements of pressure values at sensitive nodes of a network, it is possible to calculate with sufficient accuracy burst size, a number of numerical experiments have been carried out. To generate data, namely the values of the inlet flow and the pressure at sensitive nodes, a WDS simulation program specially developed by Prescott in the MATLAB package has been used (Prescott and Ulanicki 2006). This program has been implemented to provide more flexibility in performing numerical experiments, it is simple to use, includes pressure dependent leakage, has facilities for setting up different simulation scenarios and can be easily modified depending on the requirements of the experiments. There are other WDS simulation packages that could be used, such as, FINESSE (WSS 1999), EPANET (Rossman 2000) or the one which was implemented in GAMS (Brooke, Kendrick, & Meeraus 1992). All of them have some drawbacks, GAMS input and output data format is inconvenient for their further processing within the framework of

the present experiment. The other packages have the same disadvantage using their own data formats and additionally they don't model pressure dependent leakage: For carrying out the planned research experiments it is important to manipulate data easily as well as having the possibility of modifying the simulation algorithm at different stages of the experiments. In order to validate the simulation algorithm the program results have been compared with the results obtained from the previously used programs, the one implemented in GAMS and the FINESSE package.

A model of the Frizinghall network has been selected for validating the simulation program, the model which has already been available in the GAMS and in the FINESSE format. In order to validate the simulation results the same values of inlet pressure, demands and parameters of burst have been used by the three simulation programs. The testing has been carried out by changing parameters of the burst including size and location. Values of the pressure at nodes and values of the calculated inlet flow have been compared and they agree with good accuracy therefore the code has been accepted for further research.

Two DMAs with different characteristics, Ocker Hill and Shenstone, shown in Fig.5.1 and Fig.5.2 respectively have been chosen to investigate the benefits of more measurements being available. Node and element data for Ocker Hill are shown at Appendix C and for Shenstone are shown at Appendix D.

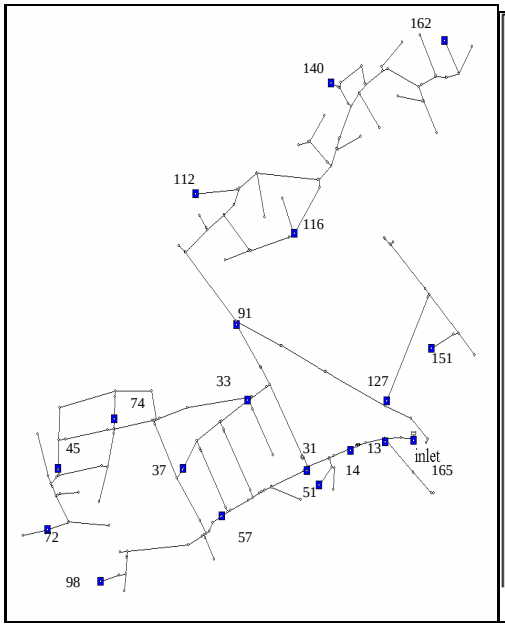

Fig. 5.1 Ocker Hill DMA schematic

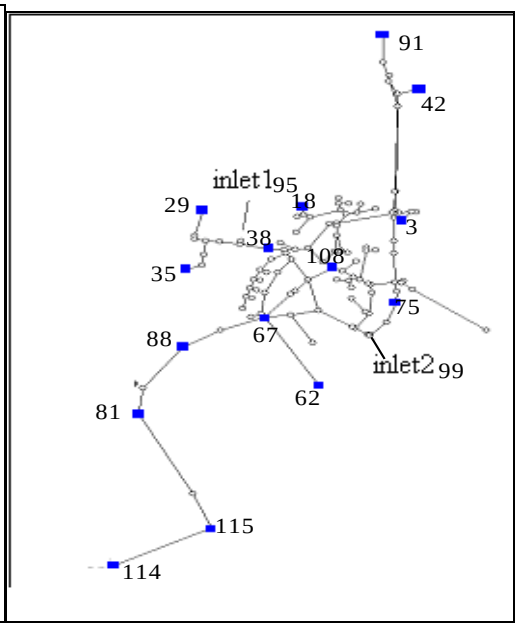

Fig. 5.2 Shenstone DMA schematic

Ocker Hill is a mostly domestic single-feed DMA supplying 1850 properties (1825 domestic, 25 commercial). The inlet is through a 6" Rollseal PRV and there is a disused PRV (4" Bermad) about 150m downstream of this. Shenstone is currently fed through two PRV inlets and supplies 1008 consumers (917 domestic, 91 commercial). The PRVs are 4" Bermad (St John) and 4" Rollseal (Lynn).

Sensitive nodes which have been obtained from the program described in Chapter 5.1.1 are marked in the DMA schematics. The pressure values at the marked nodes are used as initial indicators for calculating the burst size.

The set up of the experiment is described below:

- the inlet pressure is changed in steps in Ocker Hill from *18.94 m* to *50.47 m* (node 165) (Figure 5.3) and in Shenstone from *40.9 m* to *65.9 m* at Inlet 1 (node 95) and from *33.26 m* to *58.26 m* at Inlet 2 (node 99) (Figure 5.4).

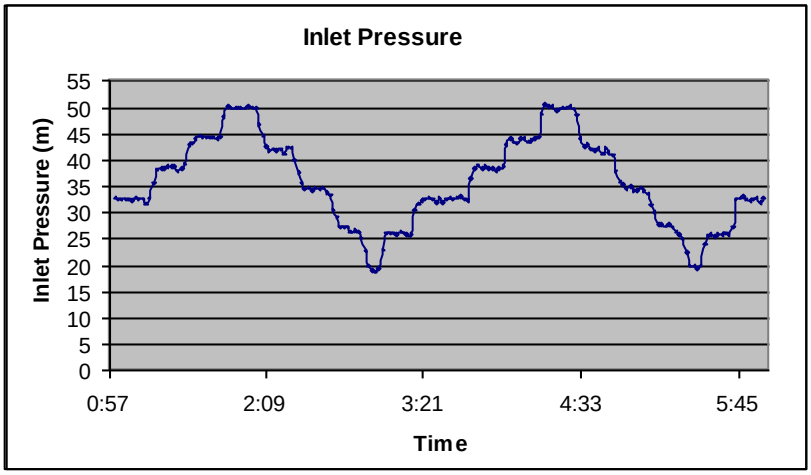

Fig. 5.3 Ocker Hill Inlet pressure.

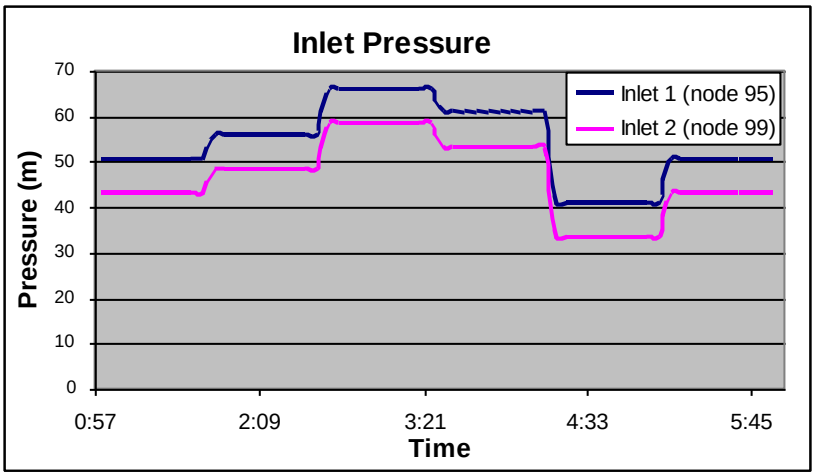

Fig. 5.4 Shenstone Inlet Pressure.

- The total demand is set within the limits from 2 to 4 *l/s* and distributed among the demand nodes in proportion to the number of consumers.
- The value of the total background leakage coefficient is set within the limits from 0 to 0.02 $l/s/m\sqrt{m}$ and random distributed among demand nodes of the network.
- The value of the burst coefficient is set within the limits from 0.2 to 0.5 $l/s/\sqrt{m}$ at a selected node of the network (a different burst coefficient value for each experiment).
- The selected values are entered into the network simulation program as input parameters. The observed output variables are: the total inlet flow and the pressure values at sensitive nodes of the network.
- Using the least squares method defined by Equation (4.2) the coefficients of the IFM are calculated, where the Average Zone Night Pressure is used in the background leakage term and pressure at a sensitive node is used to represent the burst term.

Some results of the experiments are given in Tables 5.1 and Table 5.2 below. The assumed demand and leak coefficients have been used in the simulation program to generate data whilst values of other variables have been estimated by the least squares method separately for each sensitive node.

Tables 5.1 and Table 5.2 are highlighted in yellow for the rows containing the largest values of the burst coefficients.

Table 5.1 Ocker Hill DMA calculated results

Set values: Demand flow = 4 l/s Burst coefficient at node 59 = 0.5 Total background leakage coefficient = 0.006525				Set values: Demand flow = 3 l/s Burst coefficient at node 141 = 0.37 Total background leakage coefficient = 0.01613			
Sensitive node	Demand flow	Burst coefficient	Background leakage coefficient	Sensitive node	Demand flow	Burst coefficient	Background leakage coefficient
165	4.058089	0.478309	0.006348	165	3.269832	0.305609	0.015863
37	3.80658	0.533508	0.006317	37	3.054222	0.3395	0.01604
45	4.175571	0.482332	0.006583	45	3.284707	0.30811	0.016206
91	3.341031	0.588109	0.006037	91	2.774552	0.377206	0.015912
13	4.465427	0.424752	0.006732	13	3.520386	0.269926	0.016199
31	4.451922	0.436145	0.006792	31	3.480549	0.278997	0.016327
51	4.172598	0.474184	0.006536	51	3.311559	0.303062	0.016131
72	4.380813	0.451963	0.006749	72	3.413617	0.28941	0.016309
74	3.989204	0.508653	0.006444	74	3.16787	0.324317	0.016121
151	3.38793	0.582463	0.006067	151	2.804813	0.373748	0.015939
98	4.148603	0.48765	0.00656	98	3.26764	0.31053	0.01619
162	2.850417	0.645874	0.005789	162	2.460468	0.415558	0.015782
14	4.454542	0.429002	0.006744	14	3.504668	0.273175	0.016233
127	3.76789	0.534242	0.006296	127	3.049977	0.342568	0.016081
140	3.005157	0.628148	0.005865	140	2.560595	0.404035	0.015829
112	3.177482	0.607924	0.005953	112	2.671365	0.390698	0.015879
33	3.711359	0.543539	0.006249	33	3.000119	0.346666	0.015998
57	4.267668	0.469709	0.006652	57	3.343708	0.299688	0.016246
116	2.792038	0.652447	0.00576	116	2.422476	0.419613	0.015762

Table 5.2 Shenstone DMA calculated results

Set values: Demand flow = 3.8 l/s Burst coefficient at node 98 = 0.2 Total background leakage coefficient = 0.002406				Set values: Demand flow = 2 l/s Burst coefficient at node 29 = 0.4 Total background leakage coefficient = 0			
Sensitive node	Demand flow	Burst coefficient	Background leakage coefficient	Sensitive node	Demand flow	Burst coefficient	Background leakage coefficient
95	3.236225	0.260706	0.002156	95	1.898237	0.401441	0
99	3.593154	0.222397	0.002291	99	2.425762	0.347515	0.000168
18	3.286523	0.257139	0.002183	18	1.935232	0.398993	0
91	3.440365	0.241165	0.002237	91	2.159354	0.377021	6.28E-05
42	3.437983	0.241385	0.002237	42	2.155902	0.377425	6.14E-05
3	3.147278	0.271559	0.002136	3	1.780036	0.40958	0
114	3.861908	0.190836	0.002427	114	2.815415	0.300705	0.00035
115	3.836697	0.194077	0.002413	115	2.776174	0.305679	0.00033
81	3.585625	0.224361	0.002296	81	2.385865	0.352186	0.000151
88	3.663002	0.215375	0.002329	88	2.506131	0.338376	0.000202
108	3.885163	0.188002	0.002439	108	2.850187	0.296228	0.000368
62	3.485124	0.235644	0.002254	62	2.230019	0.369494	8.91E-05
67	3.50643	0.233287	0.002263	67	2.263157	0.365866	0.000102
38	3.378799	0.246559	0.00221	38	2.07937	0.385877	3.27E-05
75	3.53757	0.229522	0.002272	75	2.325583	0.358828	0.000127
35	3.344375	0.249648	0.002194	35	2.043496	0.393223	1.69E-05
29	3.315828	0.252624	0.002184	29	2	0.4	0
Set values: Demand flow = 2 l/s Burst coefficient at node 67 = 0.2 Total background leakage coefficient = 0.00239				Set values: Demand flow = 4 l/s Burst coefficient at node 80 = 0.24 Total background leakage coefficient = 0.002216			
Sensitive node	Demand flow	Burst coefficient	Background leakage coefficient	Sensitive node	Demand flow	Burst coefficient	Background leakage coefficient
95	1.793312	0.220055	0.002301	95	3.65718	0.273442	0.002071
99	2.094677	0.18765	0.002415	99	4.031559	0.233282	0.002213
18	1.821443	0.217637	0.002321	18	3.716929	0.269285	0.002101
91	1.949842	0.204158	0.002365	91	3.876757	0.252068	0.002158
42	1.949871	0.204019	0.002367	42	3.874481	0.25247	0.002158
3	1.706537	0.229054	0.002284	3	3.570119	0.284088	0.002053
114	2.310342	0.162332	0.002525	114	4.321251	0.199451	0.002359
115	2.288989	0.165062	0.002514	115	4.294801	0.202867	0.002345
81	2.076462	0.190582	0.002416	81	4.031286	0.234779	0.002221
88	2.141971	0.183006	0.002444	88	4.11251	0.225311	0.002256
108	2.327863	0.15972	0.002534	108	4.345177	0.196395	0.002372
62	1.991531	0.200079	0.002381	62	3.925762	0.246665	0.002177
67	2.009589	0.198089	0.002388	67	3.948126	0.244182	0.002186
38	1.907202	0.208534	0.002346	38	3.81245	0.258423	0.00213
75	2.040366	0.193994	0.002396	75	3.975472	0.240345	0.002193
35	1.883588	0.210778	0.002333	35	3.771283	0.261826	0.002112
29	1.859498	0.213293	0.002325	29	3.741332	0.264948	0.002101

The estimated coefficients in the IFM are very close to the preset values. The average differences between the estimated and the preset values are as follows:

- The average difference for the demand flow is 5%, with the difference ranging from 0.1 to 0.5 litres/sec.
- The average difference for the burst coefficient is 7%, with the difference ranging from 0.01 to 0.06.
- The average difference for the background leakage coefficient is 2%, with the difference ranging from 0.00005 to 0.0003.

It is inexpedient to select average values, because the precision of burst size prediction can be low. A question arises as to what method should be used to select particular coefficient values from the obtained range?

The task is to find out an exact size of the burst. Taking inspiration from the algorithm by Prescott and Ulanicki (2006), describing the procedure of selecting sensitive nodes, the maximum value of the burst coefficient $c_1=max$ could be considered. When this suggestion is used the following estimation accuracies have been obtained:

- For the demand *d,* the average error of estimating the demand is 11%, and the absolute error increases with increasing demands, reaching about 0.2 litres/sec for the demand of 2 litres/sec and 1.2 litres/sec for the demand of 4 litres/sec.
- For the burst coefficient, the average error of estimating the burst coefficient c_1 is 12%, which corresponds to about 0.4 litres/sec (from 0.07 litres/sec up to 0.91 litres/sec depending on the set burst size).
- For the background leakage, the average error of estimating the background leakage coefficient c_2 is 5%, which corresponds to about 0.1 litres/sec.

The results are not encouraging. The maximum value of the burst coefficient corresponds to the assumption of the presence of a burst at the sensitive node. Where the sensitive node is located in an area of the network the most distant from the source (i.e. on the end of the branch where the burst has been preset). Also the difference between the inlet pressure and the end node pressure (in the presents of leaks) is rather small. Such distant sensitive nodes are: node 116 at the Ocker Hill DMA and node 3 at the Shenstone DMA. So the hypothesis of identifying the burst node through the biggest value of the burst coefficients is not correct. The solution can be found by applying a proper statistical analysis to the generated data.

5.1.3 Method of statistical analysis for determination of the burst size.

All the obtained coefficients (within the limits of a separate experiment) have been received by means of the least squares method and correspond to an average flow/pressure relationship. However, it is difficult to be satisfied with the flow values, i.e. the demand flow, the burst flow and the background leakage flow. Some of these flows depend on pressures at nodes of the network and, as a consequence, on the inlet pressure. The inlet flow is the result of summation of all the flows. The question of selecting from the set of obtained coefficient values which are close to true values should be answered by considering flows in the network and consequently the inlet flow.

Let's assume, that the inlet flow is described by means of a certain theoretical IFM:

$$q_i = d_i + c_{1i} p_i^{0.5} + c_{2i} p_{AZNP}^{1.5} \qquad (5.4)$$

where

q_i inlet flow

d_i demand

c_{1i} burst coefficient

c_{2i} background leakage coefficient

p_i pressure at a sensitive node

p_{AZNP} Average Zone Night Pressure

i identification number of sensitive nodes (number of a theoretical IFM)

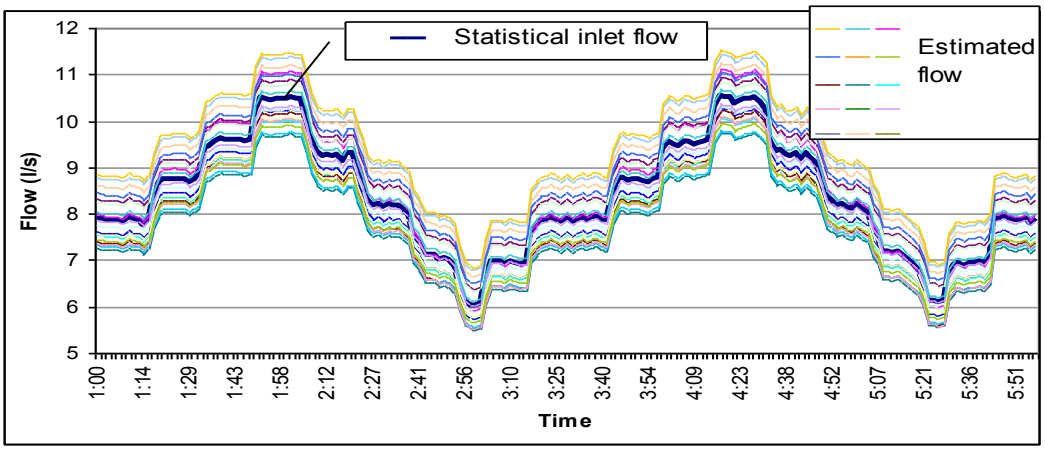

Fig. 5.5 Statistical and estimated inlet flows

No matter how well the IFM has been selected, there will be a difference between the statistical (obtained from simulation) and the estimated (calculated from equation 5.4)

data (Fig.5.5). The question arises whether these divergences are random fluctuations, related to a limited number of observations, instability of demands or inaccuracy of measurements, or they are deterministic and related to an incorrect model. The question can be answered by the so called 'goodness-of-fit' test in which on the basis of given statistical material a hypothesis *H* shall be verified, if a random variable *X* follows a certain law of distribution. This law can be set in one or another form, for example in the form of a distribution function, either in a continuous or discrete form.

In order to accept or reject the hypothesis *H*, it is necessary to choose a measure of a difference between the theoretical and statistical distributions. It is possible to use different measures, e.g. the sum of squares of deviations of the theoretical probabilities from corresponding frequencies of statistical probabilities, or the sum of the same squares with some weight coefficients, or the maximum deviation between the theoretical and statistical distribution. In any case this measure will be a random variable and the distribution law of this random variable depends on the distribution of *X* and on the number of experiments.

In order to verify the hypothesis and in our case – the compliance of the statistical and estimated values of the inlet flow, it is proposed here to use the chi-square (χ^2) criterion. A chi-square test (also chi-squared or χ^2 test) is a statistical hypothesis test in which the test statistic has a chi-square distribution when the null hypothesis is true, or in which the probability distribution of the test statistic (assuming the null hypothesis is true) can be made to approximate a chi-square distribution as closely as desired by making the sample size large enough. In probability theory and statistics, the chi-square distribution (also chi-squared or χ^2 distribution) is one of the most widely used theoretical probability distributions in inferential statistics, e.g., in statistical significance tests (Chernoff & Lehmann 1954, Plackett 1983). The chi-square statistic is calculated by finding the difference between each observed and theoretical frequency for each possible outcome, squaring them, dividing each by the theoretical frequency, and taking the sum of the results.

$$\chi^2 = \sum_i \frac{(Y_i' - Y_i)^2}{Y_i'^2} \tag{5.5}$$

where

Y_i' estimated data

Y_i statistical data

As a result of comparison of statistical values of the inlet flow obtained from simulations, with the estimated values based on Equation 5.4, the following values of χ^2 depicted in Tables 5.3 and 5.4 have been obtained.

Table 5.3 Ocker Hill DMA χ^2 values.

Burst at node 141.		Burst at node 59.	
Sensitive node	The value of χ^2	Sensitive node	The value of χ^2
165	1.45E-05	165	9.01E-07
37	6.14E-06	37	5.85E-07
45	1.19E-05	45	1.24E-06
91	2.51E-06	91	5.85E-06
13	2.64E-05	13	1.21E-05
31	2.16E-05	31	9.83E-06
51	1.39E-05	51	1.69E-06
72	1.73E-05	72	6.12E-06
74	8.53E-06	74	7.77E-09
151	2.74E-06	151	5.17E-06
98	1.14E-05	98	9.24E-07
162	6.93E-07	162	1.4E-05
14	2.46E-05	14	1.11E-05
127	5.96E-06	127	7.42E-07
140	1.09E-06	140	1.14E-05
112	1.69E-06	112	8.47E-06
33	5.3E-06	33	1.27E-06
57	1.42E-05	57	2.92E-06
116	5.78E-07	116	1.51E-05

Where the values highlighted in yellow correspond to the minimum values of χ^2.

Table 5.4 Shenstone DMA χ^2 values.

Burst at node 98.		Burst at node 29.		Burst at node 67.		Burst at node 80.	
Sensitive node	The value of χ^2	Sensitive node	The value of χ^2	Sensitive node	The value of χ^2	Sensitive node	The value of χ^2
95	1.3E-07	95	9.3E-07	95	1.3E-08	95	2.8E-08
99	2.58E-08	99	8.15E-08	99	7.23E-09	99	1.17E-09
18	1.18E-07	18	3.24E-07	18	9.7E-09	18	2.13E-08
91	7.1E-08	91	9.92E-09	91	5.45E-10	91	4.27E-09
42	7.12E-08	42	9.47E-09	42	5.12E-10	42	4.54E-09
3	1.65E-07	3	4.85E-06	3	2.47E-08	3	4.35E-08
114	5.03E-09	114	4.35E-07	114	9.13E-08	114	7.63E-08
115	1.92E-09	115	3.77E-07	115	7.61E-08	115	6.18E-08
81	2.93E-08	81	6.47E-08	81	4.36E-09	81	8.28E-10
88	1.29E-08	88	1.23E-07	88	1.49E-08	88	7.63E-09
108	9.28E-09	108	4.91E-07	108	1.1E-07	108	9.14E-08
62	5.59E-08	62	2.08E-08	62	4.99E-12	62	1.44E-09
67	4.99E-08	67	2.77E-08	67	2.26E-10	67	6.03E-10
38	8.64E-08	38	2.54E-09	38	2.6E-09	38	9.8E-09
75	4.1E-08	75	4.43E-08	75	1.68E-09	75	2.13E-11
35	9.58E-08	35	6.74E-10	35	4.06E-09	35	1.34E-08
29	1.05E-07	29	1.61E-26	29	6.05E-09	29	1.69E-08

Where the values highlighted in yellow correspond to the minimum values of χ^2.

In the ideal situation of full consistency between the statistical and the theoretical data, the value of the criteria should be equal to 0. In our experiment the pressure at a sensitive node instead of the pressure at the burst node was used and consequently $\chi^2 > 0$. In general the minimum value of χ^2 identifies the demand, the burst and the background leakage, that most correctly describe flows in a network and such cases are collected in Table 5.5 for different input data scenarios.

The accuracy of the results is influenced by the considered scenario; the simulated demand, the total background leakage and the size and the location of the burst. This will be closer investigated in Chapter 5.1.5.

Table 5.5 Obtained results

Set values	The values, obtained as a result of calculations
Ocker Hill DMA	
Demand flow = 4 l/s Burst coefficient at node 59 = 0.5 Total background leakage coefficient = 0.006525	Demand flow = 3.9892 l/s Burst coefficient at node 74 = 0.508653 Total background leakage coefficient = 0.006444
Demand flow = 3 l/s Burst coefficient at node 141 = 0.37 Total background leakage coefficient = 0.01613	Demand flow = 2.422476 l/s Burst coefficient at node 116 = 0.419613 Total background leakage coefficient = 0.015762
Shenstone DMA	
Demand flow = 3.8 l/s Burst coefficient at node 98 = 0.2 Total background leakage coefficient = 0.002406	Demand flow = 3.836697 l/s Burst coefficient at node 115 = 0.194077 Total background leakage coefficient = 0.002413
Demand flow = 2 l/s Burst coefficient at node 29 = 0.4 Total background leakage coefficient = 0	Demand flow = 2 l/s Burst coefficient at node 29 = 0.4 Total background leakage coefficient = 0
Demand flow = 2 l/s Burst coefficient at node 67 = 0.2 Total background leakage coefficient = 0.00239	Demand flow = 1.991531 l/s Burst coefficient at node 62 = 0.200079 Total background leakage coefficient = 0.002381
Demand flow = 4 l/s Burst coefficient at node 80 = 0.24 Total background leakage coefficient = 0.002216	Demand flow = 3.975472 l/s Burst coefficient at node 75 = 0.240345 Total background leakage coefficient = 0.002193

A summary of all experiments carried out by the author (about 30 experiments) including those which have not been described here is given below.

- For the demand d the average error was 1.5% (the absolute average error of 0.1 l/s for the demand of 3 l/s).
- For the burst coefficient c_1 the average error was 0.8 % (the absolute average error in the terms of the burst flow 0.03 l/s).
- For the background leakage coefficient c_2 the average error was 0.8 % (the absolute average error in the terms of the background flow 0.015 l/s).

This level of accuracy of determining the IFM coefficients is sufficiently high from the practical point of view and one should remember that the pressures to estimate the IFM coefficients were from a sensitive node and not from the exact burst node.

5.1.4 Hybrid method of burst detection

The considerations in the previous chapter allow the formulation of a hybrid method for burst detection which is based on applying a least squares method followed by a chi-square test. The description of the method is given in the following steps: data requirements including a hydraulic model and the data obtained from the field experiment, verbal description of the algorithms and the algorithm flowchart.

The following input data are required to determine the size of a burst in a network:

1. Hydraulic model data

The model of the Shenstone network used by the author is stored in a separate excel file *model.xls* (Table 5.6 and full data are contained in Appendix D) with the following fields:

A – Node number – a unique label used to identify the node.

B - Type of node – a binary value that describes the role of a node in a network: 0 for a connection node or 1 for a source node (reservoir node or PRV OUTLET node).

C - Demand factor – number of average water users allocated to a node.

D - Elevation (m) – elevation in metres above a common reference of a node. The elevation in used in the program only to compute the pressure at the node.

E - Coefficient of a burst – value of coefficient c_1 for a specific node is set in case of presence in a network of already known burst with specified characteristics.

F - Exponent of the burst term in the IFM= 0.5.

G - Coefficient of known background leakages – value of coefficient c_2 for a specific node is set up in case of presence in a network with already known background leakages with specified characteristics.

H – Exponent of the background leakage term in the IFM =1.5.

I, J – horizontal and vertical co-ordinates of a node on the map. They do not affect any other variable.

Table 5.6 Model data

A	B	C	D	E	F	G	H	I	J
1	0	2	91	0	0.5	0	1.5	411362848	304925728
2	0	2	91	0	0.5	0	1.5	411382531	304927213
3	0	8	91	0	0.5	0	1.5	411304768	304868015
4	0	0	91.08	0	0.5	0	1.5	411296376	304921239
5	0	0	91.4	0	0.5	0	1.5	411280256	305070883
…	…	…	…	…	…	…	…	…	…
91	0	100	97	0	0.5	0	1.5	411217951	306164501
92	0	5	100.714	0	0.5	0	1.5	411142464	304066560
93	0	16	102.76	0	0.5	0	1.5	410760043	304351731
94	0	0	98	0	0.5	0	1.5	411219601	305974799
95	1	0	94.1	0	0.5	0	1.5	410509041	304723406
96	0	24	103.797	0	0.5	0	1.5	410916992	304578976
97	0	0	103.8	0	0.5	0	1.5	410779338	304376098
98	0	33	105.2	0	0.5	0	1.5	411156736	304418880
99	1	0	100.74	0	0.5	0	1.5	411148846	304062094
100	0	0	105.357	0	0.5	0	1.5	410269088	302952832
…	…	…	…	…	…	…	…	…	…
120	0	15	111.712	0	0.5	0	1.5	411059714	304321608

Reservoirs represent boundary inlet points to a network in which measurements of the inlet flow and the inlet pressure are made.

2. Experimental data.

The variables which are measured during the E-FAVOR test include the pressure and flow at the inlet to a DMA and also pressure at selected sensitive nodes inside the DMA. The following should be decided before carrying out the test:

- Number of pressure measurement points – this is limited by practical aspects such as number of available loggers and number of available access points (hydrants).
- Inlet pressure stepping – it is beneficial to have many pressure steps and each step with a significant amplitude. This is again constrained by practicalities in the field, pressure of 15m has to be maintained at each node of the network to meet the OFWAT regulations and the pressure can only go as high as the inlet pressure to the PRV (PRV fully open).

After the experiment the measurements are stored in another excel file *data.xls*, which contains the following information (Figure 5.6):

- inlet node IDs (95, 99);

- nodes which are near to the inlet nodes (19, 92);
- list of sensitive nodes, at which the measurements have been made (18, 91, 42, 3, 114, 155, …);
- inlet head in metres which is manipulated (stepped) during the experiment.
- inlet flow in litres per second resulting from the changes in the inlet pressure
- pressure at the sensitive nodes in metres, which subsequently will be transformed into head at sensitive nodes (pressure + elevation)

The algorithm of determination of burst size in a network has been implemented in the MATLAB package and progresses through the following steps:

1. Read in the Excel files containing the hydraulic model data and the experimental data.
2. Prepare the matrix of pressures at the sensitive nodes and calculate the values of the Average Zonal Night Pressure.
3. In case of a network with many inlets, add all inlet flows together to form a total inlet flow. It has been found that the use of the total flow is a good compromise between the burst location accuracy and the calculation speed of the algorithm.

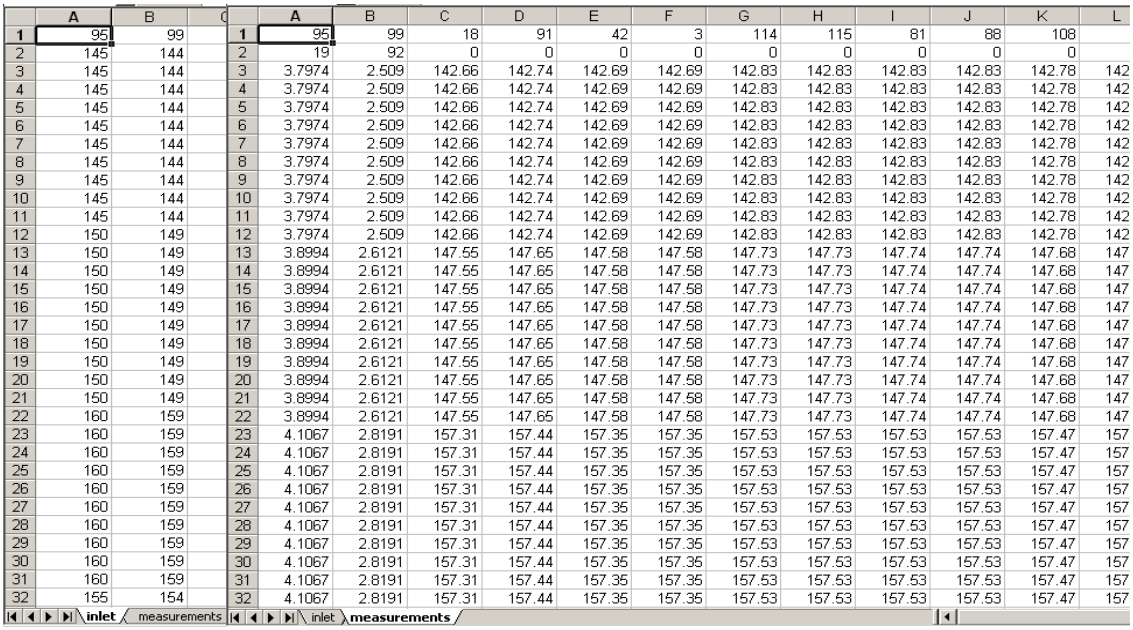

	A	B
1	95	99
2	145	144
3	145	144
4	145	144
5	145	144
6	145	144
7	145	144
8	145	144
9	145	144
10	145	144
11	145	144
12	150	149
13	150	149
14	150	149
15	150	149
16	150	149
17	150	149
18	150	149
19	150	149
20	150	149
21	150	149
22	160	159
23	160	159
24	160	159
25	160	159
26	160	159
27	160	159
28	160	159
29	160	159
30	160	159
31	160	159
32	155	154

inlet | measurements

	A	B	C	D	E	F	G	H	I	J	K	L
1	95	99	18	91	42	3	114	115	81	88	108	
2	19	92	0	0	0	0	0	0	0	0	0	
3	3.7974	2.509	142.66	142.74	142.69	142.69	142.83	142.83	142.83	142.83	142.78	142
4	3.7974	2.509	142.66	142.74	142.69	142.69	142.83	142.83	142.83	142.83	142.78	142
5	3.7974	2.509	142.66	142.74	142.69	142.69	142.83	142.83	142.83	142.83	142.78	142
6	3.7974	2.509	142.66	142.74	142.69	142.69	142.83	142.83	142.83	142.83	142.78	142
7	3.7974	2.509	142.66	142.74	142.69	142.69	142.83	142.83	142.83	142.83	142.78	142
8	3.7974	2.509	142.66	142.74	142.69	142.69	142.83	142.83	142.83	142.83	142.78	142
9	3.7974	2.509	142.66	142.74	142.69	142.69	142.83	142.83	142.83	142.83	142.78	142
10	3.7974	2.509	142.66	142.74	142.69	142.69	142.83	142.83	142.83	142.83	142.78	142
11	3.7974	2.509	142.66	142.74	142.69	142.69	142.83	142.83	142.83	142.83	142.78	142
12	3.7974	2.509	142.66	142.74	142.69	142.69	142.83	142.83	142.83	142.83	142.78	142
13	3.8994	2.6121	147.55	147.65	147.58	147.58	147.73	147.73	147.74	147.74	147.68	147
14	3.8994	2.6121	147.55	147.65	147.58	147.58	147.73	147.73	147.74	147.74	147.68	147
15	3.8994	2.6121	147.55	147.65	147.58	147.58	147.73	147.73	147.74	147.74	147.68	147
16	3.8994	2.6121	147.55	147.65	147.58	147.58	147.73	147.73	147.74	147.74	147.68	147
17	3.8994	2.6121	147.55	147.65	147.58	147.58	147.73	147.73	147.74	147.74	147.68	147
18	3.8994	2.6121	147.55	147.65	147.58	147.58	147.73	147.73	147.74	147.74	147.68	147
19	3.8994	2.6121	147.55	147.65	147.58	147.58	147.73	147.73	147.74	147.74	147.68	147
20	3.8994	2.6121	147.55	147.65	147.58	147.58	147.73	147.73	147.74	147.74	147.68	147
21	3.8994	2.6121	147.55	147.65	147.58	147.58	147.73	147.73	147.74	147.74	147.68	147
22	3.8994	2.6121	147.55	147.65	147.58	147.58	147.73	147.73	147.74	147.74	147.68	147
23	4.1067	2.8191	157.31	157.44	157.35	157.35	157.53	157.53	157.53	157.53	157.47	157
24	4.1067	2.8191	157.31	157.44	157.35	157.35	157.53	157.53	157.53	157.53	157.47	157
25	4.1067	2.8191	157.31	157.44	157.35	157.35	157.53	157.53	157.53	157.53	157.47	157
26	4.1067	2.8191	157.31	157.44	157.35	157.35	157.53	157.53	157.53	157.53	157.47	157
27	4.1067	2.8191	157.31	157.44	157.35	157.35	157.53	157.53	157.53	157.53	157.47	157
28	4.1067	2.8191	157.31	157.44	157.35	157.35	157.53	157.53	157.53	157.53	157.47	157
29	4.1067	2.8191	157.31	157.44	157.35	157.35	157.53	157.53	157.53	157.53	157.47	157
30	4.1067	2.8191	157.31	157.44	157.35	157.35	157.53	157.53	157.53	157.53	157.47	157
31	4.1067	2.8191	157.31	157.44	157.35	157.35	157.53	157.53	157.53	157.53	157.47	157
32	4.1067	2.8191	157.31	157.44	157.35	157.35	157.53	157.53	157.53	157.53	157.47	157

inlet | measurements

Fig. 5.6 File data.xls - Experimental data for the Shenstone network

4. Solve the least squares problem for each sensitive node $i \in K$:

$$\min \left\| C_i^{'} P' - Q_{in}^{*} \right\|^2 , \qquad (5.6)$$

where

$$Q_{in}^{*} = \begin{bmatrix} q_{in,1}^{*} \\ q_{in,2}^{*} \\ \dots \\ q_{in,n}^{*} \end{bmatrix}$$

is the vector of the measured inlet flow with dimension $n \times 1$ (n is the number of measurements in time);

$C_i = \begin{bmatrix} d \\ c_1 \\ c_2 \end{bmatrix}$ is the vector 3×1 of the coefficients of the IFM equation $q = d + c_1 p_i^{0.5} + c_2 p_{AZNP}^{1.5}$.

$$P = \begin{bmatrix} 1 & p_{i1}^{0.5} & p_{AZNP1}^{1.5} \\ 1 & p_{i2}^{0.5} & p_{AZNP2}^{1.5} \\ \dots & \dots & \dots \\ 1 & p_{in}^{0.5} & p_{AZNPn}^{1.5} \end{bmatrix}$$

is the matrix of the pressures with dimension $n \times 3$ (n is the number of measurements in time).

As a result the matrix of the demand and leakage coefficients is formed

$C = \begin{bmatrix} C_1' \\ C_2' \\ \dots \\ C_K' \end{bmatrix}$ with dimension $K \times 3$, where K – is number of sensitive nodes.

5. Choose the solution which corresponds to the sensitive node which gives the minimum value of the chi-square criterion using the following procedure. Estimated values of the inlet flow are obtained using the coefficients found in Step 4 and compared with the measured inlet flow using the χ^2 criterion (5.5). In this way the vector V of the χ^2 values is created which can serve as a measure of how good the description of the experimental flow is compared to the estimated (theoretical) one.

The outputs of the algorithm are the values of the IFM coefficients and the resulting theoretical inlet flows and the vector V of the χ^2 criterion values.

The flowchart of the Hybrid Algorithm for burst detection is given in Fig.5.7 and programme code is given in Appendix F

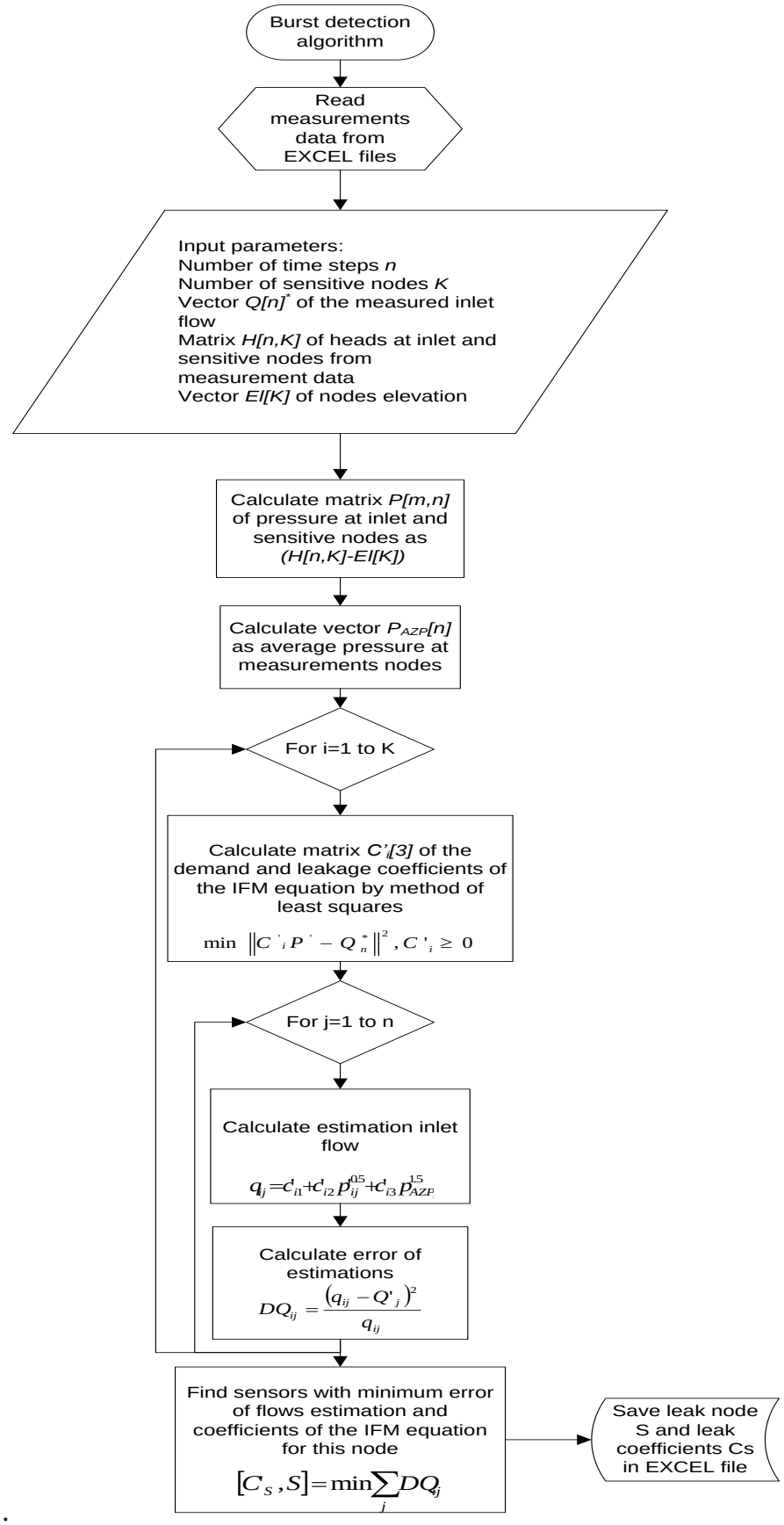

Fig. 5.7 A flowchart of a burst size estimation algorithm

5.1.5 Accuracy of the algorithm.

It was observed in the experiments described in Chapter 5.1.3, that the accuracy of the estimation of the burst size is influenced by the magnitude of the flows corresponding to the IFM three terms: the demand, the fixed area flow (burst flow) and the variable area flow (background leakage flow) and also on proportions between these flows. This issue is investigated further in this chapter.

In the above consideration the terms of the IFM have been varied within the following limits:

- Total demand flow varied from 2 l/s to 4 l/s.
- The coefficient of the fixed area leakage is varied from 0.15 to 0.4 $l/s/\sqrt{m}$.
- The coefficient of the variable area leakage is varied from 0 to 0.002 $l/s/m\sqrt{m}$ at an individual node.

It is important to know how the algorithm would behave for other coefficient values. It is also important to investigate limiting proportions between the flow components for which the accuracy of the obtained results is satisfactory.

From the literature and from other case studies provided by Water Software Systems (De Montfort University) it has been found out, that the possible values of the demand and the leakage coefficients for different DMAs can be within the following limits:

- The total demand flow: 0.2 – 11 l/s.
- The coefficient of the fixed area leakage (burst coefficient): 0.1 – 1.6 $l/s/\sqrt{m}$.
- The coefficient of the variable area leakage (background leakage coefficient): 0.005 – 0.05 $l/s/m\sqrt{m}$.

The Shenstone DMA (Figure 5.8) has been selected for these investigations because the model was already available in an electronic format and the network is well understood by the author. Additionally the accuracy of the results for typical values of the IFM coefficients is known and can be used as a benchmark to compare the accuracy for extreme flow values.

The network has two inlets, node 95 and node 99 and altogether comprises of 116 nodes. The E-FAVOR test is simulated using the model, inlet pressure has been changed in steps from *40.9 m* to *65.9 m* at Inlet 1 (node 95) and from *33.26 m* to *58.26*

m at Inlet 2 (node 99). The simulated pressure data ('measurements') are collected from 15 sensitive nodes (they are depicted in Figure 5.8 by dark blue rectangles) and the simulated inlet flow ('measurements') are collected from nodes 99 and 95.

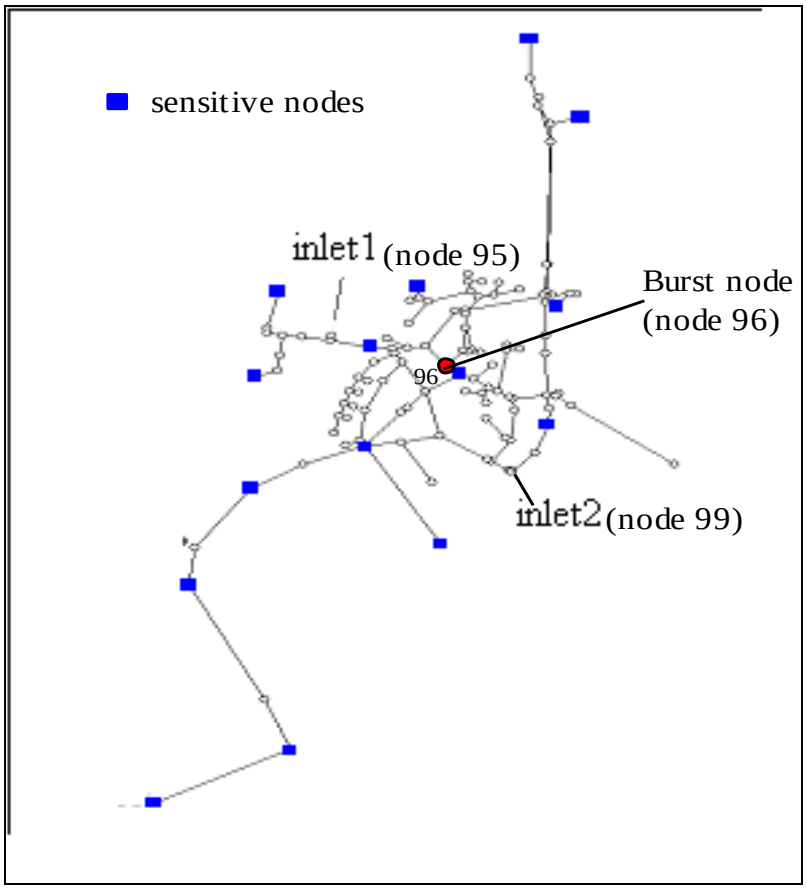

Fig. 5.8 Shenstone DMA schematic (with burst)

Node 96 is chosen as a burst node since it is equidistant from the two inlet nodes and is in the centre of the network so it should be strongly affected by the variables manipulated in the experiments.

The accuracy for this wide range of parameter values is compared to the accuracy of the method for the following average values of the parameters

- $d_{avr} = 5.5$ *l/s* - the average value of total demand;
- $c_{1\_avr} = 0.8$ – the average value of the burst coefficient;
- $c_{2\_avr} = 0.0229$ – the average value of the background leakage coefficient.

The inlet pressure has been changed in steps resulting in the total inlet flow change from 13 l/s to 22 l/s.

Applying the developed algorithm the following estimates have been obtained:

- $d_{avr} = 4.85$ *l/s* ;

- $c_{1\_avr} = 0.9$;
- $c_{2\_avr} = 0.022$

Further experiments have been carried out for different values of the parameters and the results are collected in Table 5.7.

Table 5.7 Determination of leakage coefficients

Simulated parameters				Estimated results		
Total Inlet Flow (l/s)	d l/s	c_1	c_2	d l/s	c_1	c_2
17.5 – 28.7	11	0.8	0.023	10.8	0.84	0.022
16.0 - 28.6	5.5	0.8	0.05	1.6	1.5	0.044
20.0 – 34.0	11	0.8	0.05	7.2	1.48	0.044
21.5 – 36.0	11	1.6	0.05	9.2	2	0.043
1.8 – 2.5	0.2	0.1	0.005	0.16	0.11	0.0049
2.0 – 3.0	0.2	0.15	0.005	0.11	0.16	0.0049
7.0 – 11.0	5.5	0.15	0.005	5.45	0.15	0.0049
12.5 - 19	11	0.15	0.005	11	0.15	0.005
5.8 – 11.2	0.2	0.15	0.023	0.005	0.26	0.02
9.6 – 18.6	0.2	0.15	0.047	0	0.34	0.042

More experiments have been performed and they have been divided into groups where only one parameter has been varied in a group. The level of accuracy was calculated from the equation below:

$$\varphi = \left(1 - \frac{\sum_{n} \frac{|x_m - x_c|}{x_m}}{n} \right) \cdot 100\%$$

where x_m and x_c are the simulated parameter value and the estimated parameter value, respectively and n is the number of experiments inside each group. The best accuracy corresponds to $\phi = 100\%$.

The results are presented in Figs 5.9, 5.10 and 5.11 respectively.

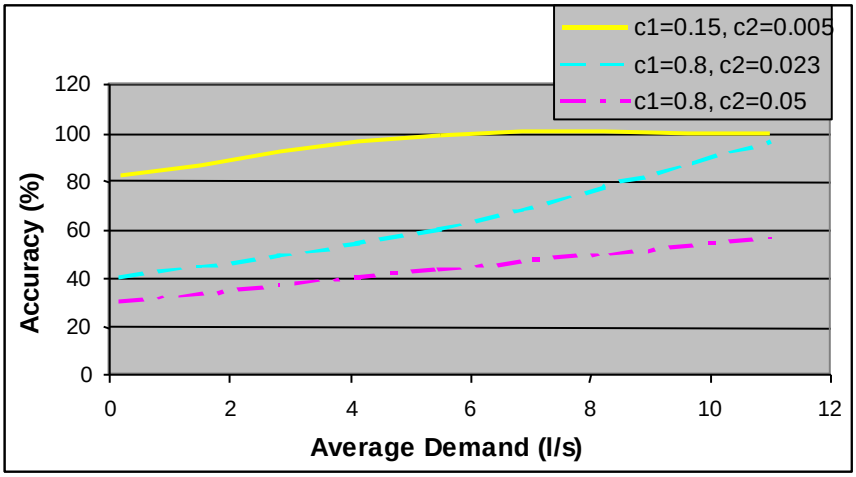

Fig. 5.9 The result's accuracy from value of Demand

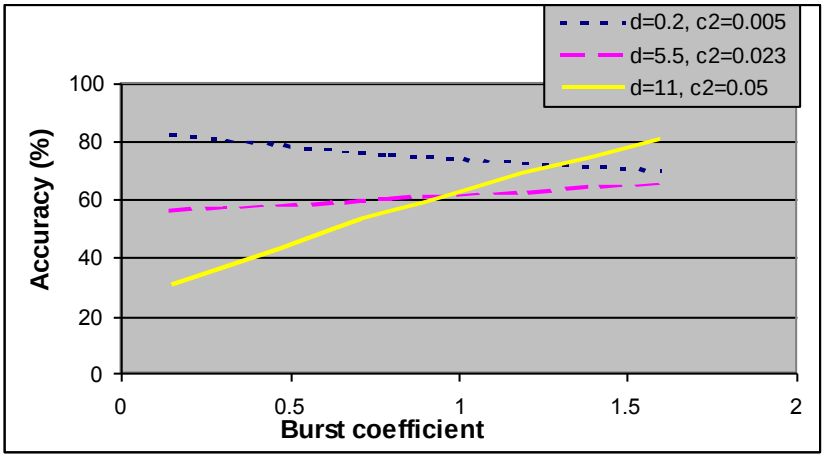

Fig. 5.10 The result's accuracy from value of the burst

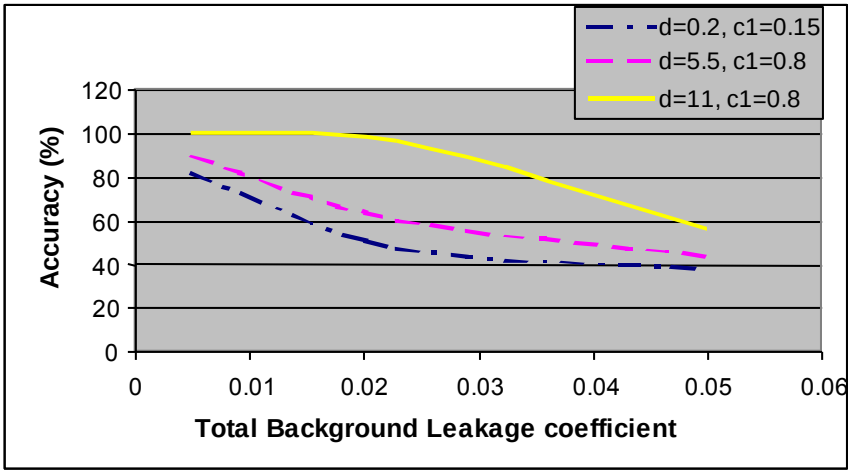

Fig. 5.11 The result's accuracy from value of the background leakage's flow

The observations from the experiments are collected below:

1. For small values of the leakage flows an increase in the demand improves the accuracy of the algorithm as shown in Fig. 5.9. For bigger values of the leakage flows an increase in the demand has also a positive effect on accuracy. In both cases the improvement in accuracy is moderate and stays slightly above 80%.
2. The leakage flows depend on pressure through different exponents, 0.5 for a burst and 1.5 for the background leakage respectively. The burst coefficient is estimated with higher accuracy for bigger burst flows as can be observed in Fig. 5.10. The opposite can be observed for the background leakage coefficient where the accuracy gets lower for bigger background leakage coefficients as illustrated in Figure 5.11.
3. Ratios between the terms in the IFM also influence the accuracy of the coefficient estimates. For small values of the background leakage the accuracy of the algorithm is high enough (> 80 %) and depends only on the ratio between the demand and the burst terms. An increase in the demand causes an increase of the estimation accuracy for the background leakage coefficient. The increase in the value of the background leakage coefficient with the two terms remaining constant reduces the estimation accuracy.

From the numerous experiments where the values of coefficients were within the limits 0.2 – 11 l/s for total demand flow, 0.1 – 1.6 $l/s/\sqrt{m}$ for burst coefficient and 0.005 – 0.05 $l/s/m\sqrt{m}$ for background leakage coefficient, it is observed that the estimation of a burst is effective if the burst is sufficiently big in comparison with the background leakage flow:

Variable area flow (background leakage) $\leq \frac{1}{2}$ fixed area flow (burst leakage).

5.1.6 Summary

The following conclusions can be made resulting from the carried out research:

- The least squares method has been used to calculate the coefficients of the IFM, where the Average Zone Night Pressure has been substituted in the background

leakage term, and the pressure at a sensitive node was used to represent the burst term.

- A burst was provisionally allocated to different sensitive nodes and the solution was selected which gives the minimum value of the chi-square criterion applied to the total inlet flow. This is the essence of the hybrid method of burst detection algorithm.
- The hybrid method helps to determine accurate values of the IFM parameters, the total demand and fixed and variable area leakage terms using the recorded data of the inlet pressure and flow and pressure at the sensitive nodes of a network.
- The accuracy of the results of determining the burst size and the burst location is influenced by the magnitude of the three flows (demand, fixed area flow and variable area flow) and by the proportions between them.

5.2 Effects of a burst on pressure in a DMA

The hybrid method of determination of burst size was based on studying flow changes in a DMA caused by the fixed area and the variable area leakage. However, the flow changes in a DMA cause a redistribution of pressure at nodes of the network. This may provide a good signature for the identification of the burst location. The remainder of this chapter is dedicated to develop this idea.

5.2.1 Influence of burst presence to pressure change in a network.

A DMA consists mainly of pipes, a head-loss along a pipe is:

$\Delta h = Rq^B$,

where Δh is the head-loss, q is the flow rate, R is the resistance coefficient, and B is flow exponent. In the Hazen-Williams formula the exponent $B = 1.852$ and subsequently $\Delta h = Rq^{1.852}$

It has been demonstrated before that the inlet flow can be separated into the three components: the total average demand d, the fixed area flow $q = c_1 p^{0.5}$ and the variable area flow $q = c_2 p_{AZNP}^{1.5}$.

In the absence of the demand and the leakage flows the pressure in the network is distributed uniformly and $\Delta h = 0$ for any pipe. When the demand only is present, the pressure drop along a pipe is pressure independent and for a constant demand is constant $\Delta h = f(d)$. This should be true when performing the e-FAVOR test for such a network. Let's use the Ocker Hill which has one inlet for simulation experiments.
The inlet head (node 165) has been changed linearly from 156 m up to 191 m (which corresponds to the change in pressure from 18.5 m up to 53.5m) and the demand *d* is set to 1 l/s. The corresponding values of pressures at all nodes of the network have been recorded and are depicted in Table 5.8.

Table 5.8 Pressure at nodes of the network (without burst)

Node number	Measurement number (n)							$\Delta p = p(n=1) - p(n=176)$
	1	2	3	…	174	175	176	
1	18.50	18.70	18.90	…	53.10	53.30	53.50	35
2	19.89	20.09	20.29	…	54.49	54.69	54.89	35
3	18.50	18.70	18.90	…	53.10	53.30	53.50	35
4	18.50	18.70	18.90	…	53.10	53.30	53.50	35
5	18.50	18.70	18.90	…	53.10	53.30	53.50	35
6	16.99	17.19	17.39	…	51.59	51.79	51.99	35
7	15.97	16.17	16.37	…	50.57	50.77	50.97	35
8	15.46	15.66	15.86	…	50.06	50.26	50.46	35
9	15.95	16.15	16.35	…	50.55	50.75	50.95	35
10	15.95	16.15	16.35	…	50.55	50.75	50.95	35
…	…	…	…	…	…	…	…	…
75	21.69	21.89	22.09	…	56.29	56.49	56.69	35
76	19.39	19.59	19.79	…	53.99	54.19	54.39	35
77	20.05	20.25	20.45	…	54.65	54.85	55.05	35
…	…	…	…	…	…	…	…	…
165	18.50	18.70	18.90	…	53.1	53.3	53.5	35

The pressure at each node of the network increases linearly with the increase of the inlet pressure, and this can be seen in Figure 5.12.

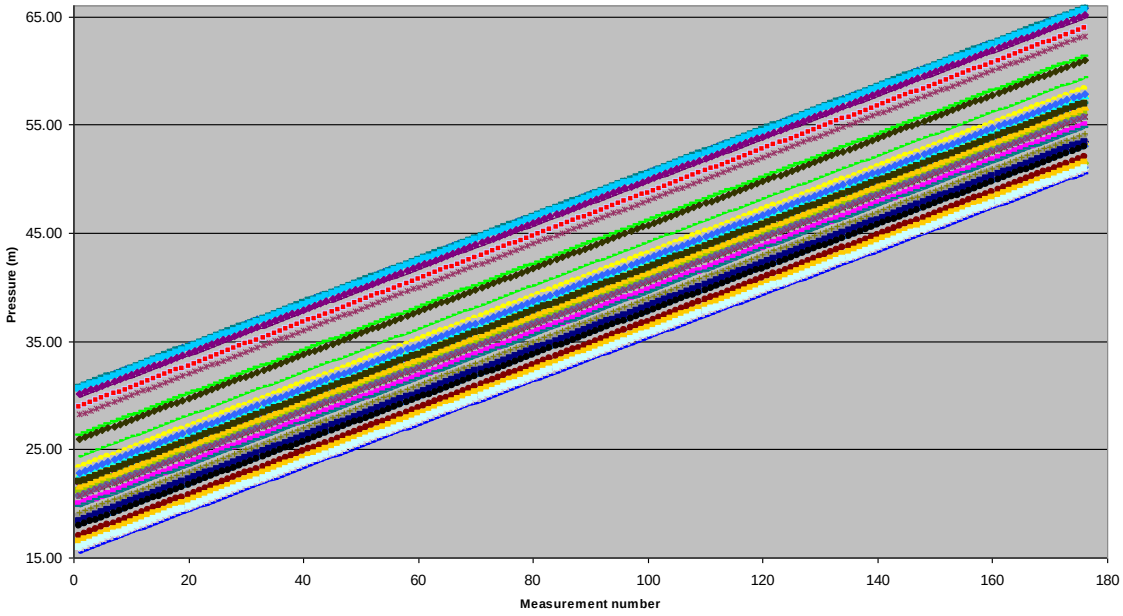

Fig. 5.12 Diagram of pressure change at nodes of the network (without burst)

If a burst is present in the network, the pressure at the burst node drops and the burst flow depends on the pressure and the size of the break in the pipe.

In the numerical experiments the inlet head (node 165) has been varied from 156 m up to 191 m (that corresponds to a change of pressure from 18.5 m up to 53.5m), the average total demand is 1 l/s and the burst at node 76 has the burst coefficient $c1=0.9$. By means of simulation the pressure values at all nodes of the network have been calculated and are presented in Table 5.9.

Table 5.9 Pressure at nodes of the network (with burst)

Node number	Measurement number (t)							$\Delta p = p(t=1) - p(t=176)$
	1	2	3	…	174	175	176	
1	18.49	18.69	18.89	…	53.07	53.27	53.47	34.98
2	18.26	18.45	18.63	…	50.74	50.93	51.12	32.86
3	18.49	18.69	18.89	…	53.09	53.29	53.49	34.99
4	18.49	18.69	18.89	…	53.07	53.27	53.47	34.98
5	18.49	18.69	18.88	…	53.07	53.27	53.47	34.98
6	16.76	16.96	17.16	…	51.08	51.27	51.47	34.71
7	15.48	15.67	15.87	…	49.43	49.63	49.83	34.35
8	14.76	14.95	15.15	…	48.45	48.65	48.84	34.08
9	15.19	15.38	15.58	…	48.79	48.98	49.18	33.99
10	15.16	15.36	15.55	…	48.74	48.93	49.12	33.96
…	…	…	…	…	…	…	…	…
75	18.72	18.89	19.07	…	49.16	49.34	49.51	30.79
76	16.09	16.27	16.44	…	46.01	46.18	46.36	30.26
77	16.96	17.13	17.30	…	47.21	47.39	47.56	30.61
…	…	…	…	…	…	…	…	…
165	18.50	18.70	18.90	…	53.1	53.3	53.5	35

Now, the pressure at the burst node and the nearby nodes follows a different law than the pressure at the inlet node and remaining nodes. A general diagram of pressure changes at all the nodes of the network is given in Figure 5.13 below.

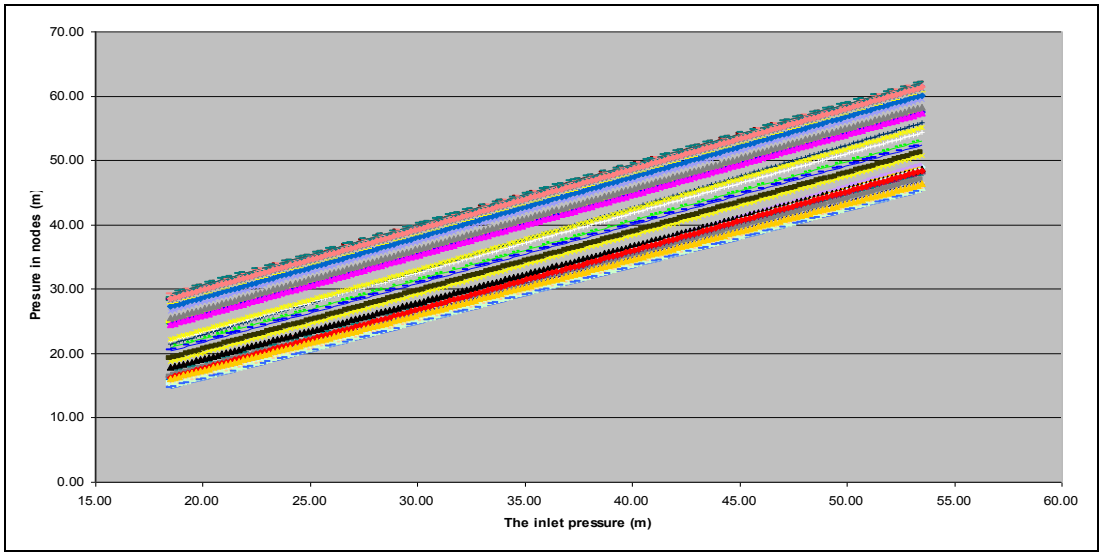

Fig. 5.13 Diagram of pressure change in the network nodes (with burst)

The diagram suggests that the pressure changes at the nodes can be approximated by straight lines. Let's consider these changes in more detail for some selected nodes. The following the network nodes have been chosen for inspection: node 3 which is adjacent to the actual input node (node 165), node 76 which is the burst node, node 75 which is

in immediate proximity to the burst, node 62 which is on the same branch as the burst and nodes 93 and 28 which are in other parts of the network (Figure 5.14).

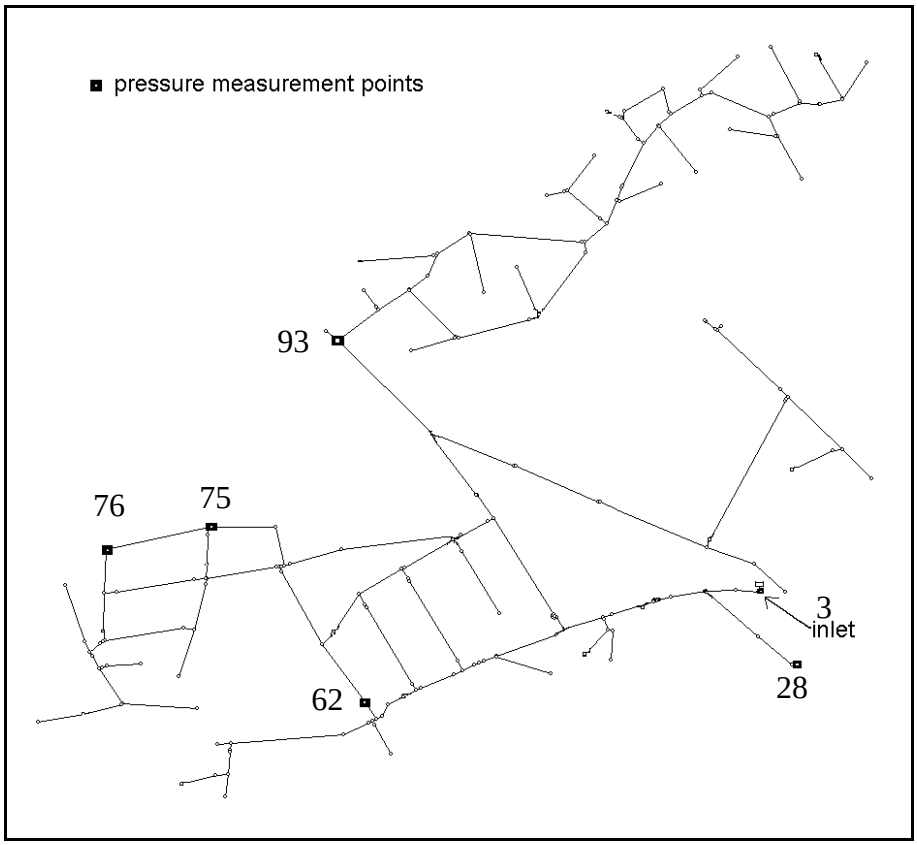

Fig. 5.14 Ocker Hill DMA schematic (pressure measurement points)

The pressure changes at the selected nodes are illustrated Figure 5.15.

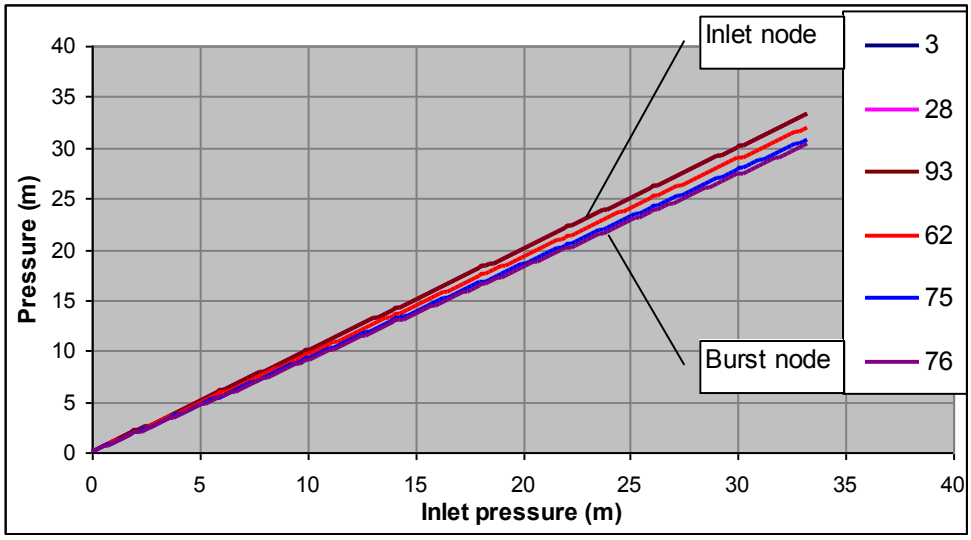

Fig. 5.15 Diagram of pressure change in the network nodes

In the diagram (Figure 5.15) differences between the gradients of the pressure lines for different nodes are quite evident. The smallest gradient is observed for the straight line representing the burst node. Also the nodes 75 and 62 which are close to the burst node have small gradients. For the remaining nodes 93 and 28 the pressure line approximation completely coincides with the pressure line approximation for the inlet node 3 (node 3 is directly connected with PRV OUTLET at node 165), which indicates that these nodes are not affected by the burst.

If a small background leakage, with the background leakage coefficient equal to 0.015, is added the general picture does not change qualitatively as is shown in Figure 5.16, the order in the gradient values is the same as previously with the smallest gradient for the burst node and the biggest gradient for the inlet node.

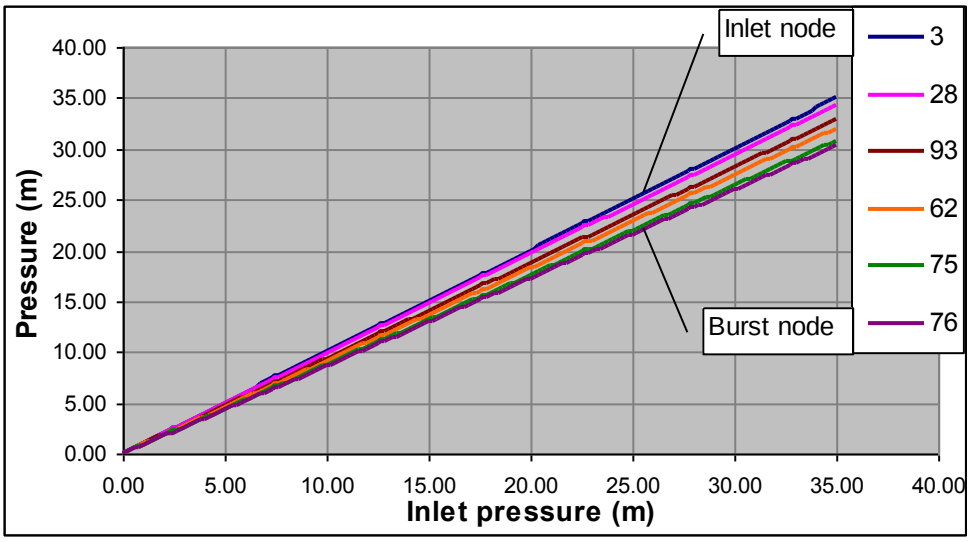

Fig. 5.16 Diagram of pressure change in the network nodes

The gradient values of the pressure approximation lines for all the nodes apart from the inlet node have been reduced but the order between the lines remained the same. The observation can be made that the gradient of the pressure approximation lines can be used to identify the burst location and that the presence of small background leakage does not invalidate this hypothesis. Further experiments have been performed which are not described in this report which independently have confirmed that by analysing the pressure lines it is possible to identify a burst location in a network.

5.2.2 The burst area location.

At the burst node the pressure changes with smaller steps compared to other nodes and potentially by measuring the pressure at all nodes it would be possible to find the burst node. In reality during a field experiment it is impossible to log all the nodes in a network for economical and technical reasons and only selected nodes can be monitored. A natural question arises as to whether it is possible to identify a burst location by investigating the pressure patterns at the sensitive nodes (Chapter 5.1.1).

Numerical experiments have been performed on the Shenstone DMA with the following set up: a hydraulic network model available in Matlab is used, the head at Inlet 1 (node 95) has been stepped from *135 m* up to *160 m* and at Inlet 2 (node 99) has been stepped from *134 m* up to *159 m*, the total demand flow was *3 l/s*, the total coefficient of the background leakage is *0.0024*.

The demand is distributed among nodes of the network according to the number of properties (houses) allocated to each node and the background leakage is distributed in a similar way. The results from the simulation program have been the pressure values at the sensitive nodes: 18, 91, 42, 3, 114, 115, 81, 88, 108, 62, 67, 38, 75, 35, 29, and the values of inlet flows.

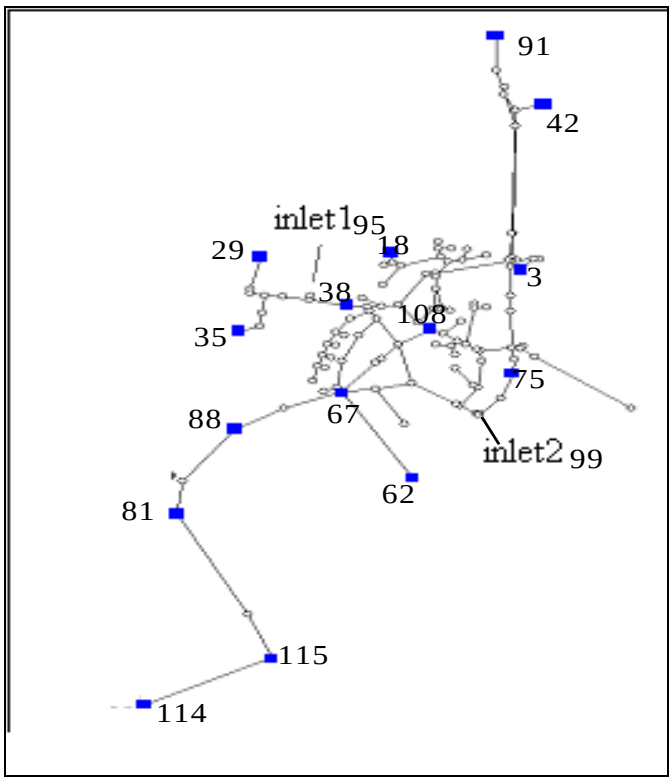

Fig. 5.17 The Shenstone DMA schematic

The simulation results have been entered as input data to the program of the burst size determination, based on the Hybrid Algorithm described in Chapter 5.1.4 and the following values are calculated:

- total demand 2.999159 l/s
- burst coefficient 0
- total coefficient of the background leakage 0.002412.

The following equation is used for approximating the pressure changes at each sensitive node:

$$p = a + bp_{inlet}$$

where

p pressure at a sensitive node

a constant coefficient of the regression line

b gradient of the regression line

p_{inlet} inlet pressure

The regression coefficients have been found by the least squares method to minimise deviations of the approximating straight line from the experimental data:

$U = \sum_{i=1}^{N} \left[p_i - (a + bp_{inlet\_i}) \right]^2 = \min$, where N is number of measurements.

Equating the respective partial derivatives to zero and simplifying gives

$$\frac{dU}{da} = \sum_{i=1}^{N} \left[p_i - (a + bp_{inlet\_i}) \right] = 0$$

$$\frac{dU}{db} = \sum_{i=1}^{N} \left[\left\{ p_i - (a + bp_{inlet\_i}) \right\} p_{inlet\_i} \right] = 0$$

which leads to a system of simultaneous linear equations with respect to a and b:

$$aN + b\sum_{i=1}^{N} p_{inlet\_i} = \sum_{i=1}^{N} p_i$$

$$a\sum_{i=1}^{N} p_{inlet\_i} + b\sum_{i=1}^{N} p_{inlet\_i}^2 = \sum_{i=1}^{N} p_i p_{inlet\_i}$$

,

The equations can be solved analytically as:

$$a = \frac{1}{N}\left(\sum_{i=1}^{N} p_i - b\sum_{i=1}^{N} p_{inlet\_i} \right)$$

$$b = \frac{\sum_{i=1}^{N} p_{inlet\_i} \sum_{i=1}^{N} p_i - N \sum_{i=1}^{N} p_i p_{inlet\_i}}{\left(\sum_{i=1}^{N} p_{inlet\_i} \right)^2 - N \sum_{i=1}^{N} p_{inlet\_i}^2}$$

Applying these formulae to the simulated data the following coefficients shown in Table 5.10 are obtained.

Table 5.10 The values of coefficients

Node number	*a*	*b*
95	0	1.0000
99	-7.64	1.0000
18	-0.62394	0.9922
91	-3.85902	0.9930
42	-3.80134	0.9925
3	2.183803	0.9925
114	-13.3392	0.9929
115	-12.7394	0.9929
81	-7.01928	0.9929
88	-8.73966	0.9929
108	-13.8839	0.9932
62	-4.84889	0.9933
67	-5.30837	0.9933
38	-2.78493	0.9965
75	-6.18396	0.9965
35	-2.22599	0.9994
29	-1.62653	0.9994

The gradients of the lines corresponding to the sensitive nodes are within the limits from 0.99 to 1 and are very close one to another. This confirms the first part of the hypothesis that the background leakage has little influence on the pressure at the sensitive nodes.

In order to verify the second part of the hypothesis, the numerical experiment is repeated for the same network model, with the same values of the inlet heads and demands. The background leakage is removed from the model and a burst is introduced at node 52 with burst coefficient $c_1=0.4$ as shown in Figure 5.18.

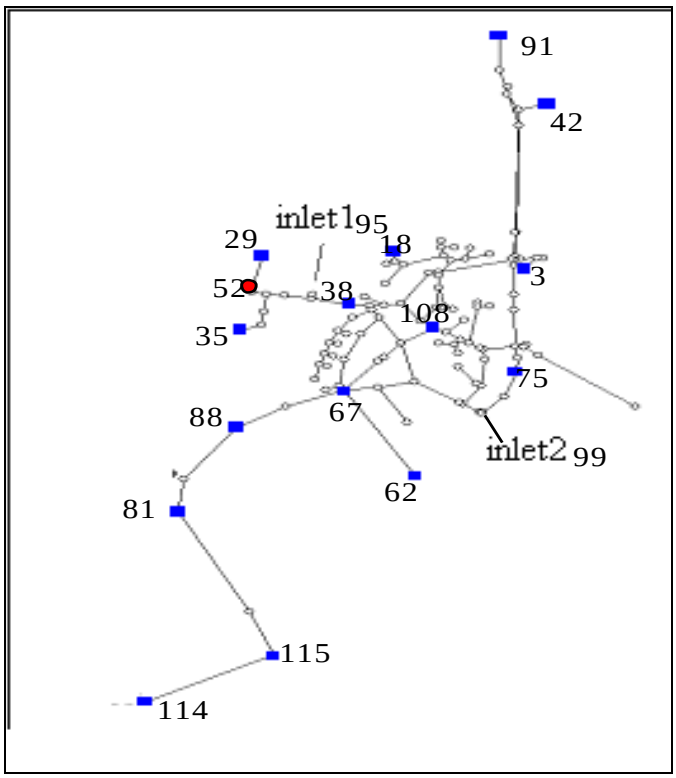

Fig. 5.18 The Shenstone DMA schematic (with burst)

Repeating the calculations has yielded the following *a* and *b* coefficients presented in Table 5.11.

Table 5.11 Received coefficients of regression lines

The number of node	*a*	*b*
95	0	1.0000
99	-7.64	1.0000
18	-0.66244	0.9994
91	-3.91534	0.9999
42	-3.86885	0.9997
3	2.118069	0.9997
114	-13.3933	0.9994
115	-12.7933	0.9994
81	-7.07294	0.9994
88	-8.79272	0.9994
108	-13.93	0.9995
62	-4.89169	0.9994
67	-5.35134	0.9994
38	-2.83102	0.9985
75	-6.222	0.9999
35	-2.34588	0.9820
29	-1.77288	0.9720

It can be seen from Table 5.11, that the smallest gradient of the pressure line *b=0.97* is observed at node 29 which is in the immediate proximity of the burst. Presence of the burst has also a significant impact on node 35 *(b=0.98),* which is located in the same branch as the burst node. The burst has lesser impact on other nodes with the gradient values of about *b=0.999.* It confirms the second part of the hypothesis that the gradients of the pressure line at sensitive nodes can be used to identify the area with the burst.

The following observations can be made:

- Presence of a burst in a network affects the gradient of regression lines approximating the pressure changes at sensitive nodes which are close to the burst
- It is possible to identify the burst area by analysis of the regression lines
- Small background leakage in a network doesn't change the order between the regression lines.

A weak point of the hypothesis is an assumption about the small background leakage. For example, a background leakage concentrated in one particular area can lead to erroneous determination of the burst site. Further numerical investigations have been performed to answer this question. The Shenstone and the Ocker Hill DMA models have been used for the experiments and different values of demand, burst and background leakage have been simulated.

Some results of the experiments are given in Tables 5.12 and 5.13 below, where *Burst area* denotes sensitive nodes located near the burst. The estimated values of the gradients of the estimated sensitive nodes are highlighted in yellow.

Table 5.12 Ocker Hill DMA calculated results.

Parameter	Set values	Estimated values	Sensitive nodes and estimated values of b			
burst node 59			98	0.87753	112	0.89546
			57	0.88002	151	0.89593
d (l/s)	4	3.9892	72	0.88223	127	0.89624
			45	0.88232	91	0.89700
c_1	0.5	0.50865	74	0.88245	31	0.90762
c_2	0.006525	0.006444	37	0.88272	51	0.92618
			33	0.89247	14	0.95076
Burst area	57, 98, 37	98, 57, 72, 45, 74, 37	162	0.89522	13	0.96887
			140	0.89526	165	1.00000
			116	0.89537		
burst node 141			162	0.81	98	0.84
			140	0.81	37	0.84
d (l/s)	3	2.422476	116	0.81	57	0.85
			112	0.81	33	0.85
c_1	0.37	0.419613	151	0.82	31	0.86
c_2	0.01613	0.015762	127	0.82	51	0.89
			91	0.82	14	0.92
Burst area	140, 162, 116, 112	162, 140, 116, 112	72	0.84	13	0.95
			45	0.84	165	1.00
			74	0.84		

Table 5.13 The Shenstone DMA calculated results.

Parameter	Set values	Estimated values	Sensitive nodes and estimated values of b			
burst node 67			114	0.983	3	0.988
			115	0.983	91	0.988
d (l/s)	2	1.99	81	0.983	38	0.993
			88	0.983	75	0.994
c_1	0.2	0.2	62	0.983	35	0.999
			67	0.983	29	0.999
c_2	0.00239	0.00238	108	0.987	95	1.000
			18	0.987	99	1.000
Burst area	67, 62, 88	114, 115, 81, 88, 62, 67	42	0.988		
burst node 80			18	0.979	67	0.982
			42	0.980	91	0.982
d (l/s)	4	3.975	3	0.980	38	0.989
			108	0.981	75	0.991
c_1	0.24	0.24	114	0.982	35	0.999
			115	0.982	29	0.999
c_2	0.002216	0.002193	81	0.982	95	1.000
			88	0.982	99	1.000
Burst area	108, 38	18, 42, 3, 108	62	0.982		
burst node 96			18	0.987	62	0.990
			42	0.988	67	0.990
d (l/s)	0.2	0.11	3	0.988	38	0.994
			108	0.989	75	0.995
c_1	0.15	0.159	91	0.990	29	0.999
			114	0.990	35	0.999
c_2	0.005	0.0049	115	0.990	95	1.000
			81	0.990	99	1.000
Burst area	108	18, 42, 3, 108	88	0.990		
burst node 96			42	0.834	62	0.874
			3	0.836	67	0.875
d (l/s)	0.2	0.05	18	0.843	75	0.926
			91	0.861	38	0.934
c_1	0.15	0.26	108	0.866	35	0.989
			114	0.871	29	0.989
c_2	0.023	0.0215	115	0.871	95	1.000
			81	0.871	99	1.000
Burst area	108	42, 3, 18, 91, 108	88	0.871		

Parameter	Set values	Estimated values	Sensitive nodes and estimated values of b			
burst node 96			42	0.65	62	0.72
			3	0.66	67	0.72
d (l/s)	0.2	0	18	0.67	38	0.85
c_1	0.15	0.34	114	0.70	75	0.85
			115	0.70	29	0.96
c_2	0.04666	0.0419	81	0.70	35	0.96
			88	0.70	95	1.00
Burst area	108	42, 3, 18	108	0.71	99	1.00
			91	0.72		
burst node 96			18	0.96	62	0.97
			42	0.96	67	0.97
d (l/s)	5.5	5.45	3	0.96	75	0.98
c_1	0.15	0.15	108	0.96	38	0.98
			91	0.96	35	1.00
c_2	0.005	0.00496	114	0.97	29	1.00
			115	0.97	95	1.00
Burst area	108	18, 42, 3, 108, 91	81	0.97	99	1.00
			88	0.97		
burst node 96			18	0.94	62	0.95
			42	0.94	67	0.95
d (l/s)	11	10.95	3	0.94	75	0.97
c_1	0.15	0.15	108	0.94	38	0.97
			91	0.95	35	1.00
c_2	0.005	0.00494	114	0.95	29	1.00
			115	0.95	95	1.00
Burst area	108	18, 42, 3, 108	81	0.95	99	1.00
			88	0.95		
burst node 98			91	0.979	62	0.984
			3	0.979	67	0.984
d (l/s)	3.8	10.95	42	0.979	75	0.989
c_1	0.2	0.15	18	0.981	38	0.992
			108	0.982	35	0.999
c_2	0.0024	0.00494	114	0.984	29	0.999
			115	0.984	95	1.000
Burst area	108	91, 3, 42, 18, 108	81	0.984	99	1.000
			88	0.984		

The performed experiments have confirmed that by investigating the pressure changes at the sensitive nodes it is possible to define an approximate area of the burst. The background leakage affects the gradients of the regression lines at the sensitive nodes but does not lead to erroneous identification of the burst area. It has been also observed

that the accuracy of burst area identification depends on the topology of a network. The Ocker Hill DMA (Figure 5.19) has a branch topology, where the root is represented by the inlet and the water arrives at an extreme node along a unique path. In this case the accuracy of burst area identification depends on the number of loggers in a branch. The identification results are normally quite accurate for such a topology.

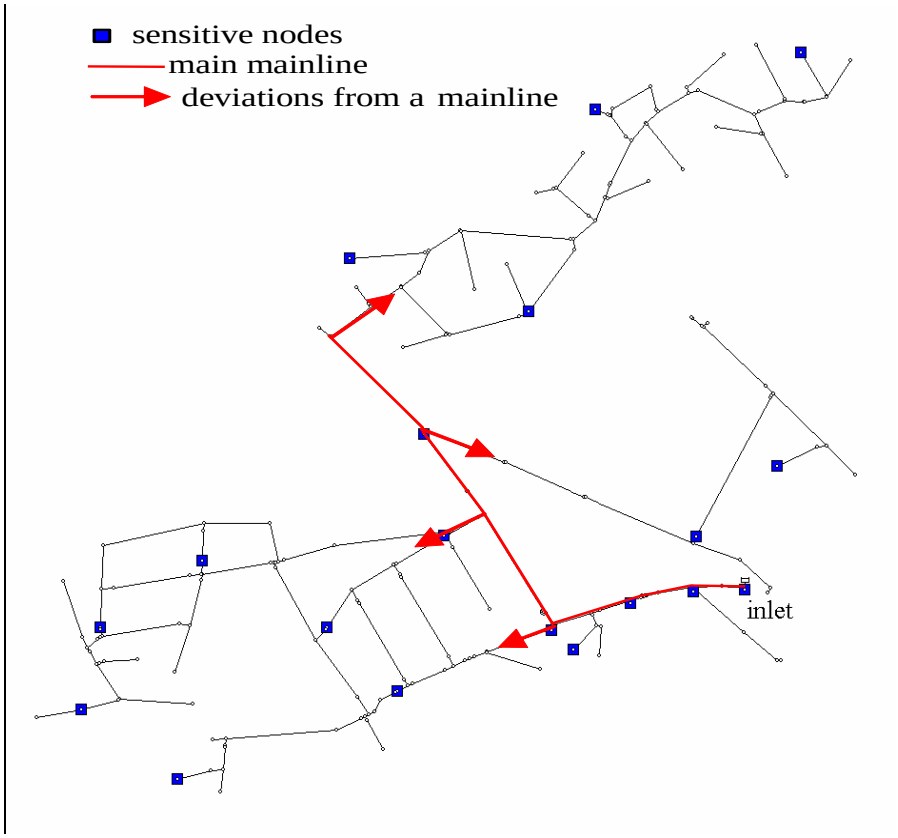

Fig. 5.19 The Ocker Hill DMA schematic

The Shenstone DMA has two inlet nodes in the network and each node is affected by both inlets which complicates the identification of the burst area. If the burst is located in the middle of the network, the burst area which is found tends to be quite big.

5.2.3 Summary

So the following conclusions have been made:

- The pressure at DMA nodes depends on the inlet pressure. The gradient of a pressure line, a plot of the pressure at a node versus the inlet pressure, is smallest for the burst node or a node close to the burst node.
- By investigating the pressure changes at the sensitive nodes it is possible to define an approximate area of the burst.
- The background leakage affects the gradients of the regression lines at the sensitive nodes but does not lead to erroneous identification of the burst area. It has been also observed that the accuracy of burst area identification depends on the topology of a network.

5.3 Algorithm for the burst location identification

The results shown in the previous Chapter 5.2 are satisfactory but for identification of burst locations with higher precision further research is required which is presented in this chapter. Two lines of investigation are possible, a deterministic approach or a statistical analysis. The decision about the choice of the approach depends on the nature of the input data available. The following data are considered to be available for the burst location identification:

- model of a network
- inlet pressure which is stepped during the field experiment
- inlet flow
- list of sensitive nodes
- pressure measurements at the sensitive nodes
- the total average demand, the burst coefficient and the total background leakage coefficient which are calculated using the hybrid method for burst detection described in Chapter 5.1.4.
- gradients of the regression pressure lines for the sensitive nodes.

The availability of the input data is limited by the scope of the field test and by the number and accuracy of the available loggers. In this situation application of deterministic methods is unrealistic and statistical methods have been employed in this research.

5.3.1 Application of statistical analysis.

Statistical methods calculate parameters of models to achieve the best match of the theoretical results and the physical processes.
First the discussion about the influence of bursts on pressure change at the sensitive nodes will be revisited. In Chapter 5.2.2 it was discovered that the regression line (approximating the pressure changes) with the minimum gradient indicates a burst in an immediate proximity. The burst affects also the pressure in nearby and hydraulically dependent nodes. Remote nodes are less affected by the burst and the gradient of the regression line is bigger and closer to 1. If the burst location is changed it will affect the pressure distribution in the whole network although to a different degree. This observation is supported by the results discussed in Chapter 5.1.3 where it was demonstrated that moving a burst location changes the total inlet flow and also in Chapter 5.2.2 where the burst location method was discussed.

There are different sources of errors in the identification of burst locations, some are introduced at the stage of determining the IMF coefficients and some are introduced by measurement errors of the pressure at the sensitive nodes. In such a situation use of statistical methods is required. The main idea is to perform the pressure stepping field experiment and record the pressure changes at the sensitive nodes. A similar experiment is performed on the simulation model using data evaluated earlier; the demand, the background leakage flow and the burst flow. The burst is allocated to different nodes of the simulation model and the theoretical gradient of the pressure line at each sensitive node is compared with the measured gradient. The comparison is done with the help of the chi-square criterion

The precise formulation of the algorithm is given below:

1. A hydraulic model of the network is prepared.
2. The field experiment is carried out. It is enough to apply three different inlet pressure values to approximate the gradient of a pressure line.
3. The hydraulic model is updated. The total demand and the total background leakage, earlier calculated with the hybrid method, are distributed according to the number of consumers at each node.

4. The burst, with the size which was calculated earlier by the hybrid method, is allocated alternately at each node of the network and the scenario is simulated.
5. Matrices of pressure changes at the sensitive nodes for each burst site are formed.
6. Gradients of the pressure lines at the sensitive nodes for each burst site are calculated.
7. The theoretical gradients of pressure lines are compared with the measured gradients at the sensitive nodes by applying the χ^2 criterion. A vector which contains χ^2 values for each theoretical burst site is constructed. The minimum value of χ^2 points to the burst site.

The flowchart of the algorithm is given in Fig.5.20 and programme code is given in Appendix F.

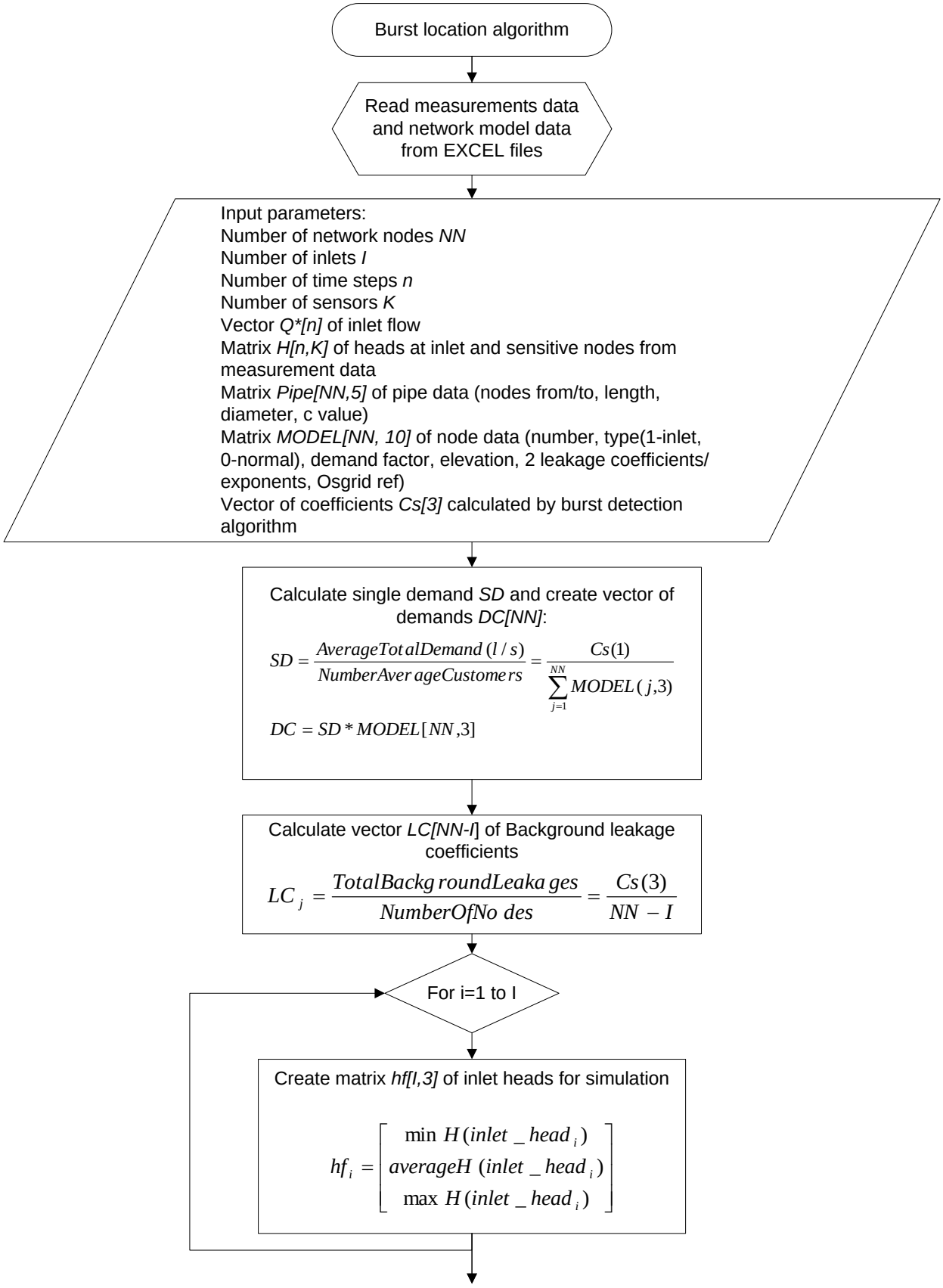
Burst location algorithm
Read measurements data and network model data from EXCEL files
Input parameters:
Number of network nodes NN
Number of inlets I
Number of time steps n
Number of sensors K
Vector Q*[n] of inlet flow
Matrix H[n,K] of heads at inlet and sensitive nodes from measurement data
Matrix Pipe[NN,5] of pipe data (nodes from/to, length, diameter, c value)
Matrix MODEL[NN, 10] of node data (number, type(1-inlet, 0-normal), demand factor, elevation, 2 leakage coefficients/ exponents, Osgrid ref)
Vector of coefficients Cs[3] calculated by burst detection algorithm
Calculate single demand SD and create vector of demands DC[NN]:
$SD = \frac{AverageTotalDemand\,(l/s)}{NumberAverageCustomers} = \frac{Cs(1)}{\sum_{j=1}^{NN} MODEL(j,3)}$
$DC = SD * MODEL[NN,3]$
Calculate vector LC[NN-I] of Background leakage coefficients
$LC_j = \frac{TotalBackgroundLeakages}{NumberOfNodes} = \frac{Cs(3)}{NN - I}$
For i=1 to I
Create matrix hf[I,3] of inlet heads for simulation
$hf_i = \begin{bmatrix} \min H(inlet\_head_i) \\ averageH(inlet\_head_i) \\ \max H(inlet\_head_i) \end{bmatrix}$

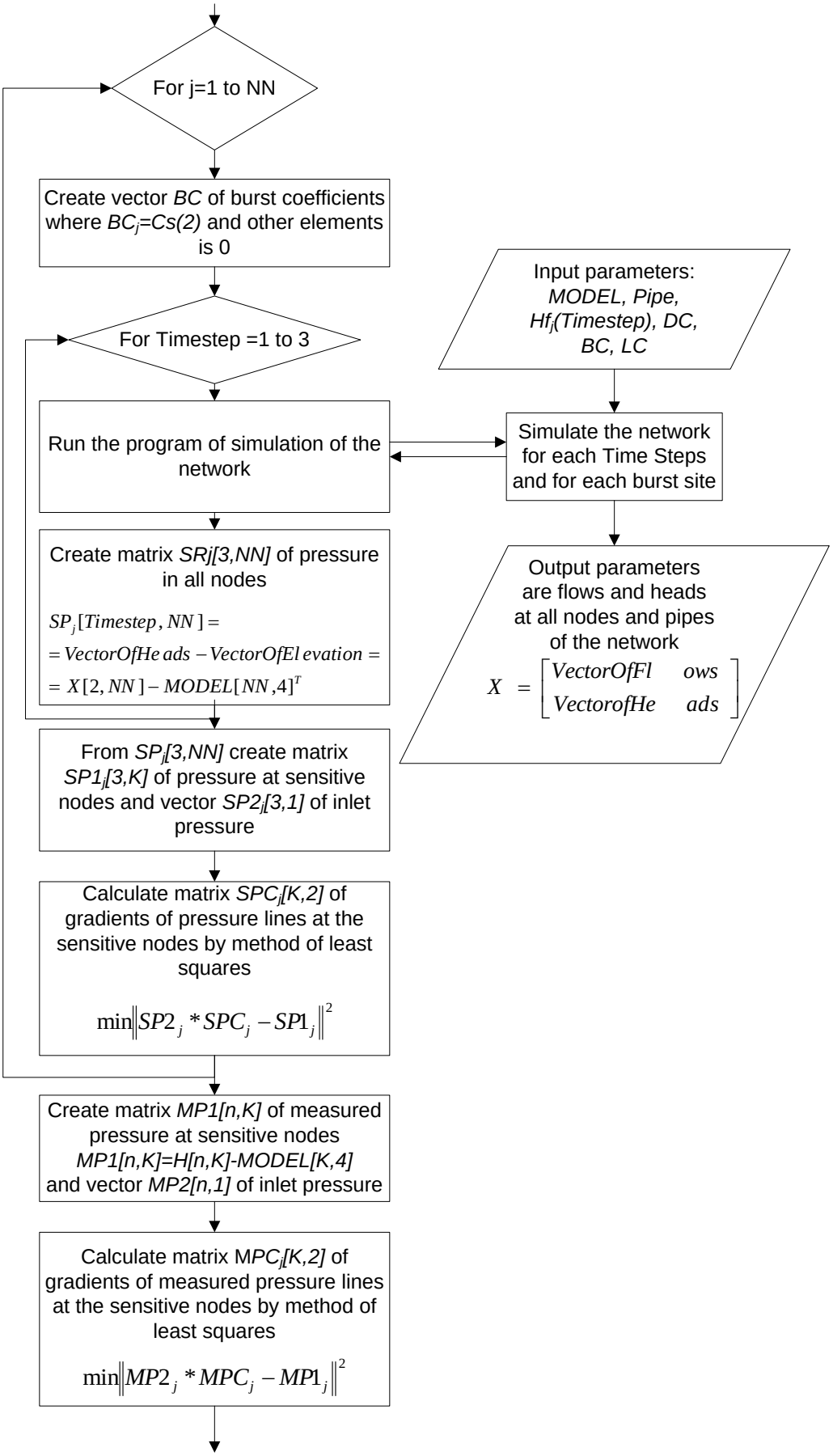
For j=1 to NN
Create vector BC of burst coefficients where BCj=Cs(2) and other elements is 0
For Timestep =1 to 3
Input parameters: MODEL, Pipe, Hfj(Timestep), DC, BC, LC
Run the program of simulation of the network
Simulate the network for each Time Steps and for each burst site
Create matrix SRj[3,NN] of pressure in all nodes
SPj[Timestep, NN] =
= VectorOfHeads − VectorOfElevation =
= X[2, NN] − MODEL[NN,4]T
Output parameters are flows and heads at all nodes and pipes of the network
X = [VectorOfFlows; VectorofHeads]
From SPj[3,NN] create matrix SP1j[3,K] of pressure at sensitive nodes and vector SP2j[3,1] of inlet pressure
Calculate matrix SPCj[K,2] of gradients of pressure lines at the sensitive nodes by method of least squares
min‖SP2j * SPCj − SP1j‖2
Create matrix MP1[n,K] of measured pressure at sensitive nodes MP1[n,K]=H[n,K]-MODEL[K,4] and vector MP2[n,1] of inlet pressure
Calculate matrix MPCj[K,2] of gradients of measured pressure lines at the sensitive nodes by method of least squares
min‖MP2j * MPCj − MP1j‖2

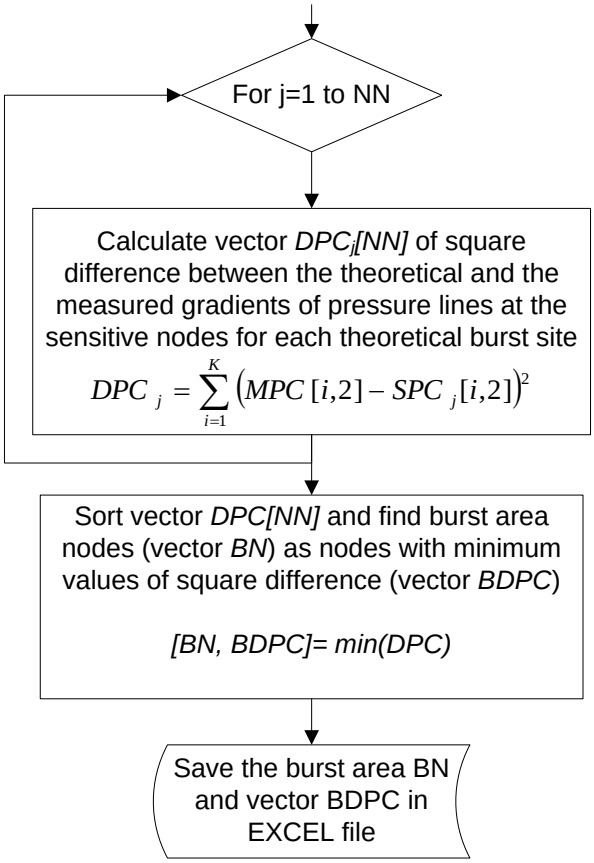

Fig. 5.20 A flowchart for burst location identification

The output from this algorithm is a set of network nodes at which a burst is most likely. The algorithm has been validated on the already considered case studies of the Shenstone and Ocker Hill DMAs shown in Figures 5.17 and 5.19.

The selected results of the experiments are given in Tables 5.14 and 5.15 below. For the Ocker Hill DMA model the inlet head (node 165) has been varied from 156 m to 191 m (which corresponds to the pressure changes from 18.5 m to 53.5m). For the Shenstone DMAs water network model the inlet head has been varied from *135 m* to *160 m* at Inlet 1 (node 95) and from *134 m* to *159 m* at Inlet 2 (node 99).

Table 5.14 Ocker Hill DMA burst location results

<table>
<tr><th>Parameter</th><th>Set values</th><th>Obtained results</th></tr>
<tr><td>burst node</td><td>59</td><td><table><tr><th>Node</th><th>The value of χ^2</th></tr><tr><td>57</td><td>2.66E-05</td></tr><tr><td>58</td><td>2.82E-05</td></tr><tr><td>55</td><td>3.27E-05</td></tr><tr><td>56</td><td>3.39E-05</td></tr><tr><td>59</td><td>3.58E-05</td></tr><tr><td>88</td><td>4.17E-05</td></tr></table></td></tr>
<tr><td>d (l/s)</td><td>4</td><td>3.9892</td></tr>
<tr><td>c_1</td><td>0.5</td><td>0.50865</td></tr>
<tr><td>c_2</td><td>0.006525</td><td>0.006444</td></tr>
<tr><td>burst node</td><td>141</td><td><table><tr><th>Node</th><th>The value of χ^2</th></tr><tr><td>141</td><td>8.74E-05</td></tr><tr><td>140</td><td>8.77E-05</td></tr><tr><td>146</td><td>8.81E-05</td></tr><tr><td>147</td><td>8.92E-05</td></tr><tr><td>139</td><td>8.92E-05</td></tr><tr><td>144</td><td>8.93E-05</td></tr><tr><td>154</td><td>8.93E-05</td></tr></table></td></tr>
<tr><td>d (l/s)</td><td>3</td><td>2.422476</td></tr>
<tr><td>c_1</td><td>0.37</td><td>0.419613</td></tr>
<tr><td>c_2</td><td>0.01613</td><td>0.015762</td></tr>
</table>

Table 5.15 Shenstone DMA burst location results

<table>
<tr><th>Parameter</th><th>Set values</th><th>Obtained results</th></tr>
<tr><td>burst node</td><td>67</td><td><table><tr><th>Node</th><th>The value of χ^2</th></tr><tr><td>67</td><td>8.44E-07</td></tr><tr><td>63</td><td>8.49E-07</td></tr><tr><td>51</td><td>8.65E-07</td></tr><tr><td>56</td><td>1.86E-06</td></tr><tr><td>61</td><td>4.69E-06</td></tr></table></td></tr>
<tr><td>d (l/s)</td><td>2</td><td>1.99</td></tr>
<tr><td>c_1</td><td>0.2</td><td>0.2</td></tr>
<tr><td>c_2</td><td>0.00239</td><td>0.00238</td></tr>
</table>

<table>
<tr><th>Parameter</th><th>Set values</th><th>Obtained results</th></tr>
<tr><td>burst node</td><td>80</td><td><table><tr><th>Node</th><th>The value of χ^2</th></tr><tr><td>80</td><td>2.26E-06</td></tr><tr><td>69</td><td>7.20E-06</td></tr><tr><td>33</td><td>8.27E-06</td></tr><tr><td>54</td><td>2.67E-05</td></tr></table></td></tr>
<tr><td>d (l/s)</td><td>4</td><td>3.975</td></tr>
<tr><td>c_1</td><td>0.24</td><td>0.24</td></tr>
<tr><td>c_2</td><td>0.002216</td><td>0.002193</td></tr>
<tr><td>burst node</td><td>96</td><td><table><tr><th>Node</th><th>The value of χ^2</th></tr><tr><td>96</td><td>4.18E-06</td></tr><tr><td>108</td><td>5.42E-06</td></tr><tr><td>80</td><td>1.44E-05</td></tr><tr><td>86</td><td>2.57E-05</td></tr><tr><td>112</td><td>2.67E-05</td></tr><tr><td>33</td><td>2.74E-05</td></tr><tr><td>69</td><td>3.04E-05</td></tr></table></td></tr>
<tr><td>d (l/s)</td><td>0.2</td><td>0.11</td></tr>
<tr><td>c_1</td><td>0.15</td><td>0.159</td></tr>
<tr><td>c_2</td><td>0.005</td><td>0.0049</td></tr>
<tr><td>burst node</td><td>96</td><td><table><tr><th>Node</th><th>The value of χ^2</th></tr><tr><td>107</td><td>2.87E-03</td></tr><tr><td>108</td><td>2.96E-03</td></tr><tr><td>96</td><td>2.98E-03</td></tr><tr><td>97</td><td>2.98E-03</td></tr><tr><td>93</td><td>3.01E-03</td></tr><tr><td>72</td><td>3.03E-03</td></tr><tr><td>61</td><td>3.06E-03</td></tr></table></td></tr>
<tr><td>d (l/s)</td><td>0.2</td><td>0</td></tr>
<tr><td>c_1</td><td>0.15</td><td>0.34</td></tr>
<tr><td>c_2</td><td>0.04666</td><td>0.0419</td></tr>
</table>

<table>
<tr><th>Parameter</th><th>Set values</th><th>Obtained results</th></tr>
<tr><td>burst node</td><td>96</td><td><table><tr><th>Node</th><th>The value of χ^2</th></tr><tr><td>66</td><td>1.04E-05</td></tr><tr><td>70</td><td>1.04E-05</td></tr><tr><td>71</td><td>1.04E-05</td></tr><tr><td>87</td><td>1.18E-05</td></tr><tr><td>96</td><td>1.37E-05</td></tr><tr><td>111</td><td>1.47E-05</td></tr><tr><td>113</td><td>1.56E-05</td></tr></table></td></tr>
<tr><td>d (l/s)</td><td>5.5</td><td>5.45</td></tr>
<tr><td>c_1</td><td>0.15</td><td>0.15</td></tr>
<tr><td>c_2</td><td>0.005</td><td>0.00496</td></tr>
<tr><td>burst node</td><td>96</td><td><table><tr><th>Node</th><th>The value of χ^2</th></tr><tr><td>87</td><td>1.55E-05</td></tr><tr><td>96</td><td>1.85E-05</td></tr><tr><td>71</td><td>1.91E-05</td></tr><tr><td>70</td><td>1.93E-05</td></tr><tr><td>66</td><td>1.96E-05</td></tr><tr><td>111</td><td>2.56E-05</td></tr><tr><td>104</td><td>2.68E-05</td></tr></table></td></tr>
<tr><td>d (l/s)</td><td>11</td><td>10.95</td></tr>
<tr><td>c_1</td><td>0.15</td><td>0.15</td></tr>
<tr><td>c_2</td><td>0.005</td><td>0.00494</td></tr>
<tr><td>burst node</td><td>98</td><td><table><tr><th>Node</th><th>The value of χ^2</th></tr><tr><td>98</td><td>2.00E-06</td></tr><tr><td>104</td><td>3.51E-06</td></tr><tr><td>103</td><td>3.92E-06</td></tr><tr><td>71</td><td>9.53E-06</td></tr><tr><td>70</td><td>9.54E-06</td></tr><tr><td>66</td><td>9.54E-06</td></tr><tr><td>111</td><td>1.15E-05</td></tr></table></td></tr>
<tr><td>d (l/s)</td><td>3.8</td><td>3.836697</td></tr>
<tr><td>c_1</td><td>0.2</td><td>0.194077</td></tr>
<tr><td>c_2</td><td>0.0024</td><td>0.002413</td></tr>
</table>

The results of the above experiment show that, at least for the data of numerical experiments, the developed algorithm identifies the burst location very precisely. It was

observed that the exponent (order) of the χ^2 value depends on the accuracy of the IFM coefficients (*d, c1, c2*), i.e. the more accurate the coefficients, the smaller the value of χ^2 is achieved.

This exponent can be used as a criterion of accuracy of the burst location identification algorithm.

- If χ^2 is of 10^{-6} order or smaller the burst node is located precisely;
- If χ^2 is bigger than 10^{-6} the area of burst is determined (not the node) and a further investigation using different methods, for example listening sticks or noise correlation should be used.

5.3.2 Influence of sensitive nodes selection.

For the field experiment loggers can only be installed at available hydrants which do not necessarily overlap with the selected sensitive nodes. The effects of random distribution of loggers on the accuracy of the burst location identification algorithms are investigated here. A group of people who are not experts in water engineering have been asked to place 15 pressure loggers in the Shenstone DMA and placement results are depicted in Fig. 5.21.

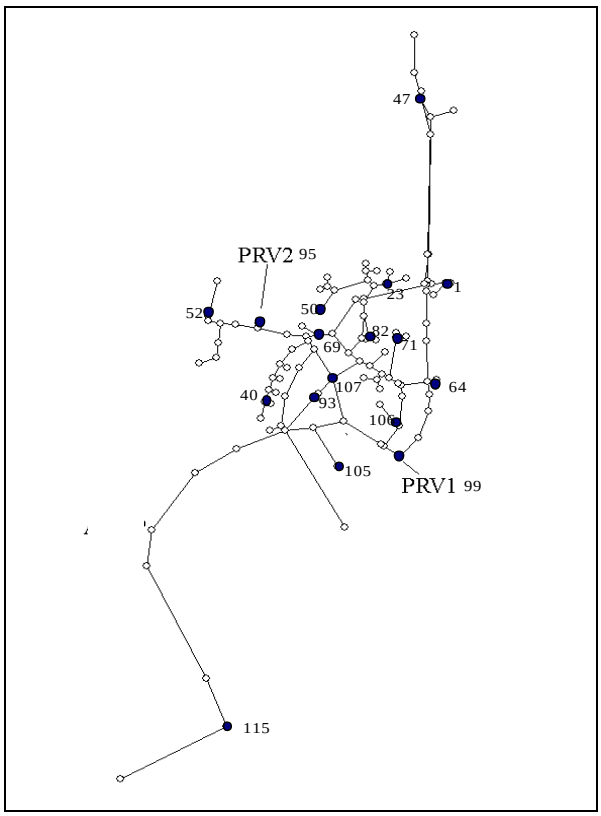

Fig. 5.21 Location of measurement points at the Shenstone DMA

The intuitive method resulted in uniform distribution of the loggers over all parts of the network.

The following conditions were set to obtain the 'experimental' data:

- inlet head has been varied from *135 m* to *160 m* on Inlet 1 (PRV 2 OUTLET node 95) and from *134 m* to *159 m* on Inlet 2 (PRV 1 OUTLET node 99);
- experimental data have been generated by the hydraulic simulations (the validity of this was investigated in Chapter 5.1.2);
- the simulations have been carried out for various values of the total demand, the various values of the total background leakage, and various burst sites;
- the following simulation results have been considered as the experimental data:
    - values of the inlet heads (nodes 99 and 95),
    - values of head at "sensitive nodes" (nodes 52, 69, 40, 82, 50, 71, 105, 64, 1, 115, 47, 93, 23, 107, 106),
    - values of inlet flows (nodes 99 and 95).

The generated experimental data have been initially processed by the hybrid method in order to obtain the estimated total demand, the estimated coefficient of the total background leakage and the estimated coefficient of the burst. Subsequently, the burst

location identification algorithm has been used to find the site of the presumed burst. The estimation results of the experiments are compared to the set values in the hydraulic simulator. The results are given in Table 5.16 below.

Table 5.16 The results of experiments with other "Sensitive nodes"

<table>
<tr><th>Parameter</th><th>Set values</th><th>Obtained results</th></tr>
<tr><td>burst node</td><td>34</td><td><table><tr><th>Node</th><th>The value of χ^2</th></tr><tr><td>34</td><td>6.84E-07</td></tr><tr><td>42</td><td>1.10E-06</td></tr><tr><td>41</td><td>2.10E-06</td></tr><tr><td>47</td><td>3.82E-06</td></tr><tr><td>6</td><td>1.26E-04</td></tr></table></td></tr>
<tr><td>d (l/s)</td><td>2</td><td>2.01433</td></tr>
<tr><td>c_1</td><td>0.15</td><td>0.149735</td></tr>
<tr><td>c_2</td><td>0.002353</td><td>0.002348</td></tr>
<tr><td>burst node</td><td>67</td><td><table><tr><th>Node</th><th>The value of χ^2</th></tr><tr><td>62</td><td>7.85E-07</td></tr><tr><td>67</td><td>7.87E-07</td></tr><tr><td>63</td><td>7.95E-07</td></tr><tr><td>51</td><td>8.44E-07</td></tr><tr><td>56</td><td>8.68E-07</td></tr><tr><td>61</td><td>1.61E-06</td></tr></table></td></tr>
<tr><td>d (l/s)</td><td>2</td><td>1.996932</td></tr>
<tr><td>c_1</td><td>0.2</td><td>0.20195</td></tr>
<tr><td>c_2</td><td>0.00239</td><td>0.002384</td></tr>
<tr><td>burst node</td><td>96</td><td><table><tr><th>Node</th><th>The value of χ^2</th></tr><tr><td>96</td><td>4.55E-04</td></tr><tr><td>108</td><td>2.01E-03</td></tr><tr><td>80</td><td>2.72E-03</td></tr><tr><td>112</td><td>3.52E-03</td></tr><tr><td>87</td><td>4.74E-03</td></tr></table></td></tr>
<tr><td>d (l/s)</td><td>5.5</td><td>4.851102</td></tr>
<tr><td>c_1</td><td>0.8</td><td>0.932311</td></tr>
<tr><td>c_2</td><td>0.0229</td><td>0.021861</td></tr>
</table>

<table>
<tr><th>Parameter</th><th>Set values</th><th>Obtained results</th></tr>
<tr><td>burst node</td><td>108</td><td><table><tr><th>Node</th><th>The value of χ^2</th></tr><tr><td>108</td><td>2.80E-03</td></tr><tr><td>96</td><td>6.80E-03</td></tr><tr><td>112</td><td>1.06E-02</td></tr><tr><td>107</td><td>1.36E-02</td></tr><tr><td>85</td><td>1.63E-02</td></tr></table></td></tr>
<tr><td>d (l/s)</td><td>5.5</td><td>1.597663</td></tr>
<tr><td>c_1</td><td>0.8</td><td>1.507342</td></tr>
<tr><td>c_2</td><td>0.05</td><td>0.043888</td></tr>
<tr><td>burst node</td><td>78</td><td><table><tr><th>Node</th><th>The value of χ^2</th></tr><tr><td>78</td><td>2.17E-03</td></tr><tr><td>68</td><td>5.53E-03</td></tr><tr><td>85</td><td>8.49E-03</td></tr><tr><td>82</td><td>1.01E-02</td></tr><tr><td>84</td><td>1.49E-02</td></tr></table></td></tr>
<tr><td>d (l/s)</td><td>11</td><td>7.199524</td></tr>
<tr><td>c_1</td><td>0.8</td><td>1.481012</td></tr>
<tr><td>c_2</td><td>0.05</td><td>0.043619</td></tr>
<tr><td>burst node</td><td>76</td><td><table><tr><th>Node</th><th>The value of χ^2</th></tr><tr><td>76</td><td>4.66E-04</td></tr><tr><td>73</td><td>2.05E-03</td></tr><tr><td>64</td><td>3.25E-03</td></tr><tr><td>75</td><td>4.36E-03</td></tr><tr><td>57</td><td>4.39E-03</td></tr></table></td></tr>
<tr><td>d (l/s)</td><td>11</td><td>10.81651</td></tr>
<tr><td>c_1</td><td>0.8</td><td>0.838669</td></tr>
<tr><td>c_2</td><td>0.0229</td><td>0.021985</td></tr>
</table>

The results show robustness of the burst location identification algorithm with respect to logger placements.

5.4 Exponent in the burst term

Recent research (Ulanicki et al. 2006) indicated that the burst term in the IFM model (the relationship between leakage flow and water pressure) can have a higher exponent than 0.5 depending on the pipe material, fluid properties for different Reynolds number and on the surrounding soil (Noack and Ulanicki 2006) from 0.5 to 2.5. In such a situation the previously described algorithms require modification. The original IMF model had the following form:

$$q = d + c_1 p_i^{0.5} + c_2 p_{AZNP}^{1.5} \tag{5.7}$$

The model is now modified to make the exponent of the burst term an unknown variable:

$$q = d + c_1 p_i^{e} + c_2 p_{AZNP}^{1.5}$$

where *e, d, c1, c2* are now the unknown parameters, which can be evaluated using Matlab. The estimated value of the exponent together with other coefficients are entered as input data to the burst detection algorithm.

So with such modification the algorithm became more universal and it will be applied in Chapter 6 where a real case study is presented.

5.5 Summary

The developed identification procedure for the burst location is more precise than other methods currently available.

The exponent of the value of χ^2 can be used as a criterion of accuracy of the burst location identification algorithm. The given criterion specifies also the accuracy of the performed experiments.

The algorithm of burst location identification developed by the author allows for finding a potential burst site with quite high precision.

6 Practical case studies

Data from real field experiments have been provided by the Water Software Systems group. It created the opportunity to test the developed algorithms in a real life model rather than purely by numerical experiments, the results are presented in this chapter.

6.1 General condition of performing the experiment.

The field tests have been an extension of the FAVOR test – apart from monitoring the inlet pressures and flows additional pressures were measured inside a DMA (e-FAVOR test).

There were several experimental parameters to be decided:

- Sampling interval – should be short enough to give a reasonable amount of data at each pressure level but large enough to avoid transients and measurement noise (e.g. flow measurement are averaged over the interval). Thirty seconds to 2 minutes has been found to be suitable.
- Accuracy of measurements – obviously the more accurate the better. They should be sufficiently accurate to record head losses across the network. The required accuracy of pressure gauges was 0.1m, and the required accuracy of flow meters was 0.1 l/s.
- Number of measurements points – again, the more the better but there are practical limits. The precision of the burst location depends on pressure changes caused by the leakage flow pattern between loggers, so the identification will be more accurate if they are closer together.
- Pressure steps – it is beneficial to have a large range of inlet pressure changes but the experiment should not upset the water customers. A pressure of 15m has to be maintained at each point in the network to meet the OFWAT requirements and the pressure can only go as high as the inlet pressure to the PRV (minus a small head loss of around 5 m across the PRV).

6.2 Ocker Hill case study

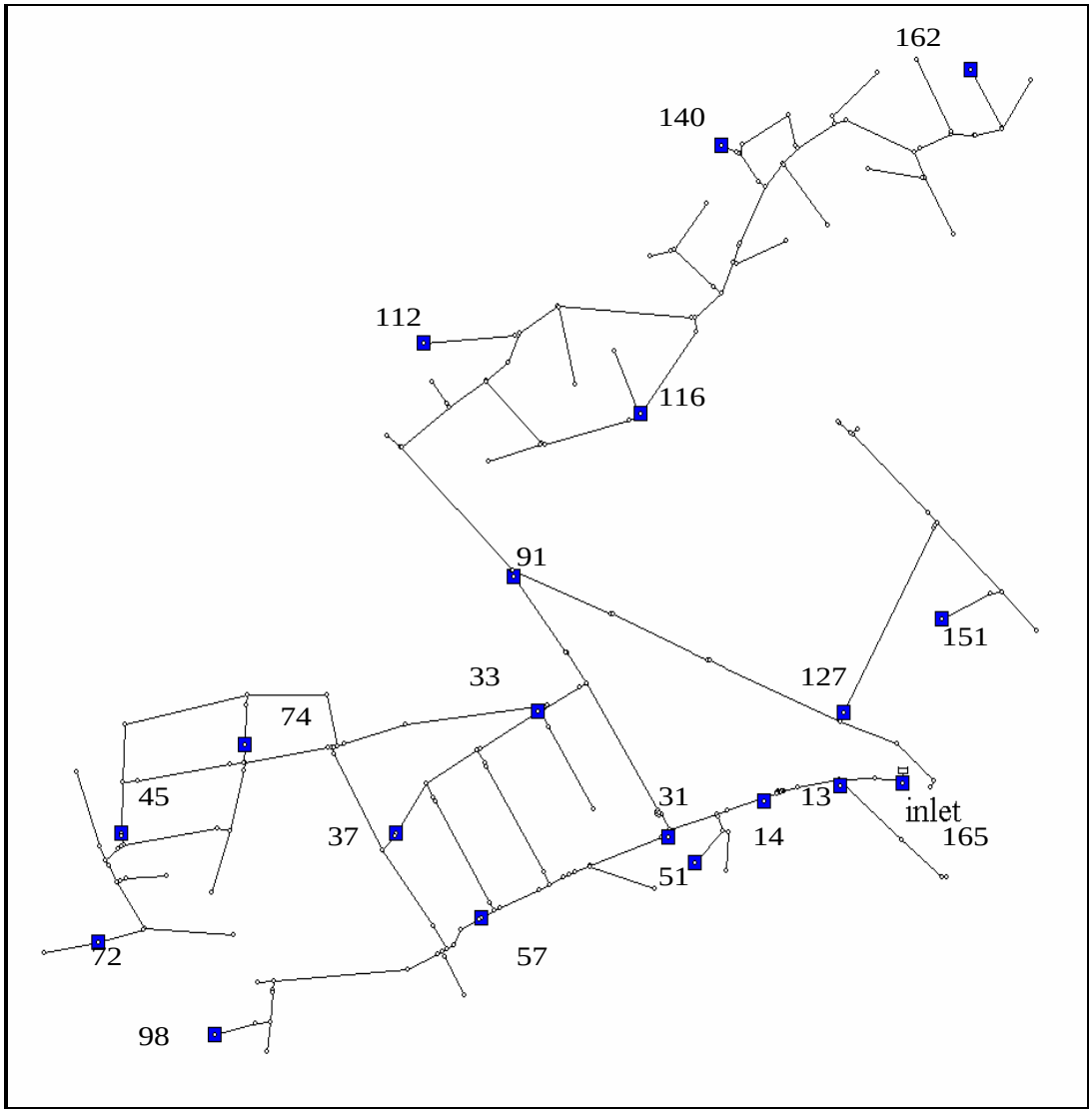

Fig. 6.1 Ocker Hill DMA schematic

Ocker Hill, shown in Fig. 6.1, is a single-feed DMA supplying 1850 domestic properties and 25 commercial customers. The inlet is through a 6" Rollseal PRV and there is one disused PRV (4" Bermad) about 150m downstream from the inlet. The experiment was performed by members of the Water Software System research group during the nights of 23rd and 24th March 2005 and consisted of a sequence of pre-programmed pressure steps, shown in Figure 6.2.

Data were recorded every 30 seconds and the measured variables were:

- Inlet flow

- PRV inlet pressure
- PRV outlet pressure
- Pressure at the following hydrants

  10 Kidd Croft

  20 Hopton Close

  41 Wooding Crescent

  27 Jackson Close

  80 Ocker Hill Road

  Corner Gospel Oak Road & Prospect St

  8 The Coppice

  37 Windsor Road

  1 North Road

  77 North Road

  8 Dick Sheppard Avenue

  5 Waring Road

  9 Shelley Avenue

  41 St Mark's Road

  1 Mott Close

  2 Solari Close

  Inlet of second PRV

  Corner Spring Street & Ocker Hill Road

The recorded data are shown in Figure 6.2. There is a clear correlation between the head and the flow measurements – when the head is decreased the flow decreases as well due to the volume of flow through leaks being reduced. The total flow reduction due to head drop of 30m is around 4.5l/s.

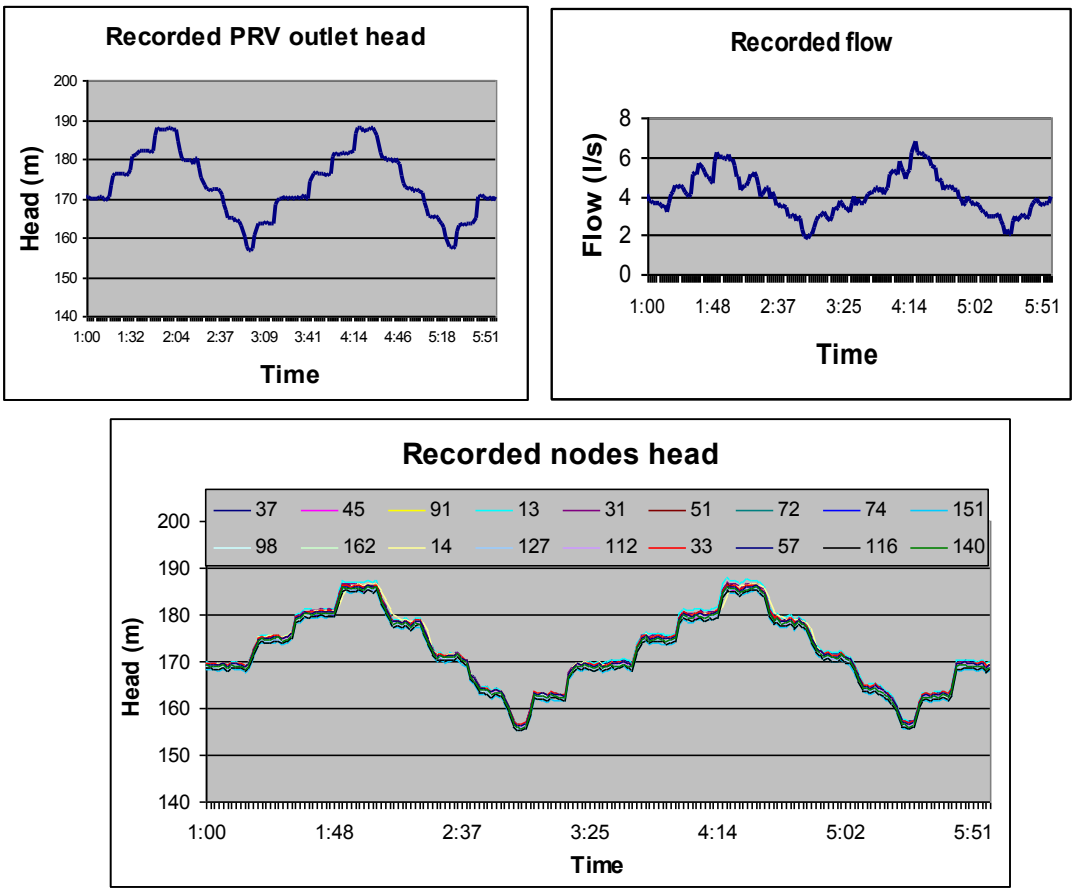

Fig. 6.2 Recorded data (Ocker Hill DMA)

The following terms of the IFM:

- demand
- fixed area burst leakage (burst coefficient) across the DMA
- variable area burst leakage (background leakage coefficient) across the DMA

have been calculated by the hybrid algorithm described in Chapter 5.1.4.

Table 6.1 Calculated results (Ocker Hill DMA)

Sensitive node	Demand factor (l/s)	Coefficient of the burst	Coefficient of the total background leakage	Value of χ^2 (difference between calculated and recorded inlet flows)
The burst exponent = 1.44968				
165	0.730393	0.021656	0	2.456042
37	0.350676	0.016086	0.003627	2.704906
45	0.590325	0	0.014098	2.715408
91	0.590325	0	0.014098	2.715408
13	0.978954	0.022717	0	2.496215
31	0.853587	0.022649	0	2.670476
51	0.683629	0.022253	0	2.677547
72	0.590325	0	0.014098	2.715408
74	0.590325	0	0.014098	2.715408
151	0.590325	0	0.014098	2.715408

98	0.590325	0	0.014098	2.715408
162	0.590325	0	0.014098	2.715408
14	0.590325	0	0.014098	2.715408
127	0.590325	0	0.014098	2.715408
140	0.082092	0.012493	0.005512	2.691486
112	0.590325	0	0.014098	2.715408
33	0.248723	0.018274	0.002202	2.687886
57	0.590325	0	0.014098	2.715408
116	0.590325	0	0.014098	2.715408

The results in yellow indicate one area of concentrated leakage with the exponent of 1.44968 near the inlet (node 165) as depicted in Figure 6.3. By looking at the exponent of the burst term and the values of parameters at other sensitive nodes, it is possible to draw a conclusion about the presence of the head loss (background leakage but not bursts) in the network. As indicated in Table 6.1, the difference between the calculated and the measured flows is big and the obtained results should be treated with caution.

Application of the burst location identification algorithm produced the following results:

Table 6.2 Results of the burst location identification algorithm (Ocker Hill DMA)

Burst node	Value of χ^2 (reflects an error in prediction of burst location)
20	1.4648E-03
19	1.6372E-03
66	1.7134E-03
21	1.8493E-03

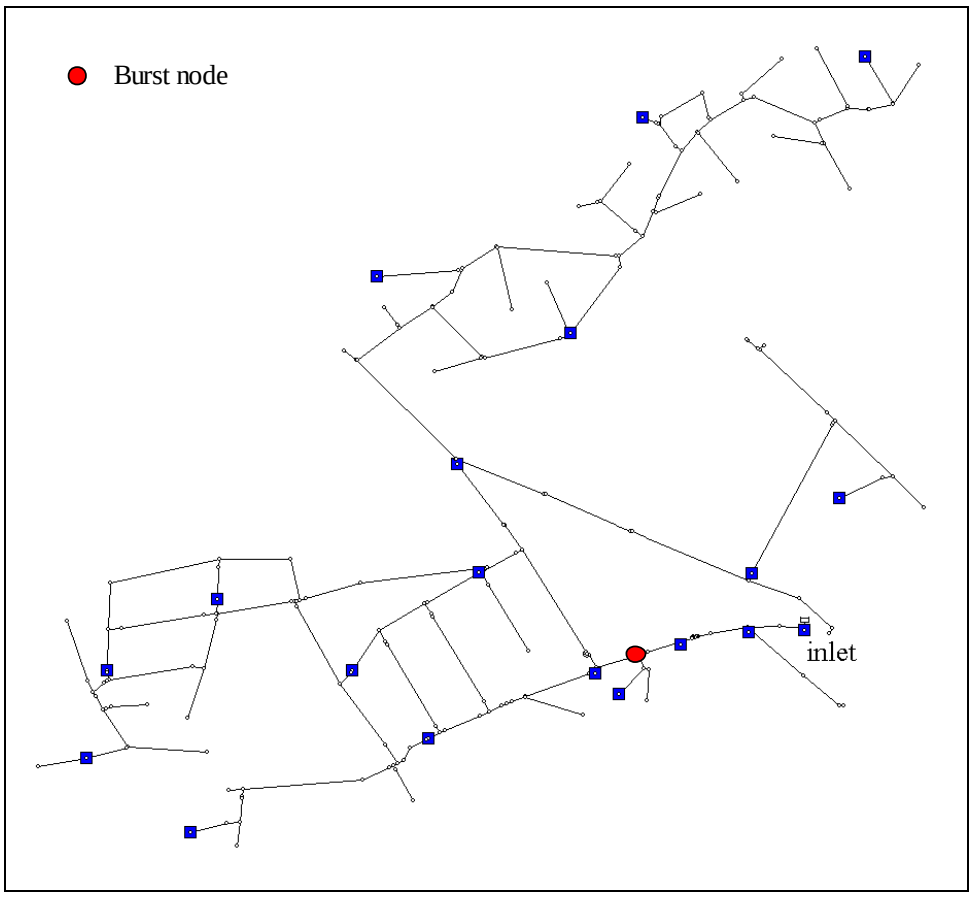

Fig. 6.3 Fixed area burst leakage in Ocker Hill DMA

The obtained results coincide with the results of the hybrid method algorithm, i.e. a small burst is indicated near the inlet, which most likely is explained by the presence of concentrated background leakage in this area.

6.3 Shenstone case study

Shenstone is fed through two PRV inlets (Figure 6.4) and supplies 1008 consumers (917 domestic and 91 commercial). The PRVs are 4" Bermad (St John) which is at the corner of St Johns Hill, and Bham Rd and 4" Rollseal (Lynn) which is in Lynne Lane.

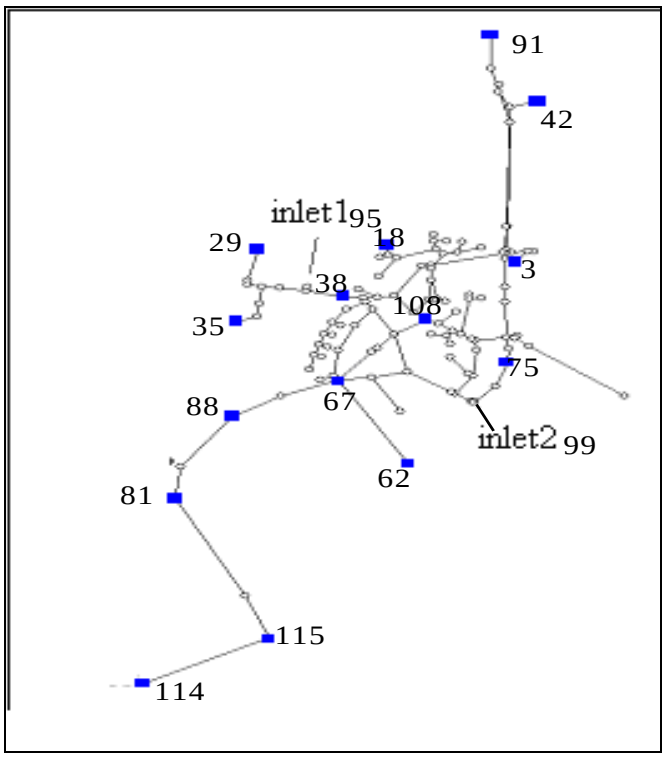

Fig. 6.4 Shenstone DMA schematic

The recorded data obtained during the field experiment are presented in Figure 6.5.

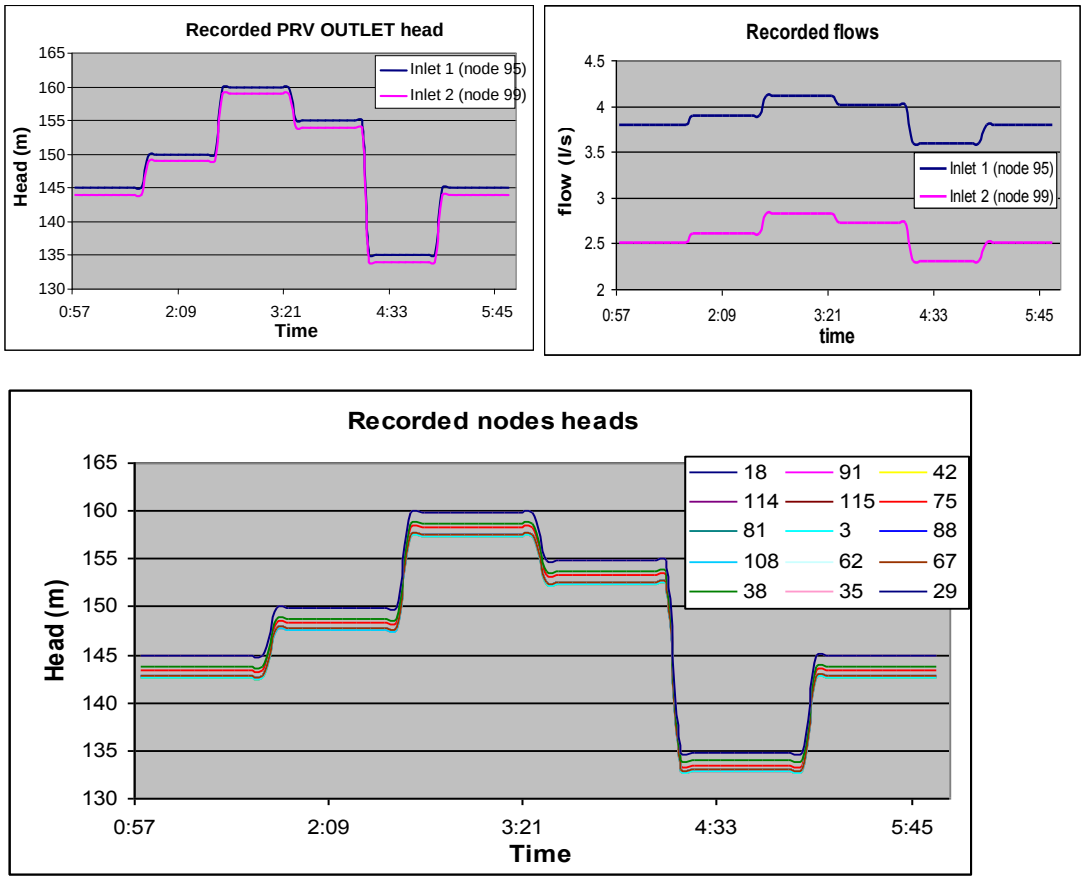

Fig. 6.5 Recorded data (Shenstone DMA)

The following terms of the IFM:

- demand
- fixed area burst leakage (burst coefficient) across the DMA
- variable area burst leakages (background leakage coefficients) across the DMA

have been calculated by the hybrid algorithm described in Chapter 5.1.4.

Table 6.3 Calculated results (Shenstone DMA)

Sensitive node	Demand factor (l/s)	Coefficient of the burst	Coefficient of the total background leakage	Value of χ^2 (difference between calculated and recorded inlet flows)
The burst exponent = 0.512104				
95	3.643539	0.284718	0.002128	4.99E-08
99	4.033422	0.242887	0.002276	9.31E-10
18	3.709304	0.279806	0.002165	3.93E-08
91	3.876389	0.261679	0.002224	5.94E-08
42	3.873712	0.262168	0.002225	1.79E-08
3	3.55773	0.294989	0.002115	7.11E-08
114	4.333455	0.208249	0.002425	7.74E-08
115	4.305799	0.211826	0.00241	6.26E-08
81	4.032276	0.244776	0.002283	2.08E-08
88	4.117065	0.234884	0.00232	1.54E-08
108	4.360773	0.204427	0.002443	1.16E-07
62	3.922307	0.257142	0.002238	6.8E-08
67	3.950318	0.253477	0.002255	1.01E-08
38	3.803718	0.269449	0.002187	1.4E-07
75	3.972916	0.250807	0.002251	1.81E-08
35	3.766198	0.271833	0.002176	1.6E-08
29	3.735147	0.275068	0.002165	1.97E-08

The results in yellow indicate both burst and background leakage in the network. The values of the χ^2 criterion confirm the high accuracy of the estimated values of the demand and the coefficients of the fixed and variable leakage terms.

Application of the algorithm for burst location identification has detected a burst site in the network:

Table 6.4 Results of the burst location identification algorithm (Shenstone DMA)

Burst node	Value of χ^2 (reflects an error in prediction of burst location)
80	3.2E-06
69	1.44E-05
33	1.67E-05

The obtained results especially the exponent of the χ^2 criterion indicates a high degree of probability of the burst presence at node 80. The value of the total demand flow is 4 l/s, the value of the coefficient of the fixed area leakage (burst) is 0.24, the value of the coefficient of the total background leakage is 0.00227.

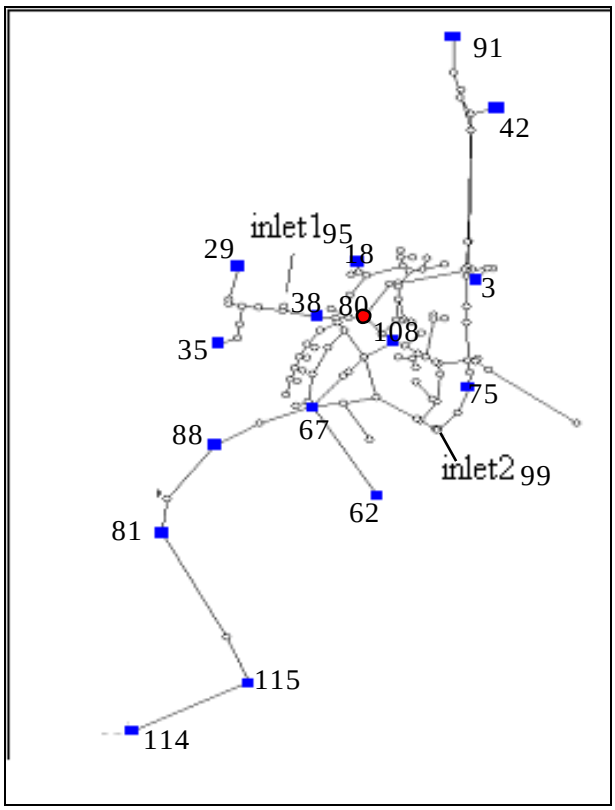

Fig. 6.6 Shenstone DMA, results of the experiment.

6.4 E054 – Drury Lane case study

E054 is a single-feed DMA supplying 253 domestic properties and 18 commercial properties of which 43 have a demand greater than 200 m^3/year. The total mains length is 9 km whilst 5 boundary valves enclose the area. There is one PRV at Walton Park (Figure 6.7). There are no major metered customers within this DMA. The experiment consisted of a sequence of pre-programmed pressure steps. It is assumed that there are 10 Cello loggers installed in the DMA. Node and element data for E054 DMA are shown at Appendix E.

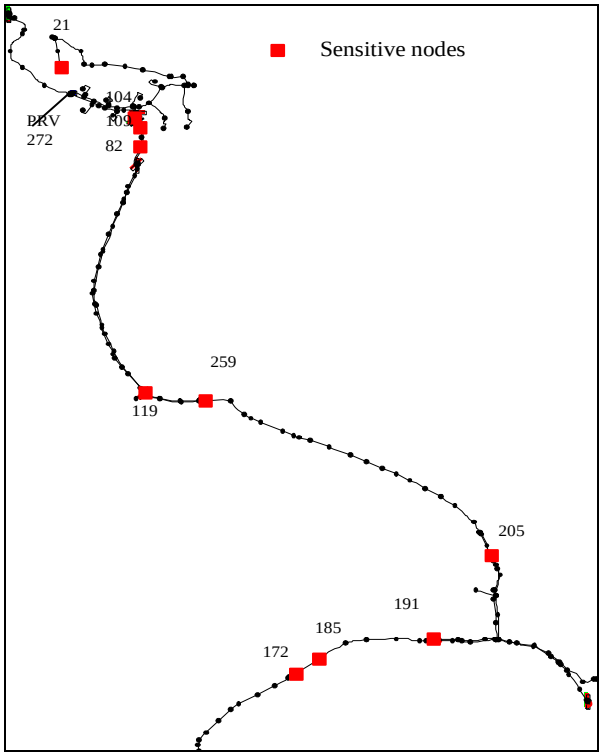

Fig. 6.7 E054 DMA schematic

The field measurements have not been available and therefore the experiment has been simulated using the program developed in Matlab and consists of two parts. The first part of the test was carried out between 22:00 hrs and 02:05 hrs. A single hydrant was opened at 5.0 l/s and the outlet pressure of the Walton Park PRV has been lowered via a number of pressure steps from 55m to 40m and then returned to 55 m using the same pressure step size. The recorded simulation data obtained during the experiment are presented in Figure 6.8.

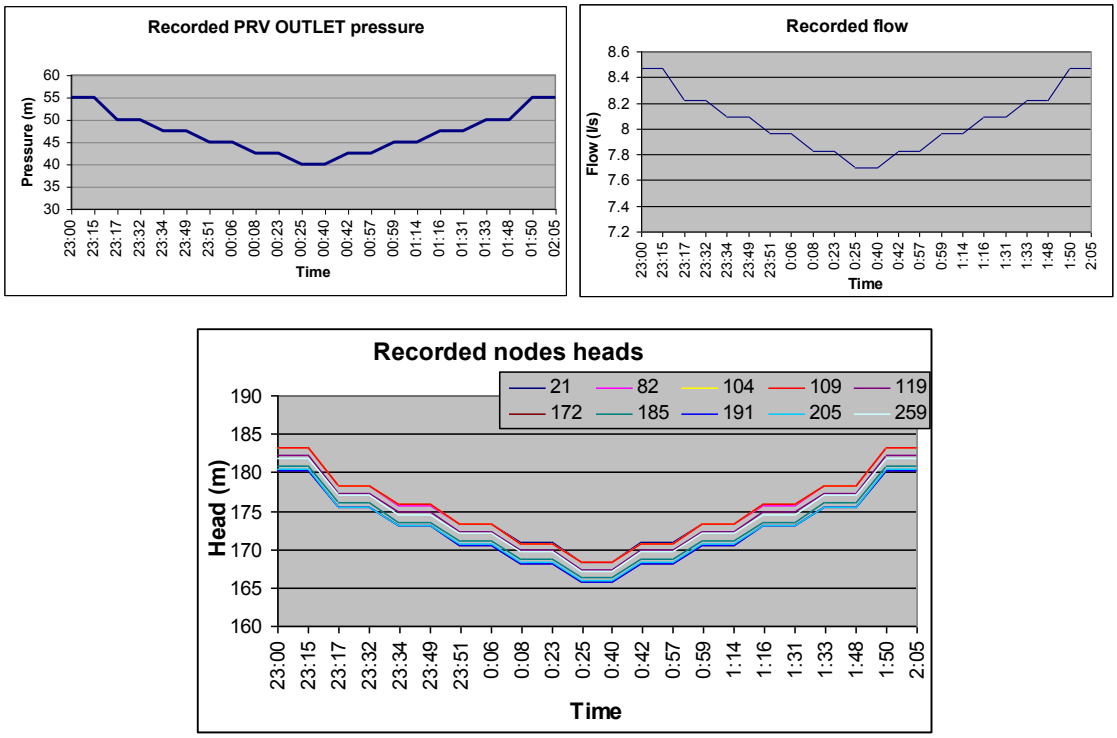

Fig. 6.8 First part of experiment. Recorded data.

The following terms of the IFM:

- demand
- fixed area burst leakages (burst coefficient) across the DMA
- variable area burst leakages (background leakage coefficients) across the DMA

have been calculated by the hybrid algorithm described in Chapter 5.1.4.

Table 6.5 Calculated results (First part of experiment)

Sensitive node	Demand factor (l/s)	Coefficient of the burst	Coefficient of the total background leakage	Value of χ^2 (difference between calculated and recorded inlet flows)
The burst exponent = 0.5				
272	4.47715	0.427843	0.002017	1.21E-07
21	4.052519	0.472961	0.001863	6.45E-08
82	6.011171	0.218857	0.002941	1.86E-06
104	6.008423	0.21928	0.002938	1.85E-06
109	6.008558	0.21926	0.002938	1.85E-06
119	5.936531	0.233564	0.002869	1.54E-06
172	0	0.800822	0.001128	1.93E-06
185	3.866816	0.497848	0.001805	4.80E-08
191	2.139402	0.654995	0.001368	1.05E-09
205	2.132612	0.655379	0.001366	1.02E-09
259	5.526152	0.299596	0.002547	6.48E-07

The results in yellow indicate both burst and background leakage in the network. The values of the χ^2 criterion confirm the high accuracy of the estimated values of the demand and the coefficients of the fixed and variable leakage terms.

Application of the algorithm for burst location identification has detected a burst site in the network:

Table 6.6 Results of the burst location identification algorithm (First part of experiment)

Burst node	Value of χ^2 (reflects an error in prediction of burst location)
206	7.04E-06
205	1.34E-05
203	1.45E-05
202	1.60E-05
204	2.09E-05

The obtained results especially the exponent of the χ^2 criterion indicate a high degree of probability of the burst presence close to node 206 (Figure 6.9). The value of the total demand flow is 2.133 l/s, the value of the coefficient of the fixed area leakage (burst) is 0.655 (which corresponds to a burst flow of about 5 l/s), the value of the coefficient of the total background leakage is 0.001366.

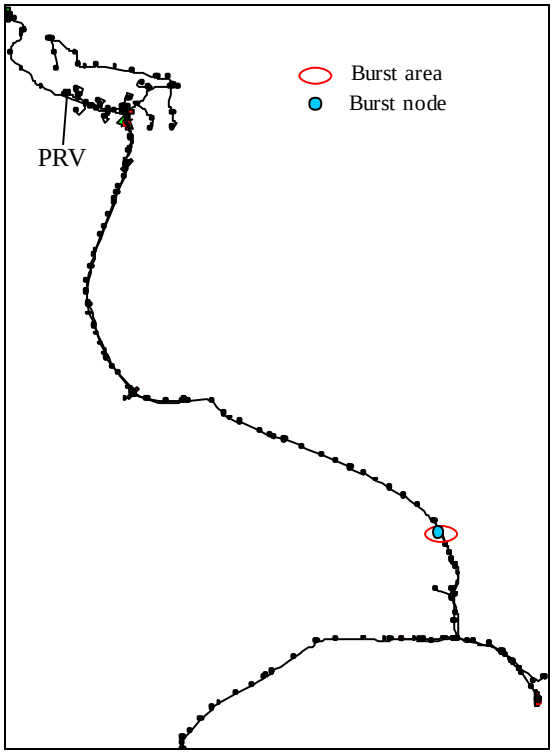

Fig. 6.9 E054 DMA. Results of first part of experiment.

The second part of test was carried out between 02:30 hrs and 05:30 hrs. A single hydrant has been opened at 1 l/s and the outlet pressure of the Walton Park PRV has been lowered via a number of pressure steps from 55m to 40m and then returned to 55 m using the same pressure step sizes. The recorded data obtained during the experiment are presented in Figure 6.10.

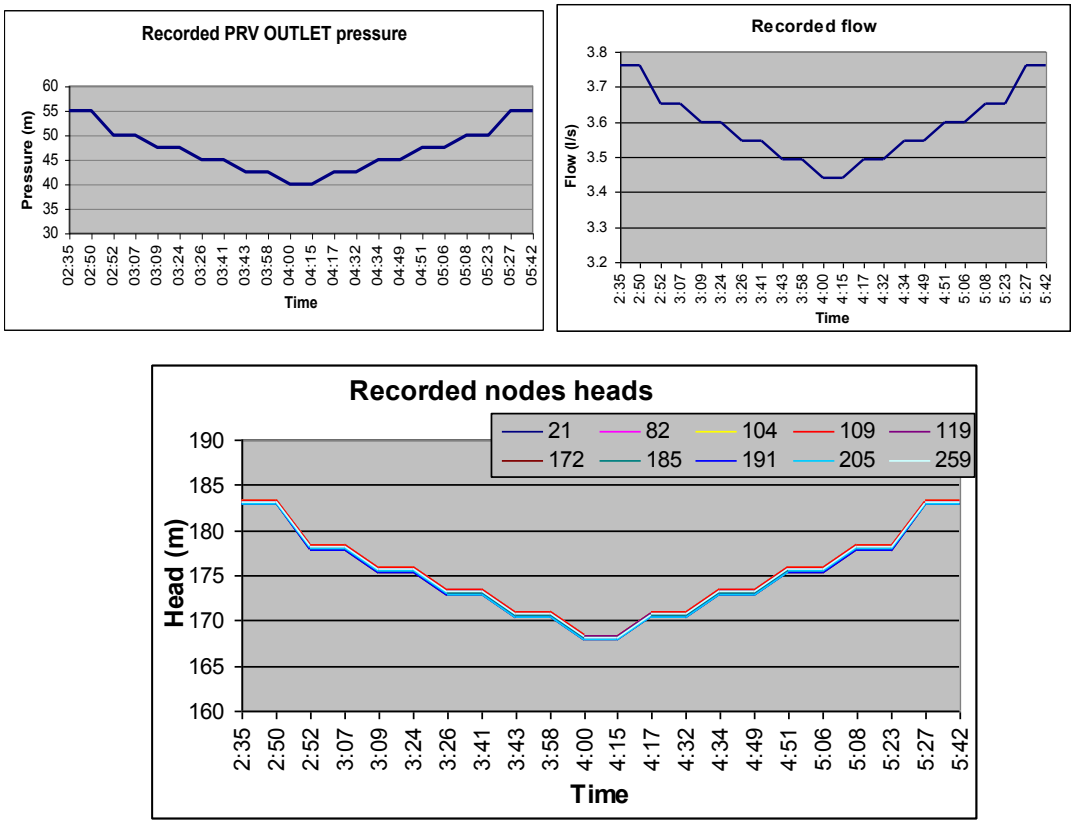

Fig. 6.10 Second part of experiment. Recorded data.

The following terms of the IFM:

- demand
- fixed area burst leakages (burst coefficient) across the DMA
- variable area burst leakages (background leakage coefficients) across the DMA

have been calculated by the hybrid algorithm described in Chapter 5.1.4.

Table 6.7 Calculated results (Second part of experiment)

Sensitive node	Demand factor (l/s)	Coefficient of the burst	Coefficient of the total background leakage	Value of χ^2 (difference between calculated and recorded inlet flows)
The burst exponent = 0.5				
272	2.563226	0.074651	0.001529	1.80E-08
21	2.488546	0.082557	0.001502	1.20E-08
82	2.829353	0.038304	0.001685	1.57E-07
104	2.829267	0.038318	0.001685	1.57E-07
109	2.829271	0.038317	0.001685	1.57E-07
119	2.811203	0.04158	0.001668	1.25E-07
172	1.743729	0.14285	0.001351	6.01E-10
185	2.445957	0.086933	0.001489	9.69E-09
191	2.149506	0.11318	0.001416	2.68E-09
205	2.14837	0.113259	0.001416	2.67E-09
259	2.737868	0.053058	0.001614	6.00E-08

The results in yellow indicate both burst and background leakage in the network. The values of the χ^2 criterion confirm the high accuracy of the estimated values of the demand and the coefficients of the fixed and variable leakage terms.

Application of the algorithm for burst location identification has detected a burst site in the network:

Table 6.8 Results of the burst location identification algorithm (Second part of experiment)

Burst node	Value of χ^2 (reflects an error in prediction of burst location)
200	1.78E-07
202	3.75E-07
203	3.95E-07
205	4.12E-07
196	4.51E-07
206	4.98E-07

The obtained results especially the exponent of χ^2 criterion indicates a high degree of probability of the burst presence close to node 200 (Figure 6.11). The value of the total demand flow is 1.7 l/s, the value of the coefficient of the fixed area leakage (burst) is 0.14 (which corresponds to a burst flow of about 1 l/s), the value of the coefficient of the total background leakage is 0.00135.

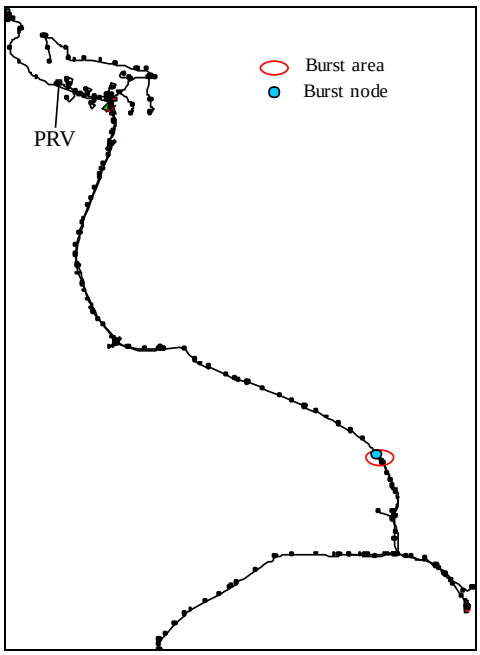

Fig. 6.11 E054 DMA. Results of second part of experiment.

The real burst for the above experiments on E054 DMA was set in the node 206 and this corresponds to the obtained results.

7 Conclusion

The research has addressed the problem of the identification of burst locations, which is a very important aspect of leakage management. The solution should help water companies to estimate the presence, the size and the location of a burst and also the total background leakage through a simple field data analysis leading to reduced water losses, improved customer service and a reduction in socio-economic disruptions.

Some aspects of searching for solutions of such issues have been expressed by the author of the present thesis during discussions at the Moscow University conference "Information and Control Systems in XXI century" (Borovik & Pavlov 2000) and have found their reflection in the published reports (Borovik & Pavlov 2007, Borovik & Yanov 2007).

The overall thesis has been that the different behaviors of background leakage and burst leakage under varying water pressure can be used to develop a method for burst detection and burst location identification which subsequently could be adopted into standard industrial practice.

Initial studies used the FAVOR test field experimental data provided by the collaborating water companies. The classical FAVOR test was performed by applying stepped pressure to the network inlet and recording the inlet flow(s). Later case studies used the e-FAVOR test experimental data. The e-FAVOR test is the same as the FAVOR test but in addition includes the pressure at internal nodes. The industrial partners provided case-study DMAs (models) and, wherever possible, the requested field measurements. However, the majority of the research had to be performed using numerical experiments and 'experimental' data generated by hydraulic simulators.

The research has been performed in three stages:

1. Detection of the presence of a burst in a network on the basis of measurements of inlet flow and inlet pressure.
2. Determination of the size of a potential burst using the measured data of inlet pressure, inlet flow and pressure at the sensitive nodes of the network.
3. Finding out burst locations in a network on the basis of measured data of inlet pressure, inlet flow and pressure changes at the sensitive nodes of a network.

In the first stage described in Chapter 4 the measurements from the FAVOR test i.e. a set of inlet pressure and flow measurement to the DMA, are used to check for the presence of bursts. Data for six various networks (DMAs) have been made available to the author. It has been shown that it is possible to distinguish the following three terms in the total inlet flow: demand (which does not depend on the inlet pressure), the burst flow and the background leakage flow. A three term inlet flow model (IFM) has been created to represent this.

Additional research has been carried out, investigating individual terms in the IFM with the help of an hydraulic simulation program implemented in GAMS. The following conclusions have been reached:

- Background leakage in a network can be accurately represented by a pressure dependent term where the Average Zone Night Pressure (AZNP) is raised to the power of 1.5.
- Burst flow is represented by a pressure dependent power term in which it is necessary to use the pressure at the burst node for accurate representation. The use of AZNP in this term creates an additional constant term which incorrectly increases the total demand term. It is impossible on the basis of input data only (inlet flow, inlet pressure and AZNP pressure) to find out precisely the burst size, but it is possible to discover its presence.
- The demand flow does not depend on the inlet pressure and has random character with a normal distribution. The probability of a demand falling within a particular range, and the demand distribution curves, have been estimated from the experimental data. However, for the reasons mentioned in the previous point it is impossible to estimate the demand accurately using only input data (inlet flow and inlet pressure).

In Stage 2 presented in Chapter 5.1 additional measurements, the pressure at sensitive nodes, have been added as input data to complement the inlet flow and pressure data. An algorithm for the selection of sensitive nodes developed by Prescott and Ulanicki (2006) has been adopted in these studies. During the research various hypotheses have been put forward and checked. Some of them, such as the hypothesis of burst size definition based on the maximal burst coefficient obtained from the ratio of inlet flow and pressure at sensitive nodes, have been rejected.

The least squares method has been used to calculate the coefficients of the IFM, where the Average Zone Night Pressure has been substituted in the background leakage term, and the pressure at a sensitive node was used to represent the burst term.
A burst was allocated to a different sensitive node and the solution was selected which gives the minimum value of the chi-square criterion applied to the total inlet flow. This is the essence of the hybrid method of burst detection algorithm. The following observations have been made:

- The hybrid method helps to determine accurate values of the IFM parameters, the total demand and fixed and variable area leakage terms using the recorded data of the inlet pressure and flow and the pressure at the sensitive nodes of a network.
- The accuracy of the results of determining the burst size and the burst location is influenced by the magnitude of the three flows (demand, fixed area flow and variable area flow) and by the proportions between them.

The main aim of the third stage of the research presented in Chapter 5.2 and 5.3 has been to propose an identification procedure for the burst location which is more precise than other methods currently available. Initially in Chapter 5.2 it was observed that the pressure at DMA nodes depends on the inlet pressure. The gradient of a pressure line, a plot of the pressure at a node versus the inlet pressure, is smallest for the burst node or a node close to the burst node. Subsequently, in Chapter 5.3, this idea was formalised and a statistical method based on the χ^2 criterion has been proposed, where the minimum value of χ^2 points to the burst site.

- The exponent of the value of χ^2 can be used as a criterion of accuracy of the burst location identification algorithm. The given criterion specifies also the accuracy of the performed experiments.
- The algorithm of burst location identification developed by the author allows for finding a potential burst site with quite high precision.

In order to validate the approach two real life case studies, Ocker Hill and Shenstone DMAs, have been analysed. In the former no burst was found but the results indicated a concentration of background leakage. In the latter case study the results were very

accurate with a burst indicated at node 80 with a high precision of $\chi^2 = 3.2 \times 10^{-6}$. These results have not been verified by the industrial partner.

An additional case study for the E054 DMA was planned, but unfortunately the field data is not currently available and numerical experiments have been carried out instead by generating data from a simulation model.

The research has developed a number of sensitive indicators to evaluate the presence, the magnitude and the location of a burst. In further research this approach can be generalized to identify the location of many bursts. At the moment a single burst is allocated to a node and the scenario is simulated, this process needs to be repeated for all nodes of the network. This process could be automated and some search algorithm (e.g. based on an evolutionary approach) could be adopted for this purpose.

Appendix A - FAVOR Test Data

Seven single-input Demand Management Areas (DMAs) were tested as well. A typical FAVOR test was carried out during the night between 1 a.m. and 5 a.m. During the period of recordings, the inlet pressure was changed stepwise over a typical range of values at 20-minute or 30-minute intervals. The inlet pressure and flow were recorded at 20-seconds intervals. The results of the FAVOR Test are shown below.

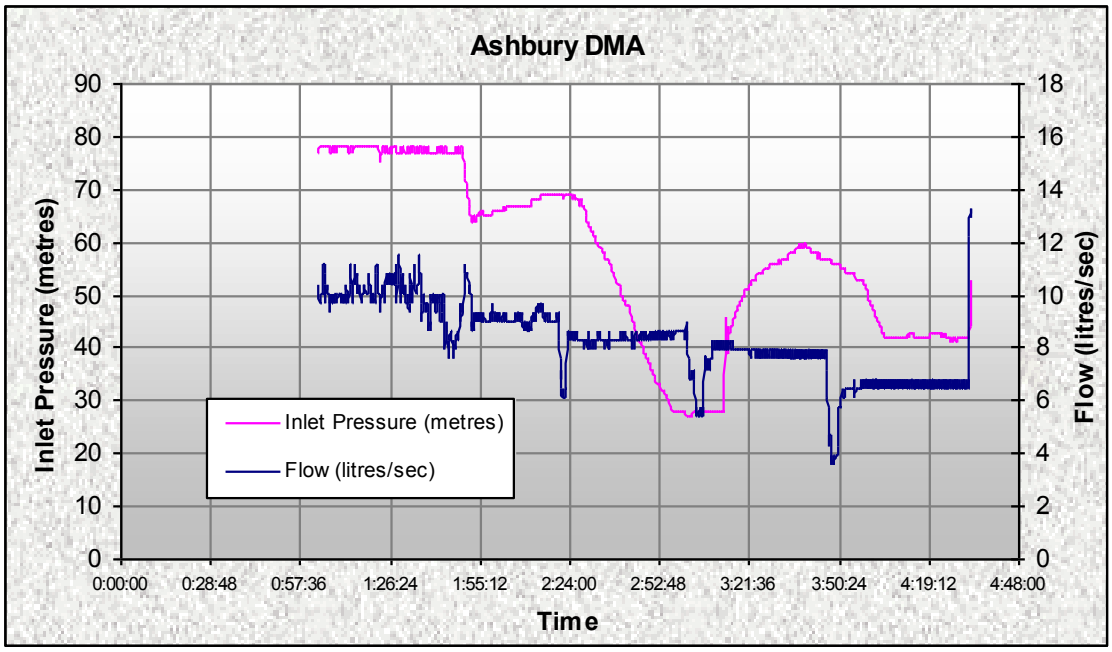

Fig. A.0.1 FAVOR Test Data. Ashbury DMA.

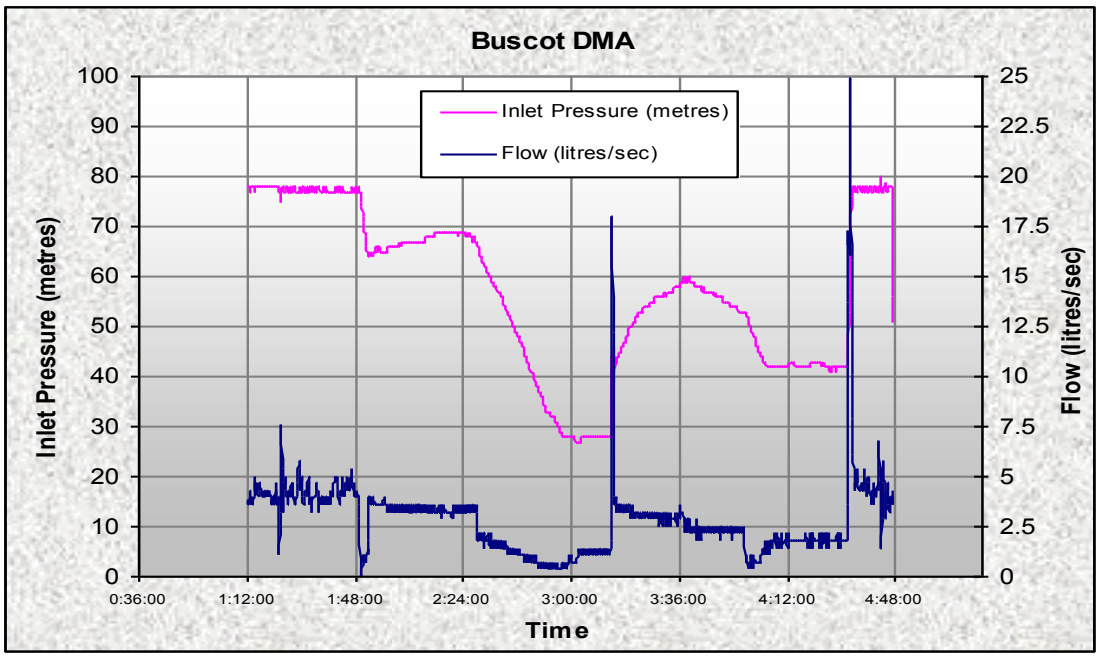

Fig. A.0.2 FAVOR Test Data. Buscot DMA.

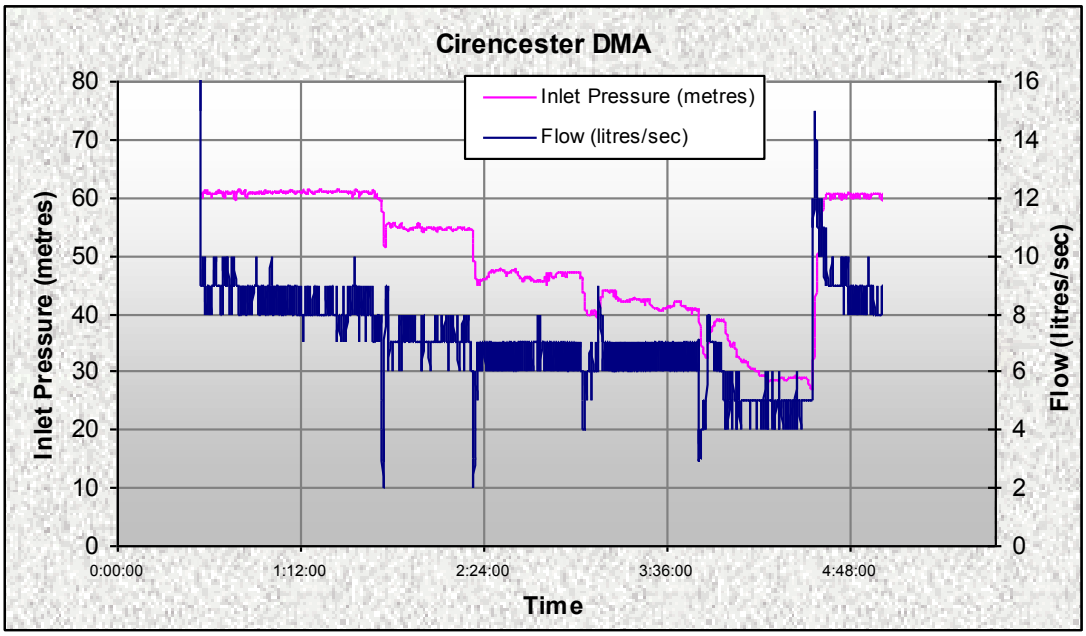

Fig. A.0.3 FAVOR Test Data. Cirencester DMA.

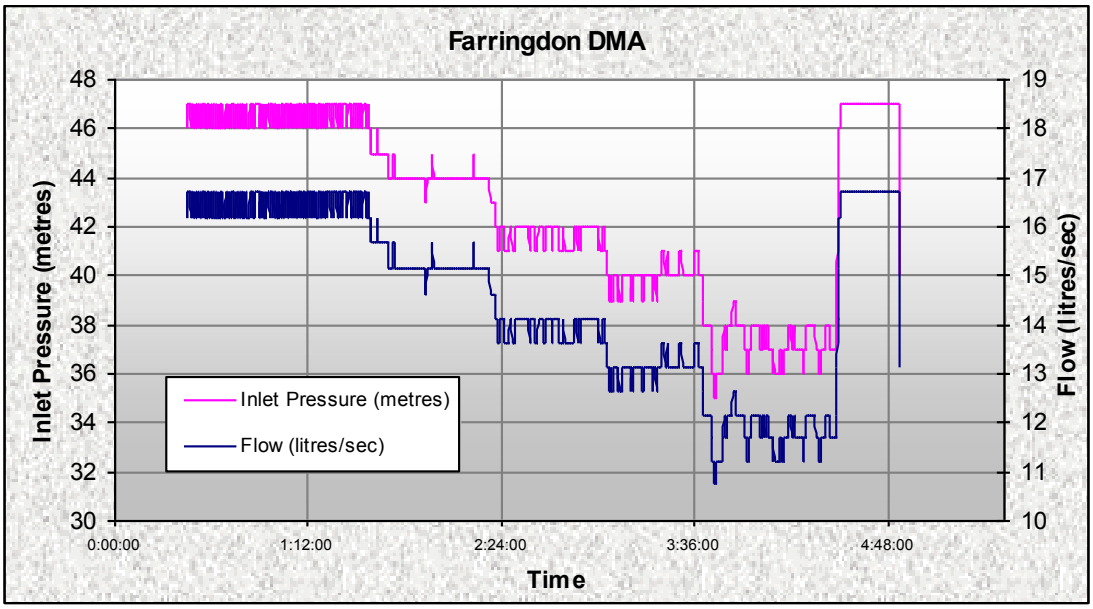

Fig. A.0.4 FAVOR Test Data. Farringdon DMA.

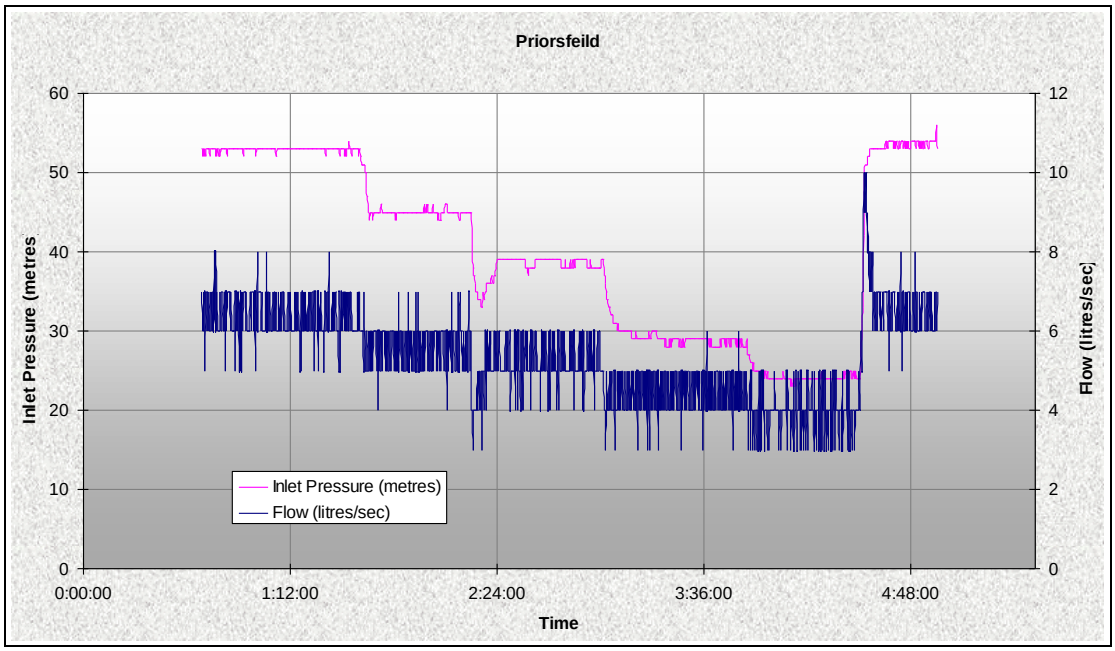

Fig. A.0.5 FAVOR Test Data. Priosfeild DMA.

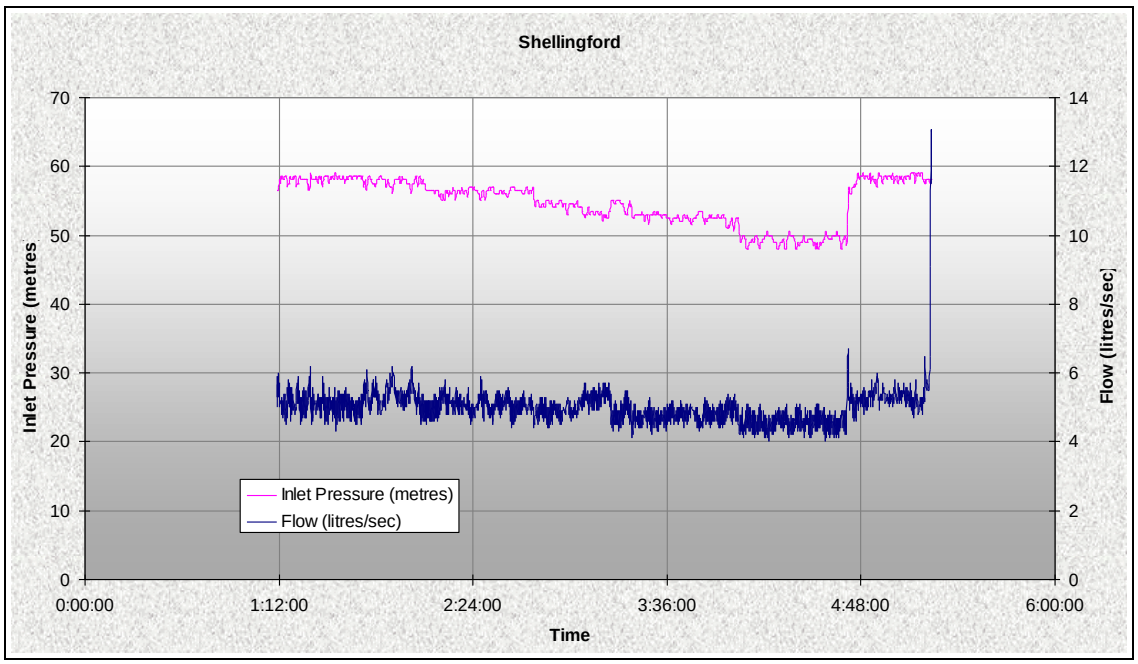

Fig. A.0.6 FAVOR Test Data. Shellingford DMA.

Appendix B - Node and Element Data for the Frizinghall DMA

Table B.0.1 Node Data for Frizinghall DMA

Node No	Node Type	Demand Factor	Elevation (m)	Horizontal Coordinate of node	Vertical Coordinate of node
5	Source node	0	148.24	90	124
10	connection node	0	114	248	238
15	connection node	0	114	264	222
20	connection node	0.086216	113	292	210
25	connection node	0	114	318	206
30	connection node	0.068742	124	320	171
35	connection node	0	136	320	137
40	connection node	0.075512	111.339	364	197
45	connection node	0	109.839	392	208
50	connection node	0.045765	109	392	219
55	connection node	0	110	425	207
60	connection node	0	110	449	193
65	connection node	0.057965	108	470	208
70	connection node	0	108	504	200
75	connection node	0.043062	109	541	193
76	connection node	0	105	541	215
77	connection node	0	102.239	525	222
80	connection node	0.090227	108	576	184
85	connection node	0	97	600	221
90	connection node	0	95	617	252
95	connection node	0.074389	96	645	235
100	connection node	0	95	673	218
104	connection node	0	107	624	167
105	connection node	0.119266	107	611	175
110	connection node	0.056677	105.519	655	145
115	connection node	0.031842	104.089	699	104
120	connection node	0.037247	99	718	141
121	connection node	0	98	696	157
125	connection node	0.079792	94	674	172
130	connection node	0	93	745	185
135	connection node	0	93	720	203
140	connection node	0.153358	85	783	244
145	connection node	0.066469	86	830	209
155	connection node	0	83	786	280
160	connection node	0	80.69	752	293
165	connection node	0.184693	86	727	256
170	connection node	0	86	674	290
175	connection node	0.109184	87.48	644	328

Node No	Node Type	Demand Factor	Elevation (m)	Horizontal Coordinate of node	Vertical Coordinate of node
180	connection node	0.157161	85	695	367
185	connection node	0	84	722	389
190	connection node	0	89	612	395
195	connection node	0.235524	87.8899	586	384
200	connection node	0	90	564	376
205	connection node	0	90	539	369
210	connection node	0	92	596	309
215	connection node	0	94	590	289
220	connection node	0	93	518	361
221	connection node	0	95	497	352
225	connection node	0.076592	97	476	345
226	connection node	0.050362	98.0999	454	338
230	connection node	0.112989	102	514	243
235	connection node	0	105	516	218
240	connection node	0	110	284	236
241	connection node	0.136793	108	304	260
242	connection node	0	106	371	262
245	connection node	0	109	268	257
246	connection node	0	99.7399	431	354
250	connection node	0.105316	90	530	380
255	connection node	0.154766	88	498	440
260	connection node	0	83.62	463	484
265	connection node	0.118223	86	468	466
270	connection node	0	85	489	454
275	connection node	0	86	509	455
280	connection node	0	82	818	438
281	connection node	0	76.62	781	449
285	connection node	0	82	564	502
290	connection node	0	82	544	506
295	connection node	0	81.33	506	531
300	connection node	0	81	508	557
305	connection node	0.0335	84.2699	305	610
310	connection node	0.075	86.97	460	674
315	connection node	0	87	470	730
320	connection node	0.079723	95	540	723
325	connection node	0	92	451	746
330	connection node	0	95	412	744
335	connection node	0.122334	95	452	766
340	connection node	0	96	411	766
345	connection node	0.1738	98.25	459	789
350	connection node	0.038347	97	368	772
351	connection node	0	88	196	711
352	connection node	0.074923	87	145	732
355	connection node	0	90	351	746
356	connection node	0	90	304	754
357	connection node	0	90	289	768

Node No	Node Type	Demand Factor	Elevation (m)	Horizontal Coordinate of node	Vertical Coordinate of node
360	connection node	0.055477	107	458	826
365	connection node	0.135497	110	369	840
370	connection node	0	110	412	840
375	connection node	0.038847	119	458	854
376	connection node	0	114.97	369	854
380	connection node	0.038169	125	458	885
385	connection node	0.090139	114	539	872

Table B.0.2 Element Data for the Frizinghall DMA

Pipe Location (Node → Node)		Length (m)	Diameter (mm)	C-Value	Pipe Location (Node → Node)		Length (m)	Diameter (mm)	C-Value
5	10	375	305	80	200	255	90	100	100
10	15	29	152	100	200	205	10	127	100
10	245	60	305	80	205	210	101	102	70
15	20	10	127	100	205	220	36	127	100
15	240	58	127	100	215	220	122	102	70
20	25	30	152	100	220	221	42	102	70
20	45	196	102	100	221	225	10	127	100
25	30	91	152	70	225	230	108	102	100
25	45	170	102	100	225	226	46	127	100
30	35	96	152	70	226	241	298	127	100
30	40	230	102	70	230	235	70	76	70
45	50	10	102	100	240	241	10	127	100
45	55	70	152	100	240	245	10	152	70
50	65	260	102	100	241	242	152	102	70
55	60	51	76	70	245	246	275	305	80
55	65	37	152	100	246	250	180	305	80
65	70	40	152	100	250	290	163	305	80
70	75	85	152	100	255	260	125	100	100
75	76	43	102	100	255	275	52	100	100
75	80	30	152	100	260	265	2.77	100	100
76	77	56	102	100	270	275	2.77	100	100
77	230	60	102	100	280	281	20	150	100
80	85	72	102	70	281	285	455	150	100
80	105	55	152	100	285	290	10	102	70
90	95	58	102	70	290	295	55	229	70
95	100	61	102	70	295	300	10	76	70
95	105	86	102	70	295	310	210	229	75
104	105	10	152	100	300	305	380	76	70
104	110	17.3	152	70	310	315	22	229	75
110	115	103	127	70	310	325	82	102	70
110	125	76	102	70	315	320	126	102	70
115	120	65	101	130	315	345	142	229	75
120	121	52	73	120	325	330	70	102	70

Pipe Location (Node → Node)		Length (m)	Diameter (mm)	C-Value	Pipe Location (Node → Node)		Length (m)	Diameter (mm)	C-Value
120	130	75	101	130	325	335	28	102	70
121	125	52	102	70	335	340	70	102	70
125	165	110	102	70	335	345	56	102	70
130	135	46	76	70	345	385	190	152	70
130	140	117	101	130	345	350	97	145	140
140	145	65	73	120	345	360	58	152	70
140	155	65	101	130	350	355	100	101	120
155	160	88	101	130	350	356	133	145	140
160	165	106	102	70	351	352	140	76	70
160	180	140	102	70	351	356	225	145	140
165	170	50	127	70	356	357	25	150	100
170	175	92	102	70	360	375	53	152	70
175	180	90	102	70	360	365	135	102	70
175	195	120	102	70	365	370	52	38	100
180	185	36	102	70	365	376	28	100	100
190	195	15	127	100	375	376	125	76	70
195	200	20	127	100	375	380	75	152	100

Appendix C - Node and Element Data for the Ocker Hill DMA

The model of the network used by the author is stored in a separate excel file *model.xls* with the following fields:

A – Node number – a unique label used to identify the node.

B - Type of node – a binary value that describes the role of a node in a network: 0 for a connection node or 1 for a source node (reservoir node or PRV OUTLET node).

C - Demand factor – number of average water users allocated to a node.

D - Elevation (m) – elevation in metres above a common reference of a node. The elevation in used in the program only to compute the pressure at the node.

E - Coefficient of a burst – value of coefficient c_1 for a specific node is set in case of presence in a network of already known burst with specified characteristics.

F - Exponent of the burst term in the IFM= 0.5.

G - Coefficient of known background leakages – value of coefficient c_2 for a specific node is set up in case of presence in a network with already known background leakages with specified characteristics.

H – Exponent of the background leakage term in the IFM =1.5.

I, J – Horizontal and vertical co-ordinates of a node on the map. They do not affect any other variable.

Table C.0.1 Complete nodes data for the Ocker Hill DMA

Node No	Node Type	Demand Factor	Elevation (m)	Coefficient of burst	Exponent of burst term	Coefficient of background leakage	Exponent of background leakage	Horizontal Coordinate of node	Vertical Coordinate of node
1	0	0	137.5	0	0.5	0	1.5	397352253	293887282
2	0	0	136	0	0.5	0	1.5	397385856	293880736
3	0	0	137.5	0	0.5	0	1.5	397352160	293889888
4	0	0	137.5	0	0.5	0	1.5	397350560	293887808
5	0	0	137.5	0	0.5	0	1.5	397349378	293887840
6	0	0	139	0	0.5	0	1.5	397316288	293889696
7	0	3	140	0	0.5	0	1.5	397272832	293889056
8	0	0	140.5	0	0.5	0	1.5	397221728	293880480
9	0	0	140	0	0.5	0	1.5	397204704	293876608
10	0	3	140	0	0.5	0	1.5	397202976	293876096
11	0	0	140	0	0.5	0	1.5	397196896	293876544

Node No	Node Type	Demand Factor	Elevation (m)	Coefficient of burst	Exponent of burst term	Coefficient of background leakage	Exponent of background leakage	Horizontal Coordinate of node	Vertical Coordinate of node
12	0	5	140.5	0	0.5	0	1.5	397277568	293884768
13	0	0	140.5	0	0.5	0	1.5	397274624	293881536
14	0	0	140	0	0.5	0	1.5	397200046	293875298
15	0	0	140	0	0.5	0	1.5	397199968	293875232
16	0	3	140	0	0.5	0	1.5	397196018	293874157
17	0	0	140	0	0.5	0	1.5	397194848	293873824
18	0	8	140	0	0.5	0	1.5	397178496	293868864
19	0	0	139.5	0	0.5	0	1.5	397133696	293854240
20	0	4	139.5	0	0.5	0	1.5	397121088	293850624
21	0	1	139	0	0.5	0	1.5	397063360	293833856
22	0	0	137	0	0.5	0	1.5	397052096	293849792
23	0	0	137	0	0.5	0	1.5	397050464	293848576
24	0	0	137	0	0.5	0	1.5	397047040	293852992
25	0	8	137	0	0.5	0	1.5	397048960	293854304
26	0	0	134	0	0.5	0	1.5	397349664	293821920
27	0	0	130	0	0.5	0	1.5	397399712	293779808
28	0	0	130	0	0.5	0	1.5	397405344	293779808
29	0	0	139	0	0.5	0	1.5	397057440	293827232
30	0	12	139	0	0.5	0	1.5	397053376	293824512
31	0	0	139	0	0.5	0	1.5	397061632	293825408
32	0	8	130.75	0	0.5	0	1.5	396959232	293996128
33	0	19	132.64	0	0.5	0	1.5	396907232	293967616
34	0	56	132.7	0	0.5	0	1.5	396902848	293965344
35	0	36	131.56	0	0.5	0	1.5	396824864	293921728
36	0	37	132.85	0	0.5	0	1.5	396761088	293884256
37	0	0	133.29	0	0.5	0	1.5	396723328	293826752
38	0	36	133.17	0	0.5	0	1.5	396706688	293809792
39	0	22	133.15	0	0.5	0	1.5	396644736	293924736
40	0	16	135.1	0	0.5	0	1.5	396536992	293908224
41	0	15	135.14	0	0.5	0	1.5	396535360	293907968
42	0	0	135.12	0	0.5	0	1.5	396518880	293905440
43	0	0	136.7	0	0.5	0	1.5	396403968	293887744
44	0	49	137	0	0.5	0	1.5	396386336	293885504
45	0	0	136.2	0	0.5	0	1.5	396384224	293829632
46	0	21	136	0	0.5	0	1.5	396387968	293816640
47	0	19	136.2	0	0.5	0	1.5	396364832	293799104
48	0	0	136.5	0	0.5	0	1.5	396356736	293814336
49	0	0	137.5	0	0.5	0	1.5	396328576	293897920
50	0	31	139	0	0.5	0	1.5	397128736	293832512
51	0	0	137	0	0.5	0	1.5	397094176	293796640
52	0	30	138.4	0	0.5	0	1.5	396963712	293793984
53	0	29	138	0	0.5	0	1.5	396914112	293772352
54	0	0	138	0	0.5	0	1.5	396901600	293766720
55	0	0	138	0	0.5	0	1.5	396852736	293745728
56	0	33	137.5	0	0.5	0	1.5	396845376	293742720

Node No	Node Type	Demand Factor	Elevation (m)	Coefficient of burst	Exponent of burst term	Coefficient of background leakage	Exponent of background leakage	Horizontal Coordinate of node	Vertical Coordinate of node
57	0	0	137	0	0.5	0	1.5	396829942	293735280
58	0	0	136.8	0	0.5	0	1.5	396827392	293733952
59	0	0	135	0	0.5	0	1.5	396804096	293722304
60	0	0	134	0	0.5	0	1.5	396795232	293705376
61	0	18	134	0	0.5	0	1.5	396786720	293700608
62	0	0	134	0	0.5	0	1.5	396770016	293725568
63	0	0	139	0	0.5	0	1.5	397135552	293830624
64	0	0	138	0	0.5	0	1.5	397132992	293787008
65	0	0	140	0	0.5	0	1.5	397179648	293864672
66	0	9	137.7	0	0.5	0	1.5	396379360	293774464
67	0	0	137.65	0	0.5	0	1.5	396389504	293778464
68	0	0	137.13	0	0.5	0	1.5	396440224	293782208
69	0	43	135.64	0	0.5	0	1.5	396518336	293831744
70	0	0	136.08	0	0.5	0	1.5	396496096	293762976
71	0	33	137	0	0.5	0	1.5	396413280	293723744
72	0	0	137.9	0	0.5	0	1.5	396355232	293707552
73	0	0	138.22	0	0.5	0	1.5	396289472	293696864
74	0	0	134.7	0	0.5	0	1.5	396537184	293928128
75	0	50	134.2	0	0.5	0	1.5	396539712	293982752
76	0	0	136.5	0	0.5	0	1.5	396389344	293950496
77	0	0	135.84	0	0.5	0	1.5	396523328	293716544
78	0	0	135.2	0	0.5	0	1.5	396535392	293899648
79	0	56	133.01	0	0.5	0	1.5	396650848	293926112
80	0	0	132.56	0	0.5	0	1.5	396638720	293983264
81	0	0	132.28	0	0.5	0	1.5	396735744	293950304
82	0	0	132.6	0	0.5	0	1.5	396911104	293971584
83	0	9	133.94	0	0.5	0	1.5	396780736	293697120
84	0	0	134.64	0	0.5	0	1.5	396738880	293677056
85	0	7	135.16	0	0.5	0	1.5	396572256	293664352
86	0	0	135.26	0	0.5	0	1.5	396552704	293664000
87	0	0	138	0	0.5	0	1.5	396906528	293786368
88	0	0	137.5	0	0.5	0	1.5	396839968	293752384
89	0	0	132	0	0.5	0	1.5	396967776	293855552
90	0	0	129.58	0	0.5	0	1.5	396934752	294030144
91	0	0	129.72	0	0.5	0	1.5	396869440	294113984
92	0	20	129.56	0	0.5	0	1.5	396868736	294122272
93	0	2	129.4	0	0.5	0	1.5	396730368	294258752
94	0	0	129.74	0	0.5	0	1.5	396712864	294271232
95	0	0	137	0	0.5	0	1.5	397044608	293767296
96	0	15	135	0	0.5	0	1.5	396568256	293619040
97	0	0	135	0	0.5	0	1.5	396550720	293617728
98	0	0	136	0	0.5	0	1.5	396499648	293605440
99	0	0	134.92	0	0.5	0	1.5	396564960	293586016
100	0	0	133.82	0	0.5	0	1.5	396784128	293691296
101	0	0	133	0	0.5	0	1.5	396808480	293649344

Node No	Node Type	Demand Factor	Elevation (m)	Coefficient of burst	Exponent of burst term	Coefficient of background leakage	Exponent of background leakage	Horizontal Coordinate of node	Vertical Coordinate of node
102	0	9	128.95	0	0.5	0	1.5	396789984	294302752
103	0	0	128.77	0	0.5	0	1.5	396768224	294331744
104	0	15	127.66	0	0.5	0	1.5	396835264	294332480
105	0	39	127.64	0	0.5	0	1.5	396904704	294262912
106	0	0	128.35	0	0.5	0	1.5	396838464	294243264
107	0	0	126.02	0	0.5	0	1.5	397013344	294289408
108	0	34	125.65	0	0.5	0	1.5	397025120	294294848
109	0	0	125.08	0	0.5	0	1.5	396993824	294366016
110	0	0	126.98	0	0.5	0	1.5	396862496	294352672
111	0	29	126.68	0	0.5	0	1.5	396875328	294382368
112	0	0	128.43	0	0.5	0	1.5	396759104	294374112
113	0	0	129.91	0	0.5	0	1.5	396992480	294072480
114	0	28	132	0	0.5	0	1.5	397119488	294017792
115	0	0	132	0	0.5	0	1.5	397118400	294015168
116	0	0	125.58	0	0.5	0	1.5	397026688	294295680
117	0	0	125	0	0.5	0	1.5	397095488	294387776
118	0	27	125.02	0	0.5	0	1.5	397093728	294403488
119	0	35	125.34	0	0.5	0	1.5	396924608	294416000
120	0	11	124.79	0	0.5	0	1.5	397127232	294430624
121	0	0	124.91	0	0.5	0	1.5	397117632	294437504
122	0	39	127.56	0	0.5	0	1.5	397067744	294478240
123	0	0	127.56	0	0.5	0	1.5	397038624	294471744
124	0	26	133	0	0.5	0	1.5	397273408	293953152
125	0	0	134	0	0.5	0	1.5	397344544	293928800
126	0	0	136	0	0.5	0	1.5	397389728	293887040
127	0	0	133	0	0.5	0	1.5	397278016	293964064
128	0	47	130.06	0	0.5	0	1.5	397394112	294175104
129	0	0	130.1	0	0.5	0	1.5	397382144	294186144
130	0	13	126.54	0	0.5	0	1.5	397286752	294274720
131	0	0	128.06	0	0.5	0	1.5	397270912	294286848
132	0	0	126.08	0	0.5	0	1.5	396946112	294328384
133	0	0	128.18	0	0.5	0	1.5	397108128	294530112
134	0	28	125.52	0	0.5	0	1.5	397141728	294464224
135	0	0	126.41	0	0.5	0	1.5	397206720	294488224
136	0	0	126.4	0	0.5	0	1.5	397149632	294485312
137	0	12	126.39	0	0.5	0	1.5	397180960	294548992
138	0	0	126.54	0	0.5	0	1.5	397173088	294554176
139	0	26	127.02	0	0.5	0	1.5	397149216	294585984
140	0	0	127.14	0	0.5	0	1.5	397126976	294594496
141	0	7	126.03	0	0.5	0	1.5	397202656	294574624
142	0	16	126	0	0.5	0	1.5	397258112	294505568
143	0	16	126.34	0	0.5	0	1.5	397220992	294591232
144	0	0	126.08	0	0.5	0	1.5	397210208	294628544
145	0	0	126.96	0	0.5	0	1.5	397152160	294596384
146	0	28	126.42	0	0.5	0	1.5	397266848	294617984

Node No	Node Type	Demand Factor	Elevation (m)	Coefficient of burst	Exponent of burst term	Coefficient of background leakage	Exponent of background leakage	Horizontal Coordinate of node	Vertical Coordinate of node
147	0	0	126.33	0	0.5	0	1.5	397264096	294627232
148	0	21	126	0	0.5	0	1.5	397319104	294675360
149	0	0	125.9	0	0.5	0	1.5	397296032	294279168
150	0	34	130	0	0.5	0	1.5	397474432	294096736
151	0	0	130.04	0	0.5	0	1.5	397399104	294067808
152	0	0	130	0	0.5	0	1.5	397516864	294055200
153	0	0	126.21	0	0.5	0	1.5	397280736	294622496
154	0	16	125.76	0	0.5	0	1.5	397365792	294587648
155	0	21	125.16	0	0.5	0	1.5	397410976	294607616
156	0	16	126	0	0.5	0	1.5	397368545	294690200
157	0	30	125.9	0	0.5	0	1.5	397377984	294559104
158	0	0	126	0	0.5	0	1.5	397308960	294568608
159	0	0	125.06	0	0.5	0	1.5	397414604	294496136
160	0	0	125.12	0	0.5	0	1.5	397441728	294606240
161	0	41	125.26	0	0.5	0	1.5	397474175	294613150
162	0	0	126	0	0.5	0	1.5	397435968	294678144
163	0	14	126	0	0.5	0	1.5	397435840	294677856
164	0	0	125.74	0	0.5	0	1.5	397510112	294667488
165	1	0	137.5	0	0.5	0	1.5	397355488	293889760

Table C.0.2 Complete element data for Ocker Hill DMA

Pipe Location (Node → Node)		Length (m)	Diameter (mm)	C-Value	Pipe Location (Node → Node)		Length (m)	Diameter (mm)	C-Value
4	1	1.76	152.7	70	47	48	17.27	101.6	70
4	3	3.62	152.4	70	48	49	91.61	101.6	70
5	4	1.12	152.4	70	50	51	60.34	90	70
5	6	33.22	152.4	35	50	63	9.97	90	70
7	6	43.49	152.4	35	52	30	102.39	101.6	40
7	8	51.84	152.4	45	53	52	54.11	101.6	40
8	9	17.48	152.4	45	53	54	13.72	101.6	40
10	9	1.8	125	40	54	55	53.18	101.6	40
11	10	7.74	125	70	55	56	7.95	101.6	50
11	16	3.23	125	70	56	57	17.12	101.6	40
12	7	6.39	101.6	70	56	88	11.08	101.6	70
12	13	4.39	76.2	70	57	58	2.88	101.6	70
14	10	3.13	125	70	58	59	26.05	101.6	40
15	16	3.75	125	70	59	60	22.42	101.6	40
17	16	1.56	125	70	60	61	9.76	152.4	70
17	18	17.09	152.4	45	61	62	30.04	101.6	70
18	19	47.12	152.4	40	61	83	6.93	152.4	70
18	65	4.36	76.2	70	62	38	105.48	101.6	70
19	20	13.12	152.4	40	63	64	44.57	90	70
20	21	61.47	152.4	40	66	47	28.6	101.6	70
20	50	19.81	90	70	66	67	10.96	80.5	70
21	22	19.51	152.4	40	67	68	51.42	80.5	70
21	29	8.89	101.6	40	69	70	73.2	101.6	70
22	23	2.02	101.6	70	69	78	70	101.6	70
22	25	5.5	152.4	70	71	66	61.13	101.6	70
23	24	9.06	101.6	70	71	77	112.57	101.6	70
24	25	2.31	101.6	70	72	71	60.81	105	70
25	32	167.94	152.4	110	73	72	66.66	100	70
26	12	95.63	101.6	25	74	75	54.71	101.6	70
27	26	65.51	101.6	70	75	76	155.83	101.6	70
28	27	5.95	101.8	85.43	75	80	102.68	101.6	70
29	30	4.91	101.6	70	76	44	65.1	101.6	70
30	31	13.63	101.6	70	78	40	8.81	101.6	70
32	90	44.04	152.4	100	79	39	6.28	101.6	70
33	32	59.3	101.6	70	79	81	88.29	101.6	70
34	33	4.94	101.6	70	80	79	58.45	101.6	70
34	89	127.57	76.2	70	81	82	204.85	101.6	70
35	34	89.38	101.6	70	82	33	6.53	101.6	70
35	87	158.09	101.6	70	83	84	46.48	152.4	70
36	35	73.97	101.6	70	83	100	6.74	101.6	70
36	37	73.31	101.6	70	84	85	168.38	152.4	70
37	38	24.1	101.6	70	85	86	19.53	152.7	70
39	38	132.08	101.6	70	85	96	45.5	101.6	70
39	40	109	101.6	70	87	53	15.97	101.6	70
40	41	1.65	101.6	70	88	36	153.67	101.6	70

Pipe Location (Node → Node)		Length (m)	Diameter (mm)	C-Value	Pipe Location (Node → Node)		Length (m)	Diameter (mm)	C-Value
41	42	16.68	101.6	70	90	91	106.31	101.6	100
41	74	20.32	101.6	70	91	92	10.43	101.6	85.43
42	43	116.24	101.6	70	92	113	134.22	152.4	90.09
43	44	17.82	101.6	70	93	92	199.14	152.4	90.09
45	44	55.91	101.6	70	93	102	88.44	155	149
46	45	13.77	101.6	70	94	93	26.74	152.7	90.09
46	69	132.39	101.6	70	95	52	119.36	80.5	70
47	46	29.03	101.6	70	96	97	17.63	101.6	70
96	99	33.17	101.8	70	128	150	112.21	101.6	85.43
97	98	52.6	101.6	70	129	130	130.43	76.2	83.09
100	101	48.5	101.6	5	130	131	19.95	76.2	83.09
102	103	36.26	80.5	147.13	130	149	10.96	125	130
102	104	54.21	155	149	134	135	111.29	80.5	147.13
104	105	100.65	105	147.67	134	136	22.52	155	149
104	110	34.39	155	149	136	137	71.2	155	149
105	106	85.71	80.5	147.13	138	137	9.43	105	147.67
107	105	114.7	105	147.67	139	138	44.63	105	147.67
108	107	12.99	105	147.67	139	145	10.85	105	147.67
108	109	78.99	80.5	147.13	140	139	27.58	80.5	147.13
110	111	32.43	155	149	141	137	33.59	155	149
111	112	120.25	80.5	147.13	141	142	93.87	80.5	147.13
111	119	61.4	155	149	141	143	24.76	155	149
113	114	138.3	152.4	90.09	143	146	53.24	155	149
114	115	2.83	76.2	83.09	144	143	49.81	105	147.67
116	108	1.77	105	147.67	145	144	72.98	105	147.67
117	116	121.03	105	147.67	146	147	9.64	105	147.67
118	117	15.86	105	147.67	146	153	14.61	155	149
118	119	173.88	155	149	147	148	133.59	105	147.67
118	120	44.58	155	149	150	151	106.22	76.2	83.09
119	132	107.95	80.5	147.13	150	152	59.37	101.8	85.43
120	121	11.79	105	147.67	153	154	100.85	155	149
120	134	36.62	155	149	154	155	49.78	105	147.67
121	122	65.21	105	147.67	154	157	31.03	155	149
122	123	35.69	80.5	147.13	155	156	124.93	105	147.67
122	133	109.82	105	147.67	155	160	30.86	105	147.67
124	114	166.95	152.4	90.09	157	158	127.16	80.5	147.13
124	125	76.65	152.4	90.09	159	157	73.2	150	149
124	127	11.85	101.6	85.43	160	161	33.47	105	147.67
126	2	7.39	180	130	161	162	105.86	105	147.67
126	125	75.62	152.4	44.03	161	164	125.22	105	147.67
127	128	242.38	101.6	85.43	162	163	0.3	105	147.67
128	129	16.3	101.6	85.43	165	3	3.33	152.4	70

Appendix D - Node and Element Data for the Shenstone DMA

The model of the network used by the author is stored in a separate excel file *model.xls* with the following fields:

A – Node number – a unique label used to identify the node.

B - Type of node – a binary value that describes the role of a node in a network: 0 for a connection node or 1 for a source node (reservoir node or PRV OUTLET node).

C - Demand factor – number of average water users allocated to a node.

D - Elevation (m) – elevation in metres above a common reference of a node. The elevation in used in the program only to compute the pressure at the node.

E - Coefficient of a burst – value of coefficient c_1 for a specific node is set in case of presence in a network of already known burst with specified characteristics.

F - Exponent of the burst term in the IFM= 0.5.

G - Coefficient of known background leakages – value of coefficient c_2 for a specific node is set up in case of presence in a network with already known background leakages with specified characteristics.

H – Exponent of the background leakage term in the IFM =1.5.

I, J – Horizontal and vertical co-ordinates of a node on the map. They do not affect any other variable.

Table D.0.1 Complete nodes data for the Shenstone DMA

Node No	Node Type	Demand Factor	Elevation (m)	Coefficient of burst	Exponent of burst term	Coefficient of background leakage	Exponent of background leakage	Horizontal Coordinate of node	Vertical Coordinate of node
1	0	2	91	0	0.5	0	1.5	411362848	304925728
2	0	2	91	0	0.5	0	1.5	411382531	304927213
3	0	8	91	0	0.5	0	1.5	411304768	304868015
4	0	0	91.08	0	0.5	0	1.5	411296376	304921239
5	0	0	91.4	0	0.5	0	1.5	411280256	305070883
6	0	0	91.44	0	0.5	0	1.5	411279275	305069651
7	0	0	91.48	0	0.5	0	1.5	411275752	304934997
8	0	16	91.5	0	0.5	0	1.5	411274833	304917103
9	0	0	91.54	0	0.5	0	1.5	411272672	304886400
10	0	0	91.56	0	0.5	0	1.5	411271864	304886489
11	0	0	91.74	0	0.5	0	1.5	411263223	304922735

Node No	Node Type	Demand Factor	Elevation (m)	Coefficient of burst	Exponent of burst term	Coefficient of background leakage	Exponent of background leakage	Horizontal Coordinate of node	Vertical Coordinate of node
13	0	7	92.3528	0	0.5	0	1.5	411182061	304951420
14	0	4	93	0	0.5	0	1.5	410997664	305024128
15	0	6	93.18	0	0.5	0	1.5	411107728	304982497
16	0	3	93.26	0	0.5	0	1.5	411048474	304986624
17	0	6	93.2808	0	0.5	0	1.5	410995968	304986848
18	0	6	93.86	0	0.5	0	1.5	410823583	304956612
19	0	4	94.0184	0	0.5	0	1.5	410504128	304700832
20	0	5	94.06	0	0.5	0	1.5	411271476	304724846
22	0	12	94.304	0	0.5	0	1.5	411005376	304942112
23	0	11	94.52	0	0.5	0	1.5	411090592	304923872
24	0	4	94.8	0	0.5	0	1.5	410823224	304910143
25	0	5	94.8192	0	0.5	0	1.5	410792477	304893857
26	0	6	94.91	0	0.5	0	1.5	411034752	304914976
27	0	0	95	0	0.5	0	1.5	410404352	304719840
28	0	21	95.3928	0	0.5	0	1.5	410856420	304888750
29	0	12	95.6808	0	0.5	0	1.5	410320515	304937621
30	0	0	96	0	0.5	0	1.5	410315008	304555616
31	0	0	96	0	0.5	0	1.5	410325759	304626559
32	0	0	96	0	0.5	0	1.5	411290764	305669396
33	0	13	96.06	0	0.5	0	1.5	410706383	304708933
34	0	3	96.112	0	0.5	0	1.5	411289856	305757248
35	0	25	96.28	0	0.5	0	1.5	410236282	304529107
36	0	18	96.34	0	0.5	0	1.5	410333344	304722848
37	0	16	96.48	0	0.5	0	1.5	411274216	304638683
38	0	0	96.496	0	0.5	0	1.5	410639657	304668288
39	0	3	96.52	0	0.5	0	1.5	410576262	304455727
40	0	3	96.8416	0	0.5	0	1.5	410538979	304335515
41	0	0	96.8684	0	0.5	0	1.5	411247108	305842936
42	0	5	96.9868	0	0.5	0	1.5	411396608	305789120
43	0	5	97	0	0.5	0	1.5	410556352	304395616
44	0	10	97	0	0.5	0	1.5	410517464	304251778
45	0	5	97	0	0.5	0	1.5	410565126	304325776
46	0	5	97	0	0.5	0	1.5	410589705	304377693
47	0	2	97	0	0.5	0	1.5	411250596	305882076
48	0	10	97.08	0	0.5	0	1.5	410604128	304524096
49	0	5	97.08	0	0.5	0	1.5	410604223	304450105
50	0	19	97.12	0	0.5	0	1.5	410787140	304784071
51	0	5	97.18	0	0.5	0	1.5	410558590	304191658
52	0	0	97.38	0	0.5	0	1.5	410280963	304761335
53	0	0	97.38	0	0.5	0	1.5	410280771	304737743
54	0	0	97.41	0	0.5	0	1.5	410725248	304658752
56	0	0	97.6	0	0.5	0	1.5	410630337	304362238
57	0	4	97.72	0	0.5	0	1.5	411319087	304445431
58	0	6	97.76	0	0.5	0	1.5	410637603	304505478
59	0	8	97.96	0	0.5	0	1.5	410736722	304639328

Node No	Node Type	Demand Factor	Elevation (m)	Coefficient of burst	Exponent of burst term	Coefficient of background leakage	Exponent of background leakage	Horizontal Coordinate of node	Vertical Coordinate of node
60	0	0	98	0	0.5	0	1.5	410661743	304597226
61	0	0	98	0	0.5	0	1.5	410693503	304505214
62	0	12	98.1	0	0.5	0	1.5	410902576	303707802
63	0	38	98.18	0	0.5	0	1.5	410608832	304212608
64	0	8	98.2	0	0.5	0	1.5	411309728	304429888
65	0	27	98.26	0	0.5	0	1.5	410988736	304848352
66	0	5	98.44	0	0.5	0	1.5	411135619	304678112
67	0	40	98.56	0	0.5	0	1.5	410627763	304190734
68	0	3	98.58	0	0.5	0	1.5	410990237	304830932
69	0	20	98.64	0	0.5	0	1.5	410782368	304666496
70	0	4	98.676	0	0.5	0	1.5	411180511	304660019
71	0	36	98.86	0	0.5	0	1.5	411137088	304656608
72	0	51	99.0312	0	0.5	0	1.5	410763165	304594261
73	0	34	99.1	0	0.5	0	1.5	411279840	304434496
74	0	0	99.14	0	0.5	0	1.5	410950592	304842336
75	0	0	99.32	0	0.5	0	1.5	411283734	304287740
76	0	0	99.56	0	0.5	0	1.5	411286272	304370944
77	0	6	99.64	0	0.5	0	1.5	411042967	304640734
78	0	17	99.852	0	0.5	0	1.5	410986592	304760224
79	0	0	99.88	0	0.5	0	1.5	410406127	304100962
80	0	35	99.9	0	0.5	0	1.5	410845216	304676224
81	0	0	100.28	0	0.5	0	1.5	409997728	303515872
82	0	9	100.444	0	0.5	0	1.5	411012224	304654592
83	0	0	100.496	0	0.5	0	1.5	410021986	303695170
84	0	0	101.042	0	0.5	0	1.5	410995328	304649056
85	0	14	101.049	0	0.5	0	1.5	410977376	304649088
86	0	0	101.286	0	0.5	0	1.5	411237227	304154713
87	0	9	101.542	0	0.5	0	1.5	411082492	304582469
88	0	0	102	0	0.5	0	1.5	410218752	303977728
89	0	16	102.18	0	0.5	0	1.5	411153947	304065817
91	0	100	97	0	0.5	0	1.5	411217951	306164501
92	0	5	100.714	0	0.5	0	1.5	411142464	304066560
93	0	16	102.76	0	0.5	0	1.5	410760043	304351731
94	0	0	98	0	0.5	0	1.5	411219601	305974799
95	1	0	94.1	0	0.5	0	1.5	410509041	304723406
96	0	24	103.797	0	0.5	0	1.5	410916992	304578976
97	0	0	103.8	0	0.5	0	1.5	410779338	304376098
98	0	33	105.2	0	0.5	0	1.5	411156736	304418880
99	1	0	100.74	0	0.5	0	1.5	411148846	304062094
100	0	0	105.357	0	0.5	0	1.5	410269088	302952832
101	0	39	105.38	0	0.5	0	1.5	411149472	304215968
102	0	17	105.543	0	0.5	0	1.5	410757474	304206308
103	0	0	105.88	0	0.5	0	1.5	411164520	304360725
104	0	0	105.92	0	0.5	0	1.5	411144530	304424386
105	0	18	106.26	0	0.5	0	1.5	410868938	304011281

Node No	Node Type	Demand Factor	Elevation (m)	Coefficient of burst	Exponent of burst term	Coefficient of background leakage	Exponent of background leakage	Horizontal Coordinate of node	Vertical Coordinate of node
106	0	0	106.72	0	0.5	0	1.5	411130647	304228809
107	0	29	107.09	0	0.5	0	1.5	410843840	304454112
108	0	9	107.12	0	0.5	0	1.5	410967872	304536256
109	0	15	107.356	0	0.5	0	1.5	411079580	304113381
110	0	0	108.244	0	0.5	0	1.5	411065308	304124492
111	0	11	108.584	0	0.5	0	1.5	411103232	304452864
112	0	11	108.76	0	0.5	0	1.5	411013600	304512000
113	0	3	109.144	0	0.5	0	1.5	411069728	304471712
114	0	1	106.6	0	0.5	0	1.5	409880391	302451828
115	0	18	106	0	0.5	0	1.5	410361272	302712532
116	0	9	110.816	0	0.5	0	1.5	411059606	304398686
117	0	10	110.96	0	0.5	0	1.5	410986567	304452345
118	0	7	111.007	0	0.5	0	1.5	411046752	304444096
119	0	19	113.704	0	0.5	0	1.5	410897472	304239488
120	0	15	111.712	0	0.5	0	1.5	411059714	304321608

Table D.0.2 Complete element data for Shenstone DMA

Pipe Location (Node → Node)		Length (m)	Diameter (mm)	C-Value	Pipe Location (Node → Node)		Length (m)	Diameter (mm)	C-Value
1	2	19.75851	76.35	59.13333	67	63	29.30625	101.8	146.6933
1	3	96.87236	90	130	67	79	241.588	101.8	35.42
1	4	66.67503	76.35	59.13333	67	93	208.2561	101.8	35.42
4	8	21.70503	76.35	59.13333	67	102	130.745	101.8	35.42
5	32	598.6205	110	130	68	78	71.08	101.8	35.42
6	34	687.6823	101.8	72.46667	69	33	155.9978	101.8	146.6933
7	6	134.7242	101.8	72.46667	69	80	64.29997	101.8	72.46667
8	7	17.91756	101.8	72.46667	71	66	21.55412	101.8	146.6933
8	65	300.6921	76.35	59.13333	71	70	43.5567	101.8	146.6933
9	8	28.74044	101.8	72.46667	73	37	206.0456	110	130
9	20	162.0679	76.35	59.13333	73	64	33.745	76.35	59.13333
10	11	37.41631	110	130	73	98	122.1518	101.8	35.42
11	5	149.5353	110	130	74	65	39.18975	76.35	59.13333
17	14	40.41073	90	130	75	76	83.34575	101.8	35.42
17	16	64.2275	90	130	76	73	63.88521	76.35	39.13333
19	38	139.7911	101.8	72.46667	78	85	140.2262	101.8	35.42
20	10	166.5803	110	130	80	74	215.4905	76.35	59.13333
22	17	48.909	90	130	80	96	123.6254	76.35	59.13333
22	28	174.0521	125	130	81	83	182.5032	101.8	146.6933
23	13	101.9956	125	130	82	77	63.4748	101.8	35.42
23	15	85.4209	90	130	82	78	130.8103	101.8	35.42
24	18	59.74524	90	130	82	84	17.8289	101.8	35.42
24	25	51.0624	90	130	83	88	385.6661	101.8	146.6933
26	22	43.86057	125	130	85	84	18.1897	101.8	35.42
26	23	57.0413	125	130	86	75	143.3626	101.8	35.42
26	68	116.7481	125	130	88	79	224.4458	101.8	146.6933
27	19	101.3468	101.8	72.46667	89	86	116.7089	101.8	35.42
28	24	40.5345	90	130	89	92	20.771	101.8	35.42
28	50	177.4136	125	130	92	109	79.32269	101.8	35.42

Pipe Location (Node → Node)		Length (m)	Diameter (mm)	C-Value	Pipe Location (Node → Node)		Length (m)	Diameter (mm)	C-Value
30	35	85.5427	100	147.6667	94	91	261.291	110	130
31	30	162.6061	100	147.6667	95	19	16.4486	101.8	72.46667
32	94	365.2932	110	130	96	85	94.7265	101.8	35.42
34	41	98.36987	101.8	72.46667	96	108	66.60058	76.35	59.13333
34	42	130.99	76.35	59.13333	97	93	31.08131	101.8	35.42
36	27	71.08533	101.8	72.46667	97	107	101.6126	76.35	83.09333
36	31	96.599	100	147.6667	98	103	58.67721	101.8	35.42
37	20	86.6142	110	130	98	104	16.51672	101.8	35.42
38	54	86.27027	101.8	72.46667	99	92	20	125	130
39	48	73.88636	100	130	100	81	642.91	101.8	146.6933
39	49	28.526	80	130	101	106	22.78926	101.8	35.42
40	44	86.50249	100	130	101	109	124.1395	101.8	35.42
40	45	27.902	80	130	102	105	240.665	101.8	35.42
41	47	39.323	101.8	72.46667	102	119	144.3587	101.8	35.42
43	39	63.32603	100	130	103	101	151.6336	101.8	35.42
43	40	62.57467	100	130	104	111	50.6176	101.8	35.42
43	46	38.123	80	130	106	120	133.7449	101.8	35.42
48	58	38.424	80	130	107	72	161.7186	76.35	59.13333
52	29	182.6855	125	130	107	108	158.3529	76.35	83.09333
52	53	23.59628	101.8	72.46667	107	119	225.2091	76.35	59.13333
53	36	64.42031	101.8	72.46667	108	112	51.77475	76.35	59.13333
54	59	22.5636	76.35	59.13333	110	109	18.0905	101.8	35.42
54	69	58.12779	101.8	72.46667	110	119	203.4917	76.35	39.13333
56	61	157.8994	101.8	146.6933	111	71	212.4508	101.8	146.6933
59	72	52.25196	76.35	59.13333	111	113	38.4417	101.8	35.42
60	48	94.51749	100	130	112	87	101.2271	101.8	35.42
60	59	90.9568	76.35	83.09333	112	113	76.554	101.8	35.42
61	72	119.2824	101.8	146.6933	113	118	36.659	101.8	35.42
63	51	55.03089	76.35	146.0267	114	115	558.7613	76.35	146.0267
63	56	161.5005	101.8	146.6933	115	100	293.4016	101.8	146.6933
64	57	18.14639	76.35	59.13333	118	116	47.22019	101.8	35.42
65	68	17.484	101.8	35.42	118	117	68.49815	101.8	35.42
67	62	566.756	101.8	72.46667					

Appendix E - Node and Element Data for the E054 DMA

The model of the network used by the author is stored in a separate excel file *model.xls* with the following fields:

A – Node number – a unique label used to identify the node.

B - Type of node – a binary value that describes the role of a node in a network: 0 for a connection node or 1 for a source node (reservoir node or PRV OUTLET node).

C - Demand factor – number of average water users allocated to a node.

D - Elevation (m) – elevation in metres above a common reference of a node. The elevation in used in the program only to compute the pressure at the node.

E - Coefficient of a burst – value of coefficient c_1 for a specific node is set in case of presence in a network of already known burst with specified characteristics.

F - Exponent of the burst term in the IFM= 0.5.

G - Coefficient of known background leakages – value of coefficient c_2 for a specific node is set up in case of presence in a network with already known background leakages with specified characteristics.

H – Exponent of the background leakage term in the IFM =1.5.

I, J – Horizontal and vertical co-ordinates of a node on the map. They do not affect any other variable.

Table E.0.1 Complete nodes data for the E054 DMA

Node No	Node Type	Demand Factor	Elevation (m)	Coefficient of burst	Exponent of burst term	Coefficient of background leakage	Exponent of background leakage	Horizontal Coordinate of node	Vertical Coordinate of node
1	0	0	109.52	0	0.5	0	1.5	430962	451406
2	0	0	109.52	0	0.5	0	1.5	430962	451404
3	0	0	108.96	0	0.5	0	1.5	430963	451403
4	0	0	109.12	0	0.5	0	1.5	430964	451402
5	0	0	108.89	0	0.5	0	1.5	430964	451405
6	0	0	109.14	0	0.5	0	1.5	430965	451402
7	0	0	109.19	0	0.5	0	1.5	430966	451402
8	0	0	109.74	0	0.5	0	1.5	430968	451396
9	0	0	109.09	0	0.5	0	1.5	430968	451405
10	0	0	113.73	0	0.5	0	1.5	430969	451272
11	0	0	110.56	0	0.5	0	1.5	430983	451389

Node No	Node Type	Demand Factor	Elevation (m)	Coefficient of burst	Exponent of burst term	Coefficient of background leakage	Exponent of background leakage	Horizontal Coordinate of node	Vertical Coordinate of node
12	0	0	110.44	0	0.5	0	1.5	430984	451392
13	0	0	113.47	0	0.5	0	1.5	431011	451335
14	0	0	117.12	0	0.5	0	1.5	431012	451216
15	0	0	113.28	0	0.5	0	1.5	431018	451348
16	0	0	122.5	0	0.5	0	1.5	431082	451151
17	0	1	116.95	0	0.5	0	1.5	431109	451323
18	0	0	117.21	0	0.5	0	1.5	431114	451321
19	0	0	117.31	0	0.5	0	1.5	431115	451319
20	0	4	119.95	0	0.5	0	1.5	431127	451271
21	0	7	123.42	0	0.5	0	1.5	431134	451216
22	0	0	129.05	0	0.5	0	1.5	431166	451119
23	0	0	129.15	0	0.5	0	1.5	431167	451118
24	0	0	129.2	0	0.5	0	1.5	431168	451118
25	0	0	129.13	0	0.5	0	1.5	431168	451121
26	0	0	129.16	0	0.5	0	1.5	431169	451123
27	0	2	129.48	0	0.5	0	1.5	431172	451117
28	0	0	129.47	0	0.5	0	1.5	431174	451124
29	0	2	129.47	0	0.5	0	1.5	431174	451125
30	0	0	124.85	0	0.5	0	1.5	431201	451274
31	0	7	136.78	0	0.5	0	1.5	431208	451063
32	0	6	132.49	0	0.5	0	1.5	431209	451141
33	0	0	134.31	0	0.5	0	1.5	431210	451112
34	0	6	128.31	0	0.5	0	1.5	431213	451226
35	0	2	134.38	0	0.5	0	1.5	431214	451118
36	0	4	130.63	0	0.5	0	1.5	431236	451221
37	0	2	139.46	0	0.5	0	1.5	431237	451083
38	0	0	148.18	0	0.5	0	1.5	431241	450416
39	0	4	139.48	0	0.5	0	1.5	431243	451095
40	0	0	148.05	0	0.5	0	1.5	431244	450425
41	0	0	147.97	0	0.5	0	1.5	431246	450457
42	0	0	148.13	0	0.5	0	1.5	431249	450376
43	0	0	148.14	0	0.5	0	1.5	431251	450371
44	0	4	148.64	0	0.5	0	1.5	431253	450343
45	0	4	141.35	0	0.5	0	1.5	431257	451080
46	0	0	147	0	0.5	0	1.5	431258	450508
47	0	0	147.14	0	0.5	0	1.5	431266	450552
48	0	0	148.43	0	0.5	0	1.5	431269	450293
49	0	0	147.99	0	0.5	0	1.5	431269	450304
50	0	0	146.89	0	0.5	0	1.5	431272	450571
51	0	0	146.86	0	0.5	0	1.5	431273	450563
52	0	4	134.34	0	0.5	0	1.5	431280	451225
53	0	0	148.38	0	0.5	0	1.5	431282	450272
54	0	2	143.57	0	0.5	0	1.5	431282	451071
55	0	2	142.52	0	0.5	0	1.5	431284	451098
56	0	0	143.95	0	0.5	0	1.5	431290	451077

Node No	Node Type	Demand Factor	Elevation (m)	Coefficient of burst	Exponent of burst term	Coefficient of background leakage	Exponent of background leakage	Horizontal Coordinate of node	Vertical Coordinate of node
57	0	0	146.47	0	0.5	0	1.5	431291	450623
58	0	4	143.9	0	0.5	0	1.5	431292	451081
59	0	0	148.84	0	0.5	0	1.5	431292	450233
60	0	7	146.41	0	0.5	0	1.5	431307	451046
61	0	0	146.53	0	0.5	0	1.5	431307	450651
62	0	0	147.92	0	0.5	0	1.5	431307	450200
63	0	0	147.65	0	0.5	0	1.5	431308	450208
64	0	0	147.8	0	0.5	0	1.5	431314	450186
65	0	0	147.45	0	0.5	0	1.5	431319	450694
66	0	4	146.61	0	0.5	0	1.5	431319	451059
67	0	0	145.98	0	0.5	0	1.5	431320	451072
68	0	0	147.24	0	0.5	0	1.5	431334	450151
69	0	0	148.35	0	0.5	0	1.5	431339	450734
70	0	0	148.89	0	0.5	0	1.5	431340	450748
71	0	0	147.66	0	0.5	0	1.5	431341	451064
72	0	6	140	0	0.5	0	1.5	431343	451219
73	0	0	149.42	0	0.5	0	1.5	431353	450770
74	0	0	146.96	0	0.5	0	1.5	431355	450131
75	0	0	150	0	0.5	0	1.5	431357	450792
76	0	2	148.85	0	0.5	0	1.5	431370	451073
77	0	4	148.55	0	0.5	0	1.5	431371	451079
78	0	0	150	0	0.5	0	1.5	431377	450831
79	0	0	149.24	0	0.5	0	1.5	431377	451073
80	0	0	150	0	0.5	0	1.5	431378	451055
81	0	4	150	0	0.5	0	1.5	431378	451053
82	0	0	150	0	0.5	0	1.5	431380	450872
83	0	0	149.19	0	0.5	0	1.5	431380	450041
84	0	0	150	0	0.5	0	1.5	431382	451053
85	0	0	150	0	0.5	0	1.5	431382	450871
86	0	0	150	0	0.5	0	1.5	431383	450874
87	0	0	150	0	0.5	0	1.5	431383	450870
88	0	0	150	0	0.5	0	1.5	431384	450870
89	0	0	150	0	0.5	0	1.5	431384	450873
90	0	0	150	0	0.5	0	1.5	431385	450867
91	0	0	150	0	0.5	0	1.5	431385	450872
92	0	0	150	0	0.5	0	1.5	431386	450853
93	0	0	150	0	0.5	0	1.5	431386	451055
94	0	0	150	0	0.5	0	1.5	431386	451053
95	0	0	150	0	0.5	0	1.5	431386	450867
96	0	2	150	0	0.5	0	1.5	431386	451046
97	0	0	148.93	0	0.5	0	1.5	431387	451017
98	0	0	150	0	0.5	0	1.5	431386	450868
99	0	0	150	0	0.5	0	1.5	431386	450875
100	0	0	148.93	0	0.5	0	1.5	431387	451022
101	0	0	150	0	0.5	0	1.5	431387	450871

Node No	Node Type	Demand Factor	Elevation (m)	Coefficient of burst	Exponent of burst term	Coefficient of background leakage	Exponent of background leakage	Horizontal Coordinate of node	Vertical Coordinate of node
102	0	0	148.93	0	0.5	0	1.5	431388	451014
103	0	0	150	0	0.5	0	1.5	431389	451013
104	0	0	150	0	0.5	0	1.5	431389	451023
105	0	0	150	0	0.5	0	1.5	431390	451016
106	0	0	150	0	0.5	0	1.5	431390	450919
107	0	0	150	0	0.5	0	1.5	431390	451020
108	0	2	150	0	0.5	0	1.5	431391	451073
109	0	6	150	0	0.5	0	1.5	431391	451016
110	0	0	148.12	0	0.5	0	1.5	431394	450078
111	0	7	148.39	0	0.5	0	1.5	431395	451106
112	0	0	150	0	0.5	0	1.5	431398	450932
113	0	0	150	0	0.5	0	1.5	431399	450968
114	0	2	141.6	0	0.5	0	1.5	431401	451206
115	0	0	148.16	0	0.5	0	1.5	431402	450063
116	0	0	141.65	0	0.5	0	1.5	431402	451206
117	0	0	148.12	0	0.5	0	1.5	431402	450062
118	0	0	148.09	0	0.5	0	1.5	431403	450064
119	0	0	148.04	0	0.5	0	1.5	431404	450065
120	0	0	147.98	0	0.5	0	1.5	431405	450058
121	0	0	147.96	0	0.5	0	1.5	431406	450062
122	0	0	147.87	0	0.5	0	1.5	431408	450060
123	0	0	147.86	0	0.5	0	1.5	431408	450057
124	0	0	147.82	0	0.5	0	1.5	431408	450058
125	0	0	147.79	0	0.5	0	1.5	431409	450058
126	0	0	147.86	0	0.5	0	1.5	431409	450056
127	0	0	147.6	0	0.5	0	1.5	431413	450059
128	0	0	147.56	0	0.5	0	1.5	431414	450060
129	0	4	148.85	0	0.5	0	1.5	431425	451090
130	0	2	148.85	0	0.5	0	1.5	431426	451089
131	0	6	144.62	0	0.5	0	1.5	431442	451165
132	0	9	146.33	0	0.5	0	1.5	431455	450039
133	0	2	146.11	0	0.5	0	1.5	431461	450040
134	0	2	144.71	0	0.5	0	1.5	431465	451146
135	0	6	144.62	0	0.5	0	1.5	431468	451144
136	0	6	147.74	0	0.5	0	1.5	431470	451000
137	0	7	147.7	0	0.5	0	1.5	431474	451034
138	0	4	142.02	0	0.5	0	1.5	431490	451183
139	0	2	141.83	0	0.5	0	1.5	431495	451182
140	0	0	144.05	0	0.5	0	1.5	431526	450032
141	0	4	144.03	0	0.5	0	1.5	431529	450029
142	0	4	140	0	0.5	0	1.5	431537	451184
143	0	6	140.8	0	0.5	0	1.5	431539	451149
144	0	9	143.4	0	0.5	0	1.5	431547	451001
145	0	2	140.07	0	0.5	0	1.5	431549	451155
146	0	9	143.37	0	0.5	0	1.5	431549	451059

Node No	Node Type	Demand Factor	Elevation (m)	Coefficient of burst	Exponent of burst term	Coefficient of background leakage	Exponent of background leakage	Horizontal Coordinate of node	Vertical Coordinate of node
147	0	0	140.16	0	0.5	0	1.5	431550	451151
148	0	0	140	0	0.5	0	1.5	431568	451151
149	0	0	140	0	0.5	0	1.5	431571	451151
150	0	2	71.95	0	0.5	0	1.5	431584	448816
151	0	11	71.57	0	0.5	0	1.5	431586	448793
152	0	0	141.94	0	0.5	0	1.5	431587	450034
153	0	6	72	0	0.5	0	1.5	431587	448833
154	0	0	141.81	0	0.5	0	1.5	431590	450035
155	0	0	141.77	0	0.5	0	1.5	431590	450037
156	0	0	141.83	0	0.5	0	1.5	431590	450034
157	0	0	141.75	0	0.5	0	1.5	431592	450034
158	0	0	144.77	0	0.5	0	1.5	431595	450032
159	0	0	141.57	0	0.5	0	1.5	431599	450032
160	0	0	141.45	0	0.5	0	1.5	431603	450032
161	0	0	71.94	0	0.5	0	1.5	431610	448859
162	0	0	73.44	0	0.5	0	1.5	431651	448900
163	0	2	140	0	0.5	0	1.5	431691	450032
164	0	0	75.43	0	0.5	0	1.5	431692	448941
165	0	0	75.68	0	0.5	0	1.5	431717	448960
166	0	0	140	0	0.5	0	1.5	431735	449985
167	0	0	139.22	0	0.5	0	1.5	431757	449971
168	0	0	76.49	0	0.5	0	1.5	431775	448991
169	0	0	137.97	0	0.5	0	1.5	431789	449957
170	0	7	78.12	0	0.5	0	1.5	431834	449022
171	0	0	135.4	0	0.5	0	1.5	431860	449926
172	0	0	80.14	0	0.5	0	1.5	431878	449053
173	0	0	80.29	0	0.5	0	1.5	431881	449055
174	0	0	134.06	0	0.5	0	1.5	431896	449911
175	0	0	81.37	0	0.5	0	1.5	431902	449067
176	0	0	133.37	0	0.5	0	1.5	431914	449904
177	0	0	132.02	0	0.5	0	1.5	431949	449892
178	0	2	85.44	0	0.5	0	1.5	431981	449120
179	0	2	130	0	0.5	0	1.5	432012	449870
180	0	0	91.39	0	0.5	0	1.5	432065	449173
181	0	0	128.67	0	0.5	0	1.5	432079	449842
182	0	4	95.86	0	0.5	0	1.5	432132	449184
183	0	4	125.36	0	0.5	0	1.5	432135	449816
184	0	2	122.88	0	0.5	0	1.5	432182	449794
185	0	0	120.47	0	0.5	0	1.5	432230	449772
186	0	2	101.69	0	0.5	0	1.5	432231	449188
187	0	4	117.16	0	0.5	0	1.5	432272	449753
188	0	2	102.17	0	0.5	0	1.5	432307	449182
189	0	66	112.3	0	0.5	0	1.5	432326	449723
190	0	0	102	0	0.5	0	1.5	432328	449182
191	0	2	102.53	0	0.5	0	1.5	432367	449181

Node No	Node Type	Demand Factor	Elevation (m)	Coefficient of burst	Exponent of burst term	Coefficient of background leakage	Exponent of background leakage	Horizontal Coordinate of node	Vertical Coordinate of node
192	0	0	102.1	0	0.5	0	1.5	432367	449184
193	0	2	102.1	0	0.5	0	1.5	432367	449186
194	0	0	110	0	0.5	0	1.5	432376	449692
195	0	0	102.85	0	0.5	0	1.5	432414	449181
196	0	12	106.88	0	0.5	0	1.5	432422	449661
197	0	4	103.87	0	0.5	0	1.5	432431	449185
198	0	0	103.5	0	0.5	0	1.5	432442	449184
199	0	4	102.88	0	0.5	0	1.5	432473	449177
200	0	5	102.69	0	0.5	0	1.5	432482	449603
201	0	11	111.18	0	0.5	0	1.5	432489	449363
202	0	0	102.66	0	0.5	0	1.5	432502	449568
203	0	0	102.65	0	0.5	0	1.5	432503	449566
204	0	4	102.63	0	0.5	0	1.5	432505	449563
205	0	0	102.5	0	0.5	0	1.5	432506	449564
206	0	0	102.49	0	0.5	0	1.5	432508	449561
207	0	0	105.79	0	0.5	0	1.5	432519	449188
208	0	2	102.79	0	0.5	0	1.5	432525	449522
209	0	17	104.2	0	0.5	0	1.5	432537	449491
210	0	0	104.11	0	0.5	0	1.5	432538	449491
211	0	0	104.84	0	0.5	0	1.5	432548	449466
212	0	2	110	0	0.5	0	1.5	432549	449330
213	0	0	110	0	0.5	0	1.5	432549	449362
214	0	7	110	0	0.5	0	1.5	432551	449361
215	0	4	106	0	0.5	0	1.5	432552	449188
216	0	6	110	0	0.5	0	1.5	432553	449344
217	0	0	106	0	0.5	0	1.5	432554	449190
218	0	4	110	0	0.5	0	1.5	432554	449343
219	0	13	110	0	0.5	0	1.5	432554	449344
220	0	2	106	0	0.5	0	1.5	432555	449185
221	0	0	106	0	0.5	0	1.5	432555	449189
222	0	2	105.3	0	0.5	0	1.5	432555	449453
223	0	0	106	0	0.5	0	1.5	432556	449185
224	0	4	110	0	0.5	0	1.5	432557	449249
225	0	8	106	0	0.5	0	1.5	432557	449190
226	0	0	106	0	0.5	0	1.5	432557	449190
227	0	0	106	0	0.5	0	1.5	432557	449189
228	0	0	106	0	0.5	0	1.5	432558	449188
229	0	2	106.12	0	0.5	0	1.5	432558	449439
230	0	11	110	0	0.5	0	1.5	432561	449276
231	0	4	106.28	0	0.5	0	1.5	432562	449185
232	0	2	106.31	0	0.5	0	1.5	432564	449185
233	0	0	106.68	0	0.5	0	1.5	432564	449188
234	0	4	106.69	0	0.5	0	1.5	432566	449188
235	0	11	106.99	0	0.5	0	1.5	432569	449415
236	0	11	106.7	0	0.5	0	1.5	432597	449177

Node No	Node Type	Demand Factor	Elevation (m)	Coefficient of burst	Exponent of burst term	Coefficient of background leakage	Exponent of background leakage	Horizontal Coordinate of node	Vertical Coordinate of node
237	0	4	108.61	0	0.5	0	1.5	432624	449174
238	0	4	110	0	0.5	0	1.5	432676	449165
239	0	15	110	0	0.5	0	1.5	432680	449167
240	0	15	110	0	0.5	0	1.5	432727	449138
241	0	2	110	0	0.5	0	1.5	432735	449127
242	0	0	110	0	0.5	0	1.5	432756	449105
243	0	6	110	0	0.5	0	1.5	432764	449108
244	0	0	110	0	0.5	0	1.5	432767	449099
245	0	0	110	0	0.5	0	1.5	432784	449077
246	0	0	110	0	0.5	0	1.5	432788	449079
247	0	11	110	0	0.5	0	1.5	432789	449080
248	0	0	110	0	0.5	0	1.5	432793	449065
249	0	0	110	0	0.5	0	1.5	432829	449012
250	0	4	110	0	0.5	0	1.5	432838	449037
251	0	0	110	0	0.5	0	1.5	432851	448974
252	0	0	110	0	0.5	0	1.5	432852	448975
253	0	0	110	0	0.5	0	1.5	432853	448970
254	0	0	111.85	0	0.5	0	1.5	432855	448967
255	0	0	110	0	0.5	0	1.5	432857	448968
256	0	0	111.79	0	0.5	0	1.5	432860	448959
257	0	4	110	0	0.5	0	1.5	432876	449049
258	0	9	110	0	0.5	0	1.5	432884	449049
259	0	0	141.4	0	0.5	0	1.5	431605	450032
260	0	0	109.12	0	0.5	0	1.5	430963	451402
262	0	0	110	0	0.5	0	1.5	432854	448970
263	0	0	150	0	0.5	0	1.5	431389	451023
266	0	0	150	0	0.5	0	1.5	431380	450871
268	0	0	110	0	0.5	0	1.5	432851	448974
269	0	0	150	0	0.5	0	1.5	431382	450871
270	0	0	147.96	0	0.5	0	1.5	431405	450063
271	0	0	109.52	0	0.5	0	1.5	430962	451405
272	1	0	128.46	0	0.5	0	1.5	431173	451125

Table E.0.2 Complete element data for E054 DMA

Pipe Location (Node → Node)		Length (m)	Diameter (mm)	C-Value	Pipe Location (Node → Node)		Length (m)	Diameter (mm)	C-Value
2	271	1.6	152	70	133	140	65.96	152	140
3	2	1.23	152	70	134	131	69.95	150	100
4	6	1.3	102	70	135	134	3.81	150	100
4	260	1.84	152	70	135	143	72.82	150	100
5	2	1.51	100	100	137	136	39.32	100	100
5	7	4.45	100	100	138	139	4.71	102	70
6	7	1.52	102	70	139	142	43.16	100	100
8	4	7.42	152	70	140	152	60.83	152	140
9	7	4.87	102	70	141	132	74.84	76	70
10	14	75.07	154	140	142	145	30.81	100	100

Pipe Location (Node → Node)		Length (m)	Diameter (mm)	C-Value	Pipe Location (Node → Node)		Length (m)	Diameter (mm)	C-Value
11	8	16.58	154	140	144	146	67.25	100	100
11	12	3.07	150	100	145	147	4.82	100	100
11	15	64	154	140	146	143	94.29	100	100
13	10	78.14	154	140	147	143	11.61	150	100
14	16	95.85	154	140	147	148	18.01	150	100
15	13	15.4	154	140	148	149	3	150	100
16	22	90.33	154	140	150	151	23.03	73	120
17	18	5.96	102	70	152	156	3.45	152	140
18	19	1.87	76	70	152	259	19.29	152	70
18	30	99.77	102	70	153	150	17.03	73	120
19	20	49.54	76	70	154	155	1.9	102	70
20	21	55.23	76	70	156	154	1.15	102	70
22	23	1.42	154	140	156	157	2.25	152	140
23	24	0.67	154	140	157	159	7.34	152	140
24	27	3.85	154	140	158	141	66.51	76	70
25	22	3.45	150	100	159	158	4.2	76	70
26	24	5.46	150	100	161	153	34.99	73	120
27	45	93.31	154	140	162	161	57.7	73	120
28	25	6.96	150	100	163	259	48.08	145	140
29	28	1.01	150	100	164	162	57.7	73	120
29	33	38.13	150	100	165	164	31.69	73	120
30	34	49.98	102	70	166	163	64.7	145	140
33	35	7.57	80	90	167	166	26.75	145	140
33	39	36.98	150	100	168	165	66.2	73	120
34	36	25.07	102	70	169	167	35.16	145	140
35	32	55.95	80	90	170	168	66.19	73	120
36	52	43.82	102	70	171	169	77.21	145	140
37	31	64.15	80	90	172	170	55.92	73	120
38	41	41.51	76	70	173	172	3.54	73	120
39	37	13.64	80	90	174	171	38.91	145	140
39	56	50.18	150	100	175	173	23.84	100	100
40	46	84.04	152	140	176	174	19.04	145	140
41	47	97.43	76	70	177	176	37.33	145	140
42	40	49.17	152	140	178	175	96.15	100	100
43	42	5.49	152	140	179	177	66.12	145	140
44	38	73.31	76	70	180	178	99.63	100	100
45	54	26.19	154	140	181	179	72.97	145	140
46	51	56.75	152	140	182	180	68.23	100	100
47	50	19.65	100	100	183	181	61.31	145	140
48	44	52.79	76	70	184	183	52.72	145	140
49	43	69.85	152	140	185	184	52.73	145	140
50	57	55.74	76	70	186	182	99.29	100	100
51	61	94.93	152	140	187	185	46.1	145	140
52	72	63.48	102	70	188	186	76.95	102	70
53	49	34.06	152	140	189	187	61.62	145	140
54	71	59.64	154	140	190	188	20.75	102	120
56	58	4.56	80	90	191	190	38.87	102	120
56	67	30.69	150	100	191	192	2.61	76	120
57	65	76.63	76	70	192	193	1.91	76	120
58	55	51.21	80	90	194	189	58.72	145	140
59	48	64.02	76	70	195	191	47.7	102	120
61	69	88.82	152	140	196	194	55.39	145	140
62	59	36.93	76	70	197	193	64.41	76	120
63	53	69.31	152	140	198	197	11.18	76	120
64	62	15.43	76	70	199	195	59.26	102	120

Pipe Location (Node → Node)		Length (m)	Diameter (mm)	C-Value	Pipe Location (Node → Node)		Length (m)	Diameter (mm)	C-Value
65	70	57.27	76	70	200	196	83.85	145	140
66	60	70.63	80	90	202	200	39.6	145	140
67	66	13.09	80	90	203	202	2.48	145	140
67	76	49.98	150	100	203	204	4.16	76	70
68	64	40.03	76	70	203	205	3.97	145	140
69	73	38.68	152	140	204	209	78.68	76	120
70	75	47.34	76	70	205	206	4.32	99	130
71	93	52.49	154	140	206	208	41.75	99	130
72	114	59.31	102	70	207	198	76.89	76	120
73	78	65.69	152	140	208	210	34.46	99	130
74	63	90.19	152	140	209	211	26.77	76	120
75	95	80.71	76	70	210	222	41.02	99	130
76	77	5.74	80	90	211	229	29.55	76	120
76	79	7.35	150	100	212	224	81.09	102	120
77	111	76.44	80	90	214	212	32.18	102	120
78	92	23.48	152	140	214	213	1.69	76	120
79	80	18.53	150	100	215	199	79.94	102	120
79	108	13.35	150	100	216	201	67.59	76	70
80	81	2.2	150	100	218	230	67.21	76	120
81	84	3.25	150	100	219	216	0.9	76	120
81	113	91.02	150	100	219	218	1.41	76	120
82	85	2.22	148	140	220	207	37.4	76	120
82	266	9.08	150	100	220	221	3.2	76	120
84	94	4.1	150	100	221	215	2.58	102	120
85	269	1.64	148	140	222	214	95.32	102	120
86	89	1.64	154	140	223	220	1.65	76	120
87	88	0.92	148	140	224	225	58.48	102	120
88	91	2.98	152	140	225	217	3	102	120
89	91	1.25	154	140	225	226	0.75	102	120
90	95	1.19	150	100	226	227	1.1	102	120
91	99	2.75	152	140	227	221	2.2	102	120
92	88	17.06	152	140	227	228	1.15	102	120
94	93	2	154	140	228	233	6.35	102	120
94	96	6.6	154	140	229	235	26.46	76	120
95	98	1.2	76	70	230	231	90.72	76	120
96	104	23.69	154	140	231	223	6	76	120
97	102	5.22	100	68	231	232	2.05	76	120
98	101	2.44	76	70	232	233	3.45	76	120
100	97	4.54	100	68	232	236	33.52	76	120
102	103	1.46	150	100	233	234	1.2	102	120
102	105	1.79	100	100	234	237	60.03	102	120
104	100	2.03	100	100	235	219	73.26	76	120
104	107	6.45	154	140	236	239	84.54	76	120
104	263	6.45	154	140	237	238	55.03	102	120
105	109	1.95	100	100	238	241	70.37	102	120
106	82	54.77	150	100	239	240	55.21	76	120
107	109	3.61	154	140	240	243	47.76	76	70
108	129	38.83	150	100	241	242	31.16	102	70
109	112	85.82	154	140	242	244	14.96	99	130
110	68	94.5	76	70	243	247	37.6	76	70
112	86	65.33	154	140	244	245	28.22	99	130
113	106	49.77	150	100	245	248	14.53	99	130
114	116	1.13	102	70	246	245	4.41	76	70
115	83	40.67	50	110	247	246	0.92	76	70
116	138	90.92	102	70	247	250	67.44	76	70

Pipe Location (Node → Node)		Length (m)	Diameter (mm)	C-Value	Pipe Location (Node → Node)		Length (m)	Diameter (mm)	C-Value
117	115	1.26	52	70	248	249	64.14	99	130
118	115	2.03	52	70	249	251	47.99	99	130
119	110	16.91	76	70	250	257	43.1	76	70
119	118	1.18	52	70	251	253	4.03	99	130
120	117	4.35	52	70	251	268	1.19	80	90
120	126	7.14	50	110	252	255	11.92	80	90
121	270	2.62	76	70	253	262	4.05	99	130
122	120	3.13	52	70	254	256	8.76	99	130
122	121	2.92	76	70	255	254	2.08	80	90
124	123	1.03	52	70	257	258	9.66	50	140
125	122	2.38	76	70	259	160	41.29	145	140
125	124	0.86	52	70	260	3	1.84	152	70
127	126	5.04	76	70	262	254	4.05	99	130
128	74	92.93	152	140	266	90	9.08	150	100
128	127	0.92	76	70	268	252	1.19	80	90
128	133	52.06	152	140	269	87	1.64	148	140
129	130	1.03	100	100	270	119	2.62	76	70
129	135	69.61	150	100	271	1	1.6	152	70
130	137	74.9	100	100	272	29	1.04	150	100
132	125	50.88	76	70					

Appendix F - Program code

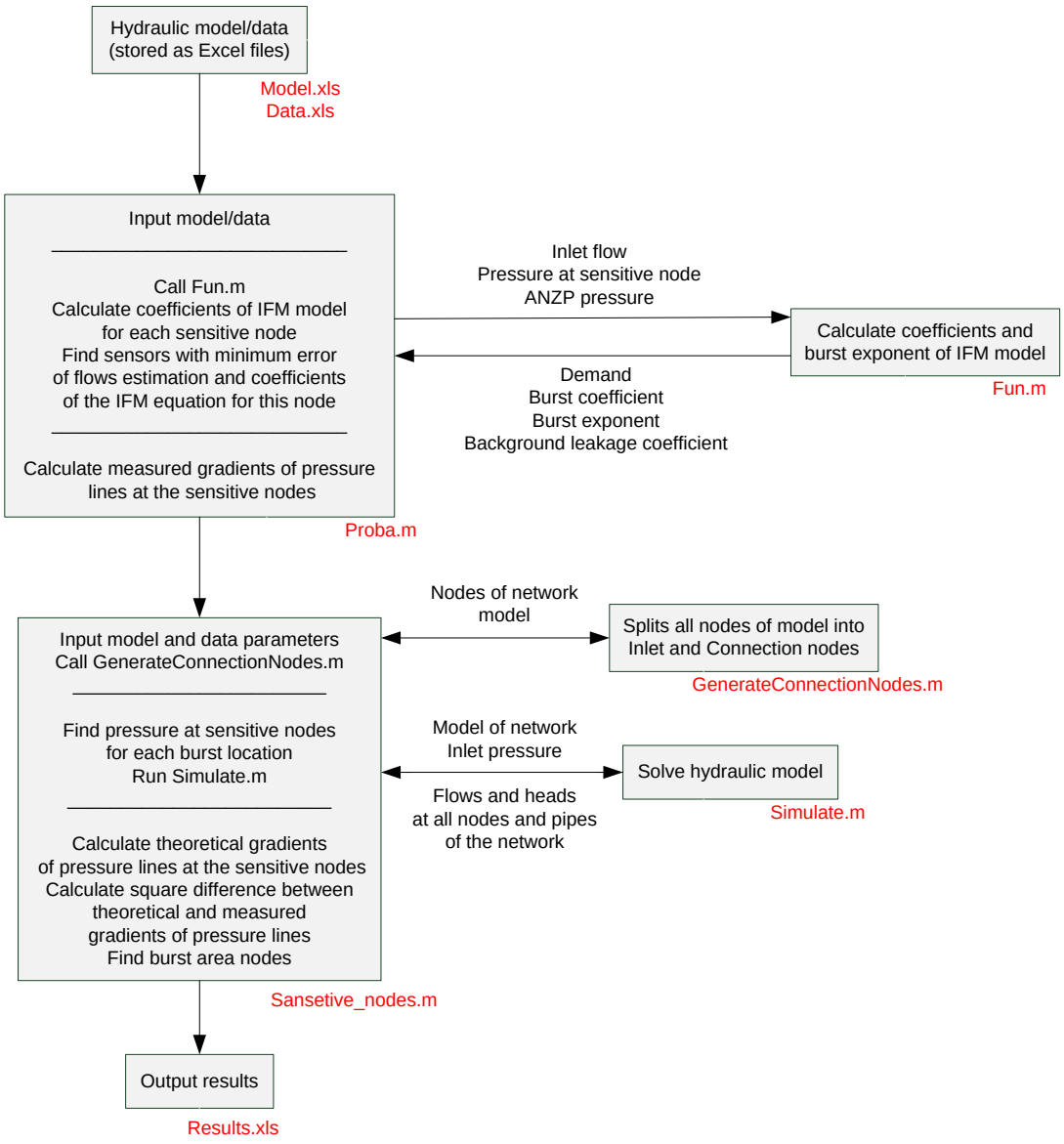

```
%%          Proba.m - identification of a burst size                    %%
%%=========================================%%

% Load input data
measurements=xlsread('data','measurements');
inlet=xlsread('data','inlet');
nodes=xlsread('model','nodes');

% Change input flows and input heads
no_input=length(inlet(1,:));
for i=1:1:no_input
   in_flow(:,i)=measurements(3:end,i);
   measurements(3:end,i)=inlet(2:end,i);
end
heads=measurements(3:end,:);

%Calculate pressures in measurements nodes from model
no_nodes=measurements(1,:);
for i=1:1:length(nodes(:,1))
   for j=1:1:length(no_nodes)
      if no_nodes(1,j)==nodes(i,1)
      elevation_p(1,j)=nodes(i,4);
      pressure(:,j)=heads(:,j)-elevation_p(1,j);
      end
   end
end
p_all=pressure';
q_all=in_flow;
NumbOfMeasurements=length(p_all(1,:));
q_first=q_all(:,1);
%q_second=q_all(:,2);                          % if there are 2 inlets
%q_dable=q_first+q_second;
q_dable=q_first;
```

```
for i=1:1:NumbOfMeasurements
   av_p(1,i)=mean(p_all(:,i));
end

% Calculate coefficients
lb=zeros(1,4);
lb(1,3)=0.5;
x=ones(1,4);
c_all_1=ones(1,4);
c_all_2=ones(1,4);
options = optimset('MaxIter', 1000, 'TolX', 10.^-20);

for j=1:1:length(no_nodes)
   for i=1:1:NumbOfMeasurements
      ak(i,1)=q_dable(i,1);
      ak(i,2)=p_all(j,i);
      ak(i,3)=av_p(1,i);
  end
   save('variables.mat', 'ak');
   c_all_2(j,:)=lsqnonlin(@func,x,lb);
end
r2_c_all=c_all_2;
r2_c_all(:,5)=no_nodes';
xlswrite('results',r2_c_all , 'c_all2');

% Calculate flow from coefficients with burst exponent c_all_2(3)
for j=1:1:length(no_nodes)
   d_p=c_all_2(j,1);
   c1=c_all_2(j,2);
   c2=c_all_2(j,4);
   expon2=c_all_2(j,3);
   for i=1:1:NumbOfMeasurements
      q2(j,i)=d_p+c1*p_all(j,i)^expon2+c2*av_p(1,i)^1.5;
```

```
        diff_q2(j,i)=((q2(j,i)-q_dable(i,1))^2)/q2(j,i);
    end
    xi_squere2(j)=sum(diff_q2(j,:));
end
r_diff2(:,1)=no_nodes';
r_diff2(:,2)=xi_squere2';
xlswrite('results',r_diff2,'diff2');

% Results
[m,k]=min(xi_squere2);
leak_node2=no_nodes(1,k);
leak_coeff2=c_all_2(k,:);
r_leak2=[leak_node2 leak_coeff2];
xlswrite('results',r_leak2,'leak2');

% Pressure coefficients
pp1=ones([1 NumbOfMeasurements]);
pp2=p_all(1,:);
p=[pp1;pp2];
p1=p';
for i=1:1:length(no_nodes)
    p2=p_all(i,:)';
    pol=p1\p2;
    pr_coeff(i,:)=pol';
end
r_pr_coeff=pr_coeff;
r_pr_coeff(:,3)=no_nodes';
xlswrite('results',r_pr_coeff,'pr_coeff');

[m,k]=min(pr_coeff(:,2));
leak_pres_node=no_nodes(1,k);
```

```
%%      sansetive_nodes.m - identification of a burst location    %%
%%=========================================%%

global lambdaf lambdac hfp d leakexp1 leakexp2 NumberPipes NumberConNodes
element_resistance elevation

% Load model
allnodes = xlsread('model','nodes');    % node data - number, type (1-inlet, 0-normal),
                                        % demand factor, elevation, 2 leakage
                                        % coefficients/exponents, OSgrid ref
pipes = xlsread('model','pipes');    % pipe data - nodes from/to, length, diameter, c value

% Generate list of connection and fixed nodes
[fixnodes,connodes]=GenerateConnectionNodes(allnodes);

NumberPipes=length(pipes(:,1));
NumberNodes=length(allnodes(:,1));
NumberFixedNodes=length(fixnodes);
NumberConNodes=length(connodes(:,1));

% Create reasonable demand curve to use in simulation (load one if you have one)
s_NumberOfMeasurements=3;
DemandLevel=leak_coeff2(1,1);           %in l/s
NumberOfProperties=sum(allnodes(:,3));
curve=(DemandLevel/NumberOfProperties)*ones(s_NumberOfMeasurements,1);

% Exceptional demand
knowndemand=zeros(NumberConNodes,s_NumberOfMeasurements);

% Create inlet head profile for simulation (load one if you have one)
% Must be of dimension  NumberFixedNodes X s_NumberOfMeasurements
elevation_res=allnodes(fixnodes,4);
pf =[min(p_all(1,:)) ((min(p_all(1,:))+max(p_all(1,:)))/2) max(p_all(1,:))];
```

```
hf=pf+elevation_res;

% Create stuff
element_location=[pipes(:,1)  pipes(:,2)];
element_resistance=1.21216*(10^10)*pipes(:,3)./((pipes(:,5).^1.852).*(pipes(:,4).^4.87)
);
demand_factors=connodes(:,3);
elevation=connodes(:,4);

leakexp1=(connodes(:,6)/0.5)*leak_coeff2(1,3);
leakexp2=connodes(:,8);
demands=(demand_factors*curve')+knowndemand;

% Create lambda, lambdac and lambdaf (node-incidence matrix thing)
lambda = zeros(NumberNodes,NumberPipes);
for (i=1:1:NumberPipes)
    from=element_location(i,1);
    to=element_location(i,2);
    aa=1;b=1;
     while from~=allnodes(aa,1)
         aa=aa+1;
     end
     while to~=allnodes(b,1)
         b=b+1;
     end
 lambda(b,i)=-1;
 lambda(aa,i)=1;
end
lambdac=lambda;
lambdaf=[];
for (i=NumberFixedNodes:-1:1)
  fxn=fixnodes(i);
  j=1;
```

```
  while fxn ~= allnodes(j,1)
    j=j+1;
  end
  lambdaf=[lambda(j,:) ; lambdaf];
  lambdac(j,:)=[];
end

% Initially simulate with no leakage
leak1=zeros(length(demand_factors),1);
leak2=ones(length(demand_factors),1).*(leak_coeff2(1,4)/length(demand_factors));

% Initialise values
x0=zeros (NumberPipes + NumberConNodes,1);
%initial flow
x0(1:NumberPipes)=0;
%initial head
x0(NumberPipes+1:NumberPipes+NumberConNodes)=mean(mean(hf));

qr=element_location;
hr=connodes(:,1);

% All flow
san_hall=zeros(NumberConNodes,NumberConNodes+2);
san_q=zeros(NumberConNodes+1,s_NumberOfMeasurements+2);
leak1=connodes(:,5);
s_p=[ones([1 s_NumberOfMeasurements]); pf];
s_p1=s_p';
for n=1:1:(NumberConNodes+1)

for (Timestep=1:1:s_NumberOfMeasurements)
  j= Timestep + 2

% Calculate flows and heads
```

```
hfp=hf(:,Timestep);
d=demands(:,Timestep);
options=optimset('Display','final','Jacobian','on','TolFun',1e-6,'MaxIter',500);
x= fsolve(@simulate,x0,options,leak1,leak2);
x0=x;
s_q(1:NumberPipes)=x(1:NumberPipes);
hc(1:NumberConNodes)=x(NumberPipes+1:NumberPipes+NumberConNodes);
qr=[qr s_q'];
hr=[hr hc'];
end
% need to change! 174 - string number of input pipe
san_q(n,:)=qr(174,1:s_NumberOfMeasurements+2);

% Calculate pressure coefficients
for i=1:1:NumberConNodes
   s_p2=(hr(i,2:end)-elevation(i,1))';
   s_pol=s_p1\s_p2;
   s_pr_coeff(i,:)=s_pol';
end

san_coef(:,n+1)=s_pr_coeff(:,2);
hr=hr*0;
hr=connodes(:,1);
leak1=connodes(:,5);
leak1(n,1)=leak_coeff2(1,2);
end
san_coef(:,1)=hr(:,1);
san_coef_leak=diag(san_coef(:,3:end));

s_no_nodes=no_nodes;
s_no_nodes(1,1)=measurements(2,1);
for i=1:1:length(no_nodes)
   ss_res(i,:)=san_coef(s_no_nodes(1,i),:);
```

```
end

for i=2:1:length(ss_res(1,:))
   ss_diff(:,(i-1))=((ss_res(:,i)-pr_coeff(:,2)).^2);
   ss_sum_diff(1,(i-1))=sum(ss_diff(:,(i-1)));
end
[ss_MC,ss_Ind]=sort(ss_sum_diff');
ss_leak_node=ss_Ind(1,1)-1;
res1=ss_res';
res2=ss_sum_diff';
xlswrite('results',res1,'s_pr_coeff');
xlswrite('results',res2,'s_pr_diff');

% Burst area
aaaa_a=ss_MC;
indii=ss_Ind;
aaaa=aaaa_a(2,1);
fl=0;
while aaaa<1
   aaaa=aaaa*10;
   fl=fl+1;
end
aaa_res=aaaa_a*(10^fl);
ii=1;
bb=5;
while aaa_res(ii,1)-aaa_res(1,1)<bb
   ff_res(ii,1)=indii(ii,1);
   ii=ii+1;
end
ff_res;
fl_res=[ss_Ind ss_MC];
xlswrite('results',fl_res,'res_area');
```

```
%%                fun.m - Function for IFM model                %%
%%=======================================%%

function F = func(x)

load variables.mat ak ;
N = length(ak(:,1));     % number of measurements
k = 1:N;
F = x(1)+x(2).*(ak(k,2)).^x(3)+x(4).*ak(k,3).^1.5-ak(k,1);



%%  GenerateConnectionNodes.m - Generate list      %%
%%   of connection and fixed nodes function          %%
%%=================================%%

function [fixnodes,connodes]= GenerateConnectionNodes(allnodes)

% Generate fixed nodes
fixnodes=[];
connodes=allnodes;
for i=length(allnodes(:,1)):-1:1
   if(allnodes(i,2))==1
      fixnodes=[allnodes(i,1) ; fixnodes];
      connodes(i,:)=[];
   end
end
```

```
%%  simulate.m - Program of simulation of the network   %%
%%=====================================%%

function [F,J]= simulate(x,leak1,leak2)

global leakexp1 leakexp2 lambdaf lambdac
global NumberPipes NumberConNodes element_resistance elevation hfp d leakage1
leakage2;

% Decoding x vector into 2 parts
q(1:NumberPipes)=x(1:NumberPipes);
hc(1:NumberConNodes)=x(NumberPipes+1:NumberPipes+NumberConNodes);
q=q';
hc=hc';
leakage1=(leak1.*((hc-elevation).^leakexp1));
leakage2=(leak2.*((hc-elevation).^leakexp2));

fun1= lambdac*q + d + leakage1 + leakage2;

dh= element_resistance.*abs(q).^0.852.*q;
a=lambdac'*hc;
b=lambdaf'*hfp;
fun2= dh - a - b;

F=[fun1;fun2];

leakbit1=diag(leak1.*leakexp1.*((hc-elevation).^(leakexp1-1)));
leakbit2=diag(leak2.*leakexp2.*((hc-elevation).^(leakexp2-1)));
leakbit=leakbit1 + leakbit2;

dnres = diag(1.852*(element_resistance.*abs(q).^0.852));
J=[lambdac leakbit;dnres -lambdac'];
```

Bibliography

1. Al-Khomairi A.M. (2005), “Use of the steady state orifice equation in the computation of transient flow through pipe leaks.” *The Arabian Journal for Science and Engineering*, 30, 1B, pp. 33-45.
2. Araujo L.S., Coelho S.T. & Ramos H.M. (2003), “Estimation of distributed pressure-dependent leakage and consumer demand in WDSs.” *Advances in Water Supply Management*, Swets & Zeitlinger B.V., Lisse, The Netherlands.
3. Babich B., Prodanovich D., and Ivetich M. (2005), “Preliminary results of water losses research in sections of Belgrade water supply system and developing of technical guidelines and procedures.” *CCWI 2005 International Conference*, Exeter University Press, Exeter, Vol.2, pp. 119-124.
4. Berardi L., Giustolisi O., Primativo F. (2007), “Exploiting multi-objective strategies for optimal rehabilitation planning”, in *Water Management Challenges in Global Change*, (Ulanicki et al. editors), Taylor & Francis Group, London, ISBN 978-0-415-45415-5, pp. 23-30.
5. Berardi L., Savic D. and Giustoloso O. (2005), “Investigation of burst-prediction formulas for water distribution systems by evolutionary computing.” *CCWI 2005 International Conference*, Exeter University Press, Exeter, Vol.2, pp. 275-280.
6. Borovik I. & Pavlov Y. (2000). “Statistical methods of an estimation and the forecast of a condition of water supply systems.” *Computer science and control systems in XXI century*, BMSTU, Moscow. (Russian)
7. Borovik I. & Pavlov Y. (2007). “Multi-factor regression analysis in applied task to control urban water supply network.” *The electronic journal " Science in formation. Engineering formation "*, ISSN 1994-0408 online. (English /Russian)
8. Borovik I. & Yanov I.O. (2007). “Mathematical model of one-dimensional water supply network.” *The electronic journal " Science in formation. Engineering formation "*, ISSN 1994-0408 online. (English /Russian)
9. Borovkov, A.A. (1976). *Probability theory*, publishing house “Science”, Moscow. (Russian)

10. Boxall J.B., O'Hagan A., Pooladsaz S., Saul A.J. and Unwin D.M. (2005), "Pipe level estimation of burst rates in water distribution mains." *CCWI 2005 International Conference*, Exeter University Press, Exeter, Vol.1, pp. 33-38.
11. Breaks and Background Estimates (BABE) (2008), Bristol Water Services Ltd. http://www.wso.us/startpage/leakagemanagement.htm, accessed on May 2008.
12. Brooke A., Kendrick, D., & Meeraus, A. (1992). *GAMS a user guide*, Boyd & Fraser – The Scientific Press Series. USA
13. Brunone B. & Ferrante M. (2001), "Detecting leaks in pressurized pipes by means of transients." *Journal of Hydraulic research*, 39(5), pp. 539-547.
14. Burnell D. (2003), "Auto-validation of district meter data." *Advances in Water Supply Management*, Swets & Zeitlinger B.V., Lisse, The Netherlands.
15. Buchberger, S.G. and L.Wu. (1995), "Model for instantaneous residential demands." *Journal of Hydraulic Engineering*, Vol. 121, No. 3, pp 232-246.
16. Buchberger, S.G. and Nadimpalli, G. (2004), "Leak Estimation in Water Distribution Systems by Statistical Analysis of Flow Readings." *Journal of Water Resources Planning and Management*, Vol. 130, No. 4, pp. 321–329.
17. Bush, C.A. and Uber, J.G. (1998), "Sampling Design Methods for Water Distribution Model Calibration." *Journal of Water Resources Planning and Management*, Vol. 124, No. 6.
18. Cascetta, F, and Vigo, P. (1992), "Location and Assessment of Water Leakage." *Measurements and Control*, Vol. 25, November.
19. Chernoff H, Lehmann E.L. (1954), "The use of maximum likelihood estimates in $\chi 2$ tests for goodness-of-fit." *The Annals of Mathematical Statistics*, Vol. 25, pp. 579-586.
20. Cheung P.B., Reis L.F.R., Formiga K.T.M., Chaudhry F.H. & Ticona W.G.C. (2003), *Evolutionary algorithms applied to the rehabilitation of water distribution: A Comparative Study, Evolutionary Multi-Criterion Optimization - Lecture notes in Computer Science*, Heidelberg: Springer-Verlag, V.2632.
21. Coulbeck B., Orr C.H., Cunningham A.E., (1989), *Computer Control of Water Supply: GINAS 5 Reference Manual*, Research report Nr 56, School of Electronic Eng., Leicester Polytechnic.

22. Covas D., Ramos H., Graham N. & Maksimovic C. (2004), "Application of transient-based techniques for leak detection in water pipe systems." *Proc. 4th World Water Congress and Exhibition*, Marrakech, IWA.
23. Covas D., Ramos H., Graham N., Maksimovic C., Kapelan Z., Savic D. & Walters G. (2003), "An assessment of the application of inverse transient analysis for leak detection: part II - collection and application of experimental data." *Computers and Control in the Water Industry (CCWI 2003)*, Imperial college London, UK.
24. Covas, D. and Ramos, H. (1999), *Leakage Detection in Single Pipelines Using Pressure Wave Behaviour, in Water Industry Systems: modelling and optimisation applications*, edited by Savic and Walters, Research Studies Press Ltd, Baldock, England.
25. Dandy G. C. and Engelhardt M. (2001), "Optimal scheduling of water pipe replacement using genetic algorithms." *Journal of Water Resources Planning and Management*, Vol. 127, N 4.
26. Deb K., Agrawal S., Pratap A. & Meyarivian T. (2000), "A fast and elitist genetic algorithm NSGAII." Technical Report N 2000001, Indian Inst.of.Tech., Kanpur, India.
27. Devi T. & Nam-Sik P. (2004), "Multiobjective Algorithms for decision of Water Distribution Networks." *Journal of Water Resources Planning and Management*, 130(1), pp. 73-82.
28. Deagle G., Green A., Scrivener J. and Tansley N. (2007), "Advanced tools for burst location", in *Water Management Challenges in Global Change*, (Ulanicki et al. editors), Taylor & Francis Group, London, ISBN 978-0-415-45415-5, pp. 307-312.
29. Economou T., Kapelan Z., Bailey T. (2007), "An aggregated hierarchical Bayesian model for the prediction of pipe failures", in *Water Management Challenges in Global Change*, (Ulanicki et al. editors), Taylor & Francis Group, London, ISBN 978-0-415-45415-5, pp. 13-16.
30. Farley, M., and Trow, S. (2003), *Losses in Water Distribution Networks*, IWA Publishing, London.

31. Ferrante M. and Brunone B. (2003), “Pipe system diagnosis and leak detection by unsteady tests. 2. Wavelet analysis.” *Advances in Water Resources*, 26, pp.107-116.
32. Final project report (2006). “Reduction of water losses and energy consumption using an effective process for burst detection.” Sustainable Technologies Initiative EPSRC & DTI, De Montfort University, February.
33. Garcia V., Cabrera E., Cabrera E. Jr. (2006), “The Minimum Night Flow Method Revisited.” *8th Annual Water Distribution Systems Analysis Symposium*, Cincinnati, Ohio, USA, August 27-30, B(1).
34. Germanopoulos, G. (1985), “A technical note in the inclusion of pressure dependent demand and leakage terms in water supply network models.” *Civil Engineering Systems*, Vol. 2.
35. Giustolisi O. & Berardi L. (2007), “Pipe level burst prediction using EPR and MCS-EPR”, in *Water Management Challenges in Global Change*, (Ulanicki et al. editors), Taylor & Francis Group, London, ISBN 978-0-415-45415-5, pp. 39-46.
36. Giustolisi O. & Laucelli D. (2007), “More realistic water distribution network design using pressure-driven demand and leakage”, in *Water Management Challenges in Global Change*, (Ulanicki et al. editors), Taylor & Francis Group, London, ISBN 978-0-415-45415-5, pp. 177-183.
37. Giustolisi O., Laucelli D. and Savic D. (2005), “A decision support framework for short-time rehabilitation planning in water distribution systems.” *CCWI 2005 International Conference*, Exeter University Press, Exeter, Vol.1, 39-44.
38. Goldman, S. (1953). *Information theory*, Constable and company, London.
39. Guo S., Liu S. & Chen R. (2004), “Optimisation Arrangement for Pressure Monitoring Points of Water Distribution Network.” *China Water & Waste Water*, Vol. 20(12), pp.82-84.
40. Hetenyi Zs., Tolnai B. and Zimmer P. (2007), “Planning reconstruction works based on risk analysis”, in *Water Management Challenges in Global Change*, (Ulanicki et al. editors), Taylor & Francis Group, London, ISBN 978-0-415-45415-5, pp. 47-54.
41. Hirner, W.H. (1997), “Unaccounted-for Water.” *Conference on Water Utility Partnership for Capacity Building*, Kampala, Uganda. October.

42. Huang T. & Cong H. (2001), “Cluster analysis for optimal locating of pressure monitoring stations in water supply network.” *China Water & Waste Water*, Vol. 17(11), pp. 50-52.
43. Kapelan Z., Savik D. and Walters G. (2003), “A Hybrid Inverse Transient Model for Leakage Detection and Roughness Calibration in Pipe Networks.” *Journal of Hydraulic Research*, 41(5), pp. 481-492.
44. Kleiner Y. & Rajani B. (2007), “Static and dynamic effects in prioritizing individual water mains for renewal”, in *Water Management Challenges in Global Change*, (Ulanicki et al. editors), Taylor & Francis Group, London, ISBN 978-0-415-45415-5, pp. 61-68.
45. Kleiner Y. and Rajani B. (2001), “Comprehensive review of structural deterioration of water mains: statistical models.” *Urban Water Journal*, No 3 (3), pp. 131-150.
46. Kleiner Y., Rajani B, Sadiq R. (2004), “Management of failure risk in large-diameter buried pipes using fuzzy-based techniques.” *4th International Conference on Decision Making in Urban and Civil Engineering*, Porto, Portugal. October.
47. Kleiner Y., Rajani B, Sadiq R. (2004), “Modelling failure risk in buried pipes using fuzzy Markov deterioration process.” *ASCE International Conference of Pipeline Engineering and Construction*, San Diego, CA. August.
48. Kleiner Y., Rajani B, Sadiq R. (2005), “Application of a Fuzzy Markov Model to Plan the Renewal of Large-Diameter Buried Pipes: A Case Study.” *CCWI 2005 International Conference*, Exeter University Press, Exeter, Vol.1, pp. 45-50.
49. Lambert, A., Myers, S., and Trow, S. (1998), *Managing Water Leakage*, Published by Financial Times Energy, London,.
50. Liggett J.A. & Chen L.C. (1994), “Inverse transient analysis in pipe networks.” *Journal of Hydraulic Engineering*, ASCE, 120(8), pp.934-955.
51. Magini R., Pallavicini I. & Verde D. (2007), “Estimation of leakages in Water Distribution Systems with measurements at few nodes”, in *Water Management Challenges in Global Change*, (Ulanicki et al. editors), Taylor & Francis Group, London, ISBN 978-0-415-45415-5, pp. 321-328.

52. Maksimovic, C., Butler, D., Memon, F.A. (2003), "Advances in Water Supply Management", *Proceedings of the International Conference an Computing and Control for the Water Industry*, London, UK, Published by Taylor and Francis group, London ISBN 9058096092, pp. 131.
53. Manual of Water Supply Practices AWWA M36 (1990). *Water Audits and Leak Detection*. ISBN 0 89867 485 0.
54. May, J. (1994), "Pressure-dependent Leakage" *World Water and Environmental Engineering*, October.
55. Mays, L.W. (2000), *Water distribution systems handbook*, McGraw-Hill International Editions.
56. Morrison J. (2004) "Managing leakage by District Metered Areas: a practical approach", for Water21 by the IWA Water Loss Task Force, UK.
57. Mounce S.R., Boxall J.B. & Machell J. (2007), "An Artificial Neural Networks/Fuzzy Logic system for DMA flow meter data analysis providing burst identification and size estimation", in *Water Management Challenges in Global Change*, (Ulanicki et al. editors), Taylor & Francis Group, London, ISBN 978-0-415-45415-5, pp. 313-320.
58. Mpesha W., Chaudry M.H. & Gassman S.L. (2000), "Leak detection in pipes by frequency response method using a step excitation." *Journal of hydraulic research*, Vol. 40, N 1, pp. 55-62.
59. Nafi A & Werey C. (2007), "An efficient multi-objective approach for water pipes renewal", in *Water Management Challenges in Global Change*, (Ulanicki et al. editors), Taylor & Francis Group, London, ISBN 978-0-415-45415-5, pp 75-84.
60. Nash G.A. & Karney B. (1999), "Efficient Inverse Transient Analysis in Pipe Systems." *Journal of Hydraulic Engineering*, ASCE, 125(7), pp.761-764.
61. Noack C. and Ulanicki B. (2006), "Modelling of soil diffusibility on leakage characteristics of buried pipes.", *8th Annual Water Distribution Systems Analysis Symposium*, Cincinnati, Ohio, USA, August 27-30.
62. Pallavicini, I., and Magini, R. (2007), "Experimental analysis of residential water demand data: Probabilistic estimation of peak coefficients at small time scales", in *Water Management Challenges in Global Change*, (Ulanicki et al.

editors), Taylor & Francis Group, London, ISBN 978-0-415-45415-5, pp.379-384.

63. Plackett, R.L. (1983), "Karl Pearson and the Chi-Squared Test." *International Statistical Review*, Vol. 51(1), pp. 59–72.
64. Prescott, S., and Ulanicki, B. (2006), Reduction of water losses and energy consumption using an effective process for burst detection, Sustainable Technologies Initiative EPSRC (GR/S25715) & DTI, Final Project Report, 19 February 2006.
65. Pudar, R.S. and Liggett, J.A. (1992), "Leaks in Pipe Networks." *Journal of Hydraulic Engineering*, ASCE 118(7), pp.1031–1046.
66. Pudar, R.S., and Liggett, J.A. (1992). *Fluid mechanics.* Mass.: WCB/McGraw-Hill, 9th edition.
67. Puust R., Kapelan Z., Savic D. and Koppel T. (2006), "Probabilistic leak detection in pipe networks using the SCEM-UA algorithm." *8th Annual Water Distribution Systems Analysis Symposium*, Cincinnati, Ohio, USA, August 27-30, A(4).
68. Rajani B. and Tesfamariam S. (2005), "Estimating time to failure of ageing cast iron water mains under uncertainties." *CCWI 2005 International Conference*, Exeter University Press, Exeter, Vol.1, pp. 57-63.
69. Rossman L.A., (2000). *EPANET 2 Users Manual*, U.S. Environmental Protection Agency, National Risk Management Research Laboratory, Cincinnati, OH 45268, September.
70. Shamir U. & Howard C.D.D. (1979), "An analytic approach to scheduling pipe replacement." *Journal of American Water Works Association*, N 71, pp. 248-258.
71. Shmoylova R.A. editor (1999). *Statistic theory*, 'The finance and statistics', Moscow. (Russian).
72. Simpson, A.R. and Vitkovsky, J.P. (1997), "A Review of Pipe Calibration and Leak Detection Methodologies for Water Distribution Networks." *Proc. 17th Federal Convention*, Australian Water and Wastewater Association, Australia, vol. 1, pp. 680–687.
73. Skipworth P.J., Cashman A., Engelhardt M.O., Saul A.J. & Savic D. (2001), "Quantification of mains failure behaviour in a whole life costing approach to

distribution system management." *ASCE EWRI conference*, Orlando, Florida. May.

74. Soares A.K., Covas D.I.C. & Reis L.F.R. (2007), "Inverse Transient Analysis for leak detection in a PVC pipe network", in *Water Management Challenges in Global Change*, (Ulanicki et al. editors), Taylor & Francis Group, London, ISBN 978-0-415-45415-5, pp.337-344.
75. Stephens M., Misiunas D., Lambert M., Simpson A., Vitkovsky J. & Nixon J. (2005), "Field verification of a continuous transient monitoring system for burst detection in water distribution systems." *CCWI 2005 International Conference*, Exeter University Press, Exeter, Vol.2, pp. 257-262.
76. Stoianov I., Karney B., Covas D., Maksimovic C. & Graham N. (2002). *Wavelet Processing of Transient Signals for pipeline Leak Location and Quantification*, Roanoke, Virginia, USA.
77. Streeter, V.L., and Wylie, K.W. (1998). *Fluid mechanics,* Mass.: WCB/McGraw-Hill, 9th edition.
78. Tabesh M. & Delavar M.R. (2003), "Application of integrated GIS and hydraulic models for unaccounted for water studies in water distribution systems." *Advances in Water Supply Management*, Swets & Zeitlinger, Lisse, The Netherlands.
79. Tabesh M., Asadiani Yekta A.H. and Burrows R. (2005), "Evaluation of Unaccounted for Water and Real Losses in Water Distribution Networks by Hydraulic Analysis of the System Considering Pressure Dependency of Leakage." *CCWI 2005 International Conference*, Exeter University Press, Exeter, Vol.2, pp. 125-130.
80. Thornton J., Lambert A. (2005) "Progress in practical prediction of pressure: leakage, pressure: burst frequency and pressure: consumption relationships", in Leakage 2005 - Conference Proceedings.
81. Trifunovich N., Umar D. (2003), "Reliability assessment of the Bekasi distribution network by the method of Cullinane." *Advances in Water Supply Management*, Swets & Zeitlinger, Lisse, The Netherlands.
82. Ulanicka K., Ulanicki B., Rance J.P. & Coulbeck B., Powell R. & Wang C. (1998), "Benchmarks for water network modelling." *Hydroinformatics'98*, Balkema, Rotterdam, ISBN 90 5410 983 1.

83. Ulanicka, K, Ulanicki, B, (2003), “Computer modelling of water supply systems – pump scheduling and reservoir control”, (ed), in *Water & Sewerage Journal*, McMillan Pub., Issue 1/2003.
84. Ulanicki B., Bounds P.L.M., Rance L.P., Reynolds L., (2000), “Open and Closed Loop Pressure Control for Leakage Reduction.” *Urban Water Journal*, Vol. 2, September.
85. Ulanicki, B. and Prescott, S. (2000), “Statistical Prediction of Leakage in Water Distribution Networks.” *Proceedings of the 45th International Scientific Colloquium*, Ilmenau Technical University, October.
86. Ulanicki, B., Bounds P.L.M., Rance J.P., and Reynolds, L. (1999), “Open Loop and Closed Loop Pressure Control for Leakage Reduction.” *Urban Water Journal*, Elsevier Science, Vol.2, pp. 105-114
87. Ulanicki, B., Prescott, S.L. and May, J. (2006). “Anatomy of leakage”, unpublished notes, Water Software Systems, De Montfort University, Leicester, UK.
88. Unwin D.M., Boxall J.B. & Saul A.J. (2003), “Data mining and relationship analysis of water distribution system databases for improved understanding of operations performance.” *Advances in Water Supply Management*, Swets & Zeitlinger, Lisse, The Netherland.
89. Van Zyl, J.E. & Clayton, CRI (2005), “The effect of pressure on leakage in water distribution systems.” *CCWI 2005 International Conference*, Exeter University Press, Exeter, Vol.2, pp. 131-136.
90. Ventcel, E.S. (1964). *Probability theory*, Major edition of the physical and mathematical literature, publishing house “Science”, Moscow. (Russian).
91. Vairavamoorthy, K, and Lumbers, J. (1998), “Leakage Reduction in Water Distribution Systems: Optimal Valve Control.” *Journal of hydraulic Engineering*, Vol.11, November.
92. Vitkovsky J.P., Simpson A.R. & Lambert M.F. (1999), “Leak Detection and Calibration of Water Distribution Systems Using Transient and Genetic Algorithm.” *Proc. of the 26th Annual Water Resources Planning and Management Conference*, June, Tempe, Arizona, USA.

93. Vitkovsky J.P., Simpson A.R. & Lambert M.F. (2000), "Leak Detection and Calibration Issues using Transient and Genetic Algorithm." *Journal of Water Resources Planning and Management*, ASCE, 126(4), pp. 262-265.
94. Vitkovsky, J.P. and Simpson, A.R. (1997). Calibration and Leak Detection in Pipe Networks Using Inverse Transient Analysis and Genetic Algorithms. Report No. R 157, Department of Civil and Environmental Engineering, University of Adelaide, p. 97.
95. WAA - Water Authorities Association UK (1980) Leakage Control Policy & Practice, Report 26, UK Water Authorities Association.
96. Wallingford Software (2008), www.wallingfordsoftware.com/products/infoworks_ws, accessed on July 2008.
97. Walski T.M. & Pelliccia A. (1982), "Economic analysis of water main breaks." *Journal of American Water Works Association*, N 74, pp. 140-147.
98. Wang X.J., Lambert M.F., Simpson A.R., Liggett J.A. & Vitkovsky J.P. (2002), "Leak Detection in Pipelines using Damping of Fluid Transients." *Journal of Hydraulic Engineering*, ASCE, 128(7), pp. 697-711.
99. WHO - World Health Organisation, (2001), *Leakage Management and Control - A Best Practice Manual*, WHO, Geneva.
100. WRc-UK Water Industry. (1994). *Managing Leakage – Summary report*, Report A.
101. WRc-UK Water Industry. (1994a). *Managing Leakage – Managing Water Pressure*, Report G.
102. WRc-UK Water Industry. (1994b). *Managing Leakage – Using Night Flow Data*, Report F.
103. WSS. (1999) "FINESSE: On-line Operational Modelling and Modelling environment", [On-line], UK, available from: http://www.eng.dmu.ac.uk/wssys/software.htm. [Accessed: 7/1/00].
104. Wu Z.Y. & Sage P. (2007), " Pressure dependent demand optimisation for leakage detection in water distribution systems", in *Water Management Challenges in Global Change*, (Ulanicki et al. editors), Taylor & Francis Group, London, ISBN 978-0-415-45415-5, pp.353-361.
105. Xi J., Bin Z.H., Jie Z. & Fang W. (2007), "Optimal placement of pressure monitors in water supply network with elitist Genetic Algorithm", in *Water*

Management Challenges in Global Change, (Ulanicki et al. editors), Taylor & Francis Group, London, ISBN 978-0-415-45415-5, pp.115-121.

106. Zecchin A.C., White L.B., Lambert M.F. and Simpson A.R. (2005), "Frequency-Domain hypothesis testing approach to leak detection in single fluid line." *CCWI 2005 International Conference*, Exeter University Press, Exeter, Vol.2, pp. 149-154.
107. Zhou S. & Xu S. (2005), "Studying Optimal Locating of Pressure Monitoring Stations in Urban. Water Distribution System." *Journal of Nanhua University* (Science and Technology), Vol. 19(1), pp. 59-63.

Dictionary

AZNP	average zonal night pressure, $p_{AZNP} = \frac{\sum_{i \in Nodes} p_i \cdot Demand\_Allocation\_Factor_i}{\sum_{i \in Nodes} Demand\_Allocation\_Factor_i}$
Background leakage	water losses with flow rates from 0.005 litres/second to 0.05 litres/second which occur mainly at joints, connections and fittings
Burst	water losses from pipe breaks or cracks with flow rates from 0.1 litres/second to 10 litres/second
Demand	node outflow representing water consumption
Demand_Allocation_Factor	Proportion of total demand *d* applied to node *i*
DMA	District Metering Area, a part of a WDS which have closed boundaries except for a small number of metered inlets and outlets
Equivalent area of a leak	The coefficient *c* in the formula $q_{leak} = c(p) \times p^{0.5}$ relating leakage flow to pressure
Experiment	This thesis refers to simulation experiments and field experiments. Unless otherwise stated 'experiment' refers to simulation experiment.
FAVOR test	Fixed And Variable Orifice area test - the type of experiment where inlet pressure of DMA is being stepped down and up and the inlet flow and inlet pressure (head) are measured
Extended FAVOR test	FAVOR test where additionally pressure (head) at a number of selected internal nodes of a DMA are measured
Fixed area leakage	leakage flow for which an equivalent leakage area is constant

IFM	Inflow Flow Model, a three term model of the total inlet flow to a DMA which comprises demand, fixed area leakage and variable area leakage
Pressure line	a plot of a functional relationship between the inlet pressure to a DMA and pressure at a selected node
Regression pressure line	A linear regression line approximation to a pressure line
RMS error	Root mean square error
Sensitive nodes	representative nodes in a DMA which are particularly sensitive to an occurrence of a burst according to a certain criterion
Variable area leakage	leakage flow for which an equivalent leakage area changes with pressure
WDS	Water Distribution System – a general term to describe a part of a clean water system from outputs of treatment works to water consumers.
χ^2 criterion	Statistical significance test

List of symbols

q	Flow (litres/sec), (l/s)
h	Head (metres), (m)
p	Pressure (metres), (m)
g	Acceleration due to gravity (m/s/s)
v	Speed of the water (m/s)
c_1	Burst coefficient ($l/s/\sqrt{m}$)
c_2	Background leakage coefficient ($l/s/m\sqrt{m}$)
d	Demand flow (l/s)
p_{AZNP}	Average zonal night pressure (m)
a, b	Coefficients
r	Resistance coefficient
δ	Standard deviation
$f(x)$	Function of x
χ^2	The chi-square statistic
φ	Level of accuracy